

**Signalling properties at single synapses and within the interneuronal
network in the CA1 region of the rodent hippocampus**

Thesis submitted for the degree of
“Doctor Philosophiae”

S.I.S.S.A.
Neurobiology Sector

CANDIDATE:
Federico Minneci

SUPERVISOR:
Prof. Enrico Cherubini

TABLE OF CONTENTS

NOTES.....	5
ABBREVIATIONS.....	6
ABSTRACT.....	8
INTRODUCTION.....	11
SECTION I.....	11
1. The Hippocampus.....	11
1.1 Anatomy of the hippocampus	12
1.2 The hippocampal circuitry	13
2. Synaptic transmission.....	15
2.1 Chemical synapses and neurotransmitter release.....	15
2.2 Synaptic efficacy.....	19
2.2.1 <i>Modulation of synaptic efficacy</i>	21
2.3 Quantal analysis and estimation of quantal parameters.....	23
2.3.1 <i>Presynaptic issues</i>	24
2.3.2 <i>Time course of synaptic signalling</i>	25
2.3.3 <i>Postsynaptic issues</i>	26
2.3.4 <i>Methods: classical approaches and novel ideas</i>	27
2.4 Univesicular versus multivesicular release	28
SECTION II.....	31
1. Interneurons of the hippocampus: overview	31
1.1 Towards a classification of the interneurons.....	33
1.1.1 <i>Morphological classification</i>	34
1.1.2 <i>Neurochemical classification</i>	36
1.1.3 <i>Functional classification</i>	37
2. Functional role of interneurons.....	38
2.1 Chemical synaptic activity	39
2.1.1 <i>Postsynaptic actions on the principal cells</i>	40

2.1.2	<i>Synaptic plasticity</i>	42
2.2	Networks of interneurons	43
2.2.1	<i>Gap junctions between interneurons</i>	43
2.2.2	<i>Inhibition in networks of coupled neurons</i>	45
2.2.3	<i>Network activity and oscillations</i>	46
3.	Molecular and genetic variety of the interneurons	49
3.1	Correlating molecular and functional studies: new ideas for a classification	49
METHODS AND RESULTS		52
Multivesicular release at developing Schaffer collateral-CA1 synapses: an analytic approach to describe experimental data.		52
Signalling properties of <i>stratum oriens</i> interneurons of the hippocampus of transgenic mice expressing EGFP in a subset of somatostatin-containing cells		53
CONCLUSIONS AND FUTURE PERSPECTIVES		94
REFERENCES		98
ACKNOWLEDGEMENTS		118

NOTES

The work described in this dissertation was carried out at the International School for Advanced Studies, Trieste, between November 2002 and August 2006, and was included in the following papers. All work reported here, with the exception listed below, arises from my own experiments and data analysis.

The theoretical work described in the first paper was done in collaboration with Federico Ricci-Tersenghi. The immunocytochemical experiments described in the second paper were carried out by Natasa Dragicevic and Daniela Avossa.

Ricci-Tersenghi F, Minneci F, Sola E, Cherubini E & Maggi L (2006). Multivesicular release at developing Schaffer collateral-CA1 synapses: an analytic approach to describe experimental data. *J Neurophysiol.* 96: 15-26. E-pub 5 Apr 2006.

Minneci F, Janahmadi M, Dragicevic N, Avossa D, Migliore M & Cherubini E. Signalling properties of stratum oriens interneurons in the hippocampus of transgenic mice expressing EGFP in a subset of somatostatin-containing cells. In preparation.

The following publication, arising from a collaborative project in which I am co-author, was not included in the present thesis:

Maggi L, Sola E, Minneci F, Le Magueresse C, Changeux JP & Cherubini E (2004). Persistent decrease in synaptic efficacy induced by nicotine at Schaffer collateral-CA1 synapses in the immature rat hippocampus. *J Physiol.* 559: 863-74. E-pub 22 Jul 2004.

ABBREVIATIONS

[]:	concentration
ACh:	acetylcholine
AMPA:	α -amino-3-hydroxy-5-methyl-4-isoxazole propionic acid
ATP:	adenosine 5'-triphosphate
cAMP:	3'-5'-cyclic adenosine monophosphate
CA1/4	<i>cornu ammonis</i> regions 1/4
CB:	calbindin
CCK:	cholecystokinin
CNS:	central nervous system
CR:	calretinin
CV:	coefficient of variation
EPSC:	excitatory postsynaptic current
EPSP:	excitatory postsynaptic potential
D-AP5:	DL-2-amino-5-phosphonopentanoic acid
DCG-IV:	(2S,2'R,3'R)-2-(2',3'-dicarboxycyclopropyl) glycine
DG:	dentate gyrus
DMSO:	dimethylsulphoxide
DNQX:	6,7-dinitroquinoxaline-2,3-dione
EGFP:	enhanced green fluorescent protein
EGTA:	ethylene glycol-bis(2-aminoethylether)-N,N,N',N'-tetraacetic acid
GABA:	γ -aminobutyric acid
GAD:	glutamic acid decarboxylase
GIN:	GFP-expressing Inhibitory Neurons (line of transgenic mice from the Jackson Laboratory, Bar Harbor, ME, USA)
G-proteins:	GTP-binding proteins
HEPES:	N-2-hydroxyethylpiperazine-N'-2-ethanesulfonic acid
IPSC:	inhibitory postsynaptic current
IPSP:	inhibitory postsynaptic potential
LM-PP:	<i>lacunosum moleculare</i> –perforant path

LM-R-PP:	<i>lacunosum moleculare-radiatum</i> –perforant path
LTD:	long-term depression
LTP:	long-term potentiation
<i>m</i> :	quantal content
m2:	muscarinic receptor type 2
MF:	mossy fibres
mGluR:	metabotropic glutamate receptor
<i>N</i> :	number of independently releasable vesicles (in univesicular multi-site release: number of release sites)
nAChR:	nicotinic acetylcholine receptor
NMDA:	N-methyl-D-aspartate
NMJ:	neuromuscular junction
NPY:	neuropeptide tyrosine
NSF:	N-emthylmaleimide-sensitive factor
PBS:	phosphate buffer saline
PPR:	paired-pulse ratio
<i>p</i> :	release probability of a single vesicle
P:	postnatal day
<i>P_r</i> :	probability of release of the synapse
PV:	parvalbumin
<i>Q</i> :	quantal size
RRP:	readily releasable pool of vesicles
SM:	somatostatin
SNAP:	soluble NSF attachment protein
SNARE:	SNAP receptor
TTX:	tetrodotoxin
VAMP:	vesicle-associated membrane protein
VGLUT3:	vesicular glutamate transporter 3
σ :	standard deviation

ABSTRACT

Understanding how the complexity of connections among the neurons in the brain is established and modified in an experience- and activity-dependent way is a challenging task of Neuroscience. Although in the last decades many progresses have been made in characterising the basic mechanisms of synaptic transmission, a full comprehension of how information is transferred and processed by neurons has not been fully achieved.

In the present study, theoretical tools and patch clamp experiments were used to further investigate synaptic transmission, focusing on quantal transmission at single synapses and on different types of signalling at the level of a particular interneuronal network in the CA1 area of the rodent hippocampus.

The simultaneous release of more than one vesicle from an individual presynaptic active zone is a typical mechanism that can affect the strength and reliability of synaptic transmission. At many central synapses, however, release caused by a single presynaptic action potential is limited to one vesicle (univesicular release). The likelihood of multivesicular release at a particular synapse has been tied to release probability (P_r), and whether it can occur at Schaffer collateral–CA1 synapses, at which P_r ranges widely, is controversial. In contrast with previous findings, proofs of multivesicular release at this synapse have been recently obtained at late developmental stages; however, in the case of newborn hippocampus, it is still difficult to find strong evidence in one direction or another.

In order to address this point, in the first part of this study a simple and general stochastic model of synaptic release has been developed and analytically solved. The model solution gives analytical mathematical expressions relating basic quantal parameters with average values of quantities that can be measured experimentally. Comparison of these quantities with the experimental measures allows to determine the most probable values of the quantal parameters and to discriminate the univesicular from the multivesicular mode of glutamate release. The model has been validated with data previously collected at glutamatergic CA3-CA1 synapses in the hippocampus from newborn (P1-P5 old) rats. The results strongly support a multivesicular type of release process requiring a variable pool of immediately releasable vesicles. Moreover, computing quantities that are functions of the model parameters, the mean amplitude of the synaptic response to the

release of a single vesicle (Q) was estimated to be 5-10 pA, in very good agreement with experimental findings. In addition, a multivesicular type of release was supported by various experimental evidences: a high variability of the amplitude of successes, with a coefficient of variation ranging from 0.12 to 0.73; an average potency ratio a_2/a_1 between the second and first response to a pair of stimuli bigger than 1; and changes in the potency of the synaptic response to the first stimulus when the release probability was modified by increasing or decreasing the extracellular calcium concentration. This work indicates that at glutamatergic CA3-CA1 synapses of the neonatal rat hippocampus a single action potential may induce the release of more than one vesicle from the same release site.

In a more systemic approach to the analysis of communication between neurons, it is interesting to investigate more complex, network interactions. GABAergic interneurons constitute a heterogeneous group of cells which exert a powerful control on network excitability and are responsible for the oscillatory behaviour crucial for information processing in the brain. They have been differently classified according to their morphological, neurochemical and physiological characteristics.

In the second part of this study, whole cell patch clamp recordings were used to further characterize, in transgenic mice expressing EGFP in a subpopulation of GABAergic interneurons containing somatostatin (GIN mice), the functional properties of EGFP-positive cells in *stratum oriens* of the CA1 region of the hippocampus, in slice cultures obtained from P8 old animals. These cells showed passive and active membrane properties similar to those found in *stratum oriens* interneurons projecting to *stratum lacunosum-moleculare*. Moreover, they exhibited different firing patterns which were maintained upon membrane depolarization: irregular (48%), regular (30%) and clustered (22%). Paired recordings from EGFP-positive cells often revealed electrical coupling (47% of the cases), which was abolished by carbenoxolone (200 μ M). On average, the coupling coefficient was 0.21 ± 0.07 . When electrical coupling was particularly strong it acted as a powerful low-pass filter, thus contributing to alter the output of individual cells. The dynamic interaction between cells with various firing patterns may differently control GABAergic signalling, leading, as suggested by simulation data, to a wide range of interneuronal communication. In additional paired recordings of a presynaptic EGFP-

positive interneuron and a postsynaptic principal cell, trains of action potentials in interneurons rarely evoked GABAergic postsynaptic currents (3/45 pairs) with small amplitude and slow kinetics, and that at 20 Hz exhibited short-term depression. In contrast, excitatory connections between principal cells and EGFP-positive interneurons were found more often (17/55 pairs) and exhibited a frequency and use-dependent facilitation, particularly in the gamma band. In conclusion, it appears that EGFP-positive interneurons in *stratum oriens* of GIN mice constitute a heterogeneous population of cells interconnected *via* electrical synapses, exhibiting particular features in their chemical and electrical synaptic signalling. Moreover, the dynamic interaction between these interneurons may differentially affect target cells and neuronal communication within the hippocampal network.

INTRODUCTION

SECTION I

1. The Hippocampus

The hippocampus is among the best characterised brain structures, mainly because its layered organisation (Andersen *et al.*, 1971) is particularly suitable for anatomical and physiological investigations, but also because, since the early 1950s, it has been recognised to play a fundamental role in some forms of learning and memory (Kandel, 2001).

Evidence implicates the hippocampus in storing and processing spatial information. Studies in rats have shown that neurons in the hippocampus have spatial firing fields; these cells are called “place cells” (Muller, 1996). Some cells fire when the animal finds itself in a particular location, regardless of direction of navigation, while most are at least partially sensitive to head direction and direction of navigation.

The discovery of place cells led to the idea that the hippocampus might act as a “*cognitive map*” of the neural representation of the layout of the environment. Recent evidence has cast doubt on this perspective, indicating that the hippocampus might be crucial for more fundamental processes within navigation. Regardless, studies with animals have shown that an intact hippocampus is required for simple spatial memory tasks (for instance, finding the way back to a hidden goal) (Kwok & Buckley, 2006), and moreover, neurological patients with damage to the hippocampal formation show memory deficits.

From these clinical origins, a diverse field of memory research has flowed (Morris, 2006). The specific functional contributions of the hippocampus and those of related structures (the entorhinal cortex, the dentate gyrus, the individual CA fields and the subicular complex) remain a matter of dispute. Rival neuropsychological theories include proposals for a role in cognitive mapping and scene memory (O'Keefe & Nadel, 1978; Gaffan, 2001), declarative and relational memory (Squire, 1992; Eichenbaum & Cohen, 2001), the rapid acquisition of configural or conjunctive associations (Sutherland & Rudy, 1989; O'Reilly & Rudy, 2001), context-specific encoding and retrieval of specific

events (Hirsh, 1974; Good & Honey, 1991) and the proposal that the hippocampal formation is critical for certain aspects of episodic and/or episodic-like memory (Tulving, 1983; Mishkin *et al.*, 1997; Morris & Frey, 1997; Vargha-Khadem *et al.*, 1997; Aggleton & Brown, 1999). To complement this complexity, neural network modelling studies indicate that the intrinsic anatomy and synaptic physiology of the hippocampus could mediate the rapid encoding and distributed storage of a large number of arbitrary associations (Marr, 1971; McNaughton & Morris, 1987; McClelland *et al.*, 1995; Rolls & Treves, 1998). Both approaches suggest that in all mammals, be they man, monkey or mouse, the hippocampus is a particular kind of associative memory network. It does not operate in isolation as several excitatory inputs and outputs reflect important functional interactions with the neocortex (Amaral & Witter, 1989; Witter *et al.*, 2000) and inputs from midbrain and other forebrain nuclei modulate its activity in critical ways for memory formation (Matthies *et al.*, 1990).

1.1 Anatomy of the hippocampus

The hippocampus is an elongated structure located on the medial wall of the lateral ventricle, whose longitudinal axis forms a semicircle around the thalamus. Due to its layered organisation through this axis, when the hippocampus is cut across its transverse axis (the septotemporal one), it is possible to identify a particular structure that is preserved in all slices taken with this orientation. The hippocampus *proper* and its neighbouring cortical regions, the dentate gyrus (DG), subiculum and entorhinal cortex, are collectively termed “hippocampal formation”. As shown in Figure 1, the hippocampus *proper* is divided in *stratum oriens* (1), *stratum pyramidale* (2), *stratum radiatum* (3), and *stratum lacunosum-moleculare* (4). Excitatory neurones (pyramidal cells) are arranged in a layer that forms the *stratum pyramidale*, traditionally divided in four regions CA1-CA4. In general, CA4 is considered the initial part of CA3 and the small CA2 is often included in CA1 (but see for example Lein *et al.*, 2005). All pyramidal neurones bear basal dendrites that arborise and form the *stratum oriens* and apical dendrites that are radially oriented in the *stratum radiatum* and *lacunosum-moleculare*. In the DG, granule cells represent the principal neurones, while the area between DG and the CA3 region is called the *hilus*.

1.2 The hippocampal circuitry

The main inputs to the hippocampus come from the enthorinal cortex, the septum and the controlateral hippocampus, whereas a unique unidirectional progression of excitatory pathways links each region of the hippocampus, creating a sort of trisynaptic circuit (Figure 1). The perforant path, originated from the enthorinal cortex, passes through the subicular complex and terminates mainly in the dentate gyrus, making synapses on granule cells. Then, the distinctive unmyelinated axons of the granule cells (mossy fibres)

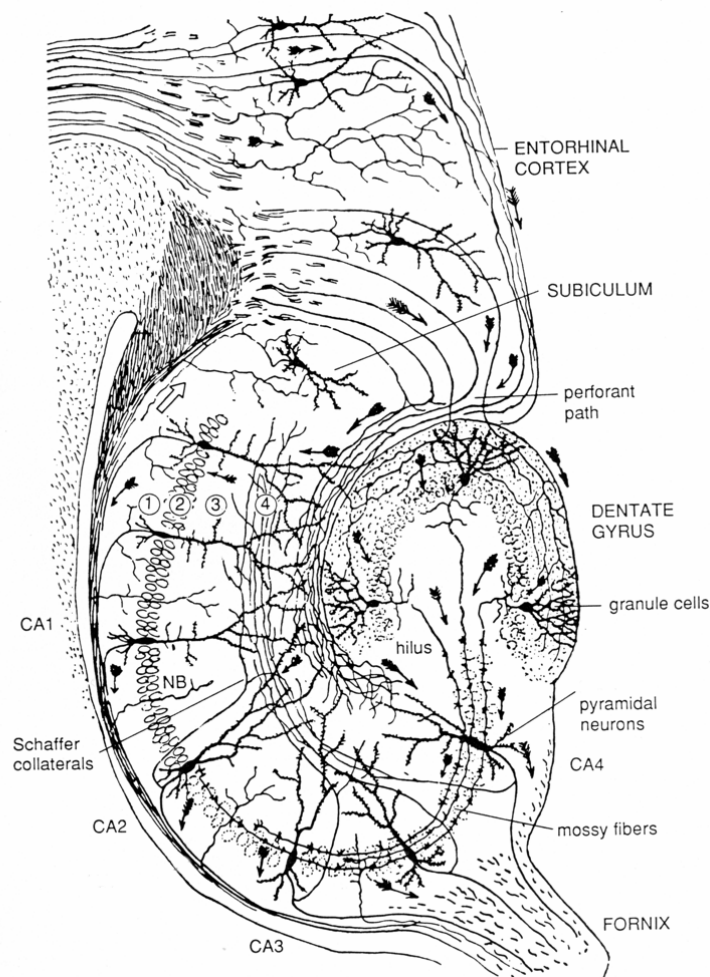


Figure 1. Neuronal elements of the hippocampal formation. Labelled areas include the subiculum, part of the enthorinal cortex, the fornix, the dentate gyrus and the region CA1 to CA4. The hippocampus *proper* is divided into *stratum oriens* (1), *stratum pyramidale* (2; cell bodies drawn as ovals), *stratum radiatum* (3) and *stratum lacunosum-moleculare* (4). (Modified from Ramón y Cajal, 1911)

project to the *hilus* and to the *stratum lucidum* of the CA3 region. Here they make synapses *en passant* on CA3 pyramidal neurones showing the large, presynaptic varicosities typical of mossy fibres-CA3 contacts. These presynaptic expansions form a unique synaptic complex with equally intricate postsynaptic processes called *thorny excrescences* and may contain tens of release sites (Jonas *et al.*, 1993). Information is therefore transferred, through Schaffer collaterals, from CA3 to CA1 pyramidal neurones, which therefore send their axons to the subiculum and the deep layers of entorhinal cortex. Then, signal is sent back to many of the same cortical areas. Thus, information entering the entorhinal cortex from a particular cortical area can traverse the entire hippocampus and return to the cortical area from which it originated. The transformations that take place during this process are presumably essential for information storage (Johnston & Amaral, 1998). Furthermore, commissural associative fibres provide synaptic contacts between CA3 pyramidal neurones and between the two hippocampi, *via* the fornix. Excitatory postsynaptic currents or potentials elicited by MF stimulation can be discriminated from those evoked by commissural fibres on the basis of their faster kinetics (Yeckel *et al.*, 1999) and their sensitivity to the selective agonist for metabotropic glutamate receptors 2/3, (2S,2'R,3'R)-2-(2',3'-dicarboxycyclopropyl) glycine (DCG-IV; Kamiya *et al.*, 1996). The recurrent connections between pyramidal neurones are particular of the CA3 region and are responsible for making this region quite unstable. The simultaneous activation of a certain percentage of these connections is sufficient for generating epileptiform activity, characterised by spontaneous, synchronised and rhythmic firing in a large number of neurones (Miles & Wong, 1986; Traub & Miles, 1991). This feature accounts for the selective generation of seizures in this region following the application of convulsive agents (Ben-Ari & Cossart, 2000). The hippocampus is known to be crucial for certain forms of learning and memory, and the recurrent associative network formed by CA3 pyramidal cells have recently been shown to play an important role in associative memory recall (Nakazawa *et al.*, 2002). A critical role in controlling the communication between pyramidal neurones, especially but not only in this case, is accomplished by local inhibitory interneurons and a balance is set between excitation and inhibition. In contrast to the rather uniform population of excitatory neurones, interneurons, which are distributed in the entire hippocampus, show

a great variability and are classified in several families according to their morphology and axonal and dendritic arborisation (see Section II). Among all the differences in morphology and in active and passive membrane properties between neurones, a particular feature of pyramidal cells, known as accommodation, is the possibility to limit the maximal firing frequency upon injection of a depolarising current step. This property distinguishes pyramidal neurones from interneurons that, on the contrary, are able to fire up to 400 Hz (Lacaille, 1991).

2. Synaptic transmission

Synaptic contacts between neurones occur primarily between small swellings, known as *boutons*, either at the terminal or along (*en passant*) axonal profiles of the presynaptic neurone and small fingerlike processes (spines) of postsynaptic dendrites (axospinous synapses). However, other types of synapses have been characterised and have been termed depending on the contact elements (for example axosomatic, axoaxonic, dendrodendritic).

Two structurally and functionally distinct forms of synapses exist: electrical and chemical. At electrical synapses, specialised channels (gap junctions) form a direct electrical connection between the presynaptic and the postsynaptic neurones. At chemical synapses, the cells are electrically disconnected from one another: the electrical signal is translated into a chemical one in the presynaptic neurone and only afterwards is reconverted to an electrical signal in the postsynaptic cell. Electrical synapses have the virtue that transmission occurs without delay, but they are far less rich in possibilities for adjustment and control than chemical synapses, that, in fact, represent the predominant way of communication between neurones. In this Section, the attention will be focused on chemical synapses, in particular on glutamatergic excitatory ones.

2.1 Chemical synapses and neurotransmitter release

Chemical synapses operate through the release, from the presynaptic neurone, of a neurotransmitter that diffuses in the synaptic cleft and provokes electrical changes in the postsynaptic cell by binding to a selective membrane protein present on the postsynaptic membrane (receptor). Neurotransmitter molecules are initially stored in the synaptic

vesicles described, long time ago, by ultrastructural studies (Palade 1954; Palay, 1954). Most vesicles are retained in a large pool behind the plasma membrane, whereas a small part of them approaches the presynaptic membrane, and eventually fuse with it, through a particular cycle that can be divided in several steps and involves a very large number of proteins (reviewed in Südhof, 1995). The vesicles immediately available for release belong to the so-called readily releasable pool of vesicles (RRP; Rosenmund & Stevens, 1996; Südhof, 2000; for a review see Rizzoli and Betz 2005). Synaptic vesicles are usually anchored to a network of cytoskeletal filaments by synapsins, a family of protein presenting phosphorylation sites for both cAMP and calcium-calmodulin dependent protein kinases. Phosphorylation is able to free vesicles from the cytoskeleton constrain, allowing them to move into the active zone, where they dock through the interaction between proteins in the vesicular membrane and proteins in the plasma membrane. Candidates for these protein-protein interactions include the vesicular membrane proteins synaptotagmin and Rab3 (Benfenati *et al.*, 1999). After docking, synaptic vesicles go through a maturation process, known as priming, during which a highly stable core complex is formed between the synaptic vesicle protein VAMP/synaptobrevin and the presynaptic membrane proteins syntaxin and SNAP-25. These three proteins are known as SNAP receptors or SNAREs, as they form a high affinity binding site for cytosolic α -SNAP (soluble NSF attachment protein), which itself becomes a receptor site for NSF (N-ethylmaleimide-sensitive factor). Under steady-state conditions, specific protein interactions, between VAMP and synaptophysin at the vesicle membrane and between syntaxin and munc 18 (or munc 13) at the plasma membrane, inhibit the formation of the core complex that would otherwise assemble outside the active zones (Thomson, 2000). The “unlocking” of these proteins occurs during docking and is modulated by phosphorylation and by calcium, suggesting that it may be an important rate-dependent step in the supply of fusion-competent vesicles during repetitive activity. Once the fusion core complexes are formed, they have to be disassembled for release to occur. The hydrolysis of ATP by NSF provides the energy required to regenerate the SNARE monomers that will be used in the next cycle. Rapid fusion and exocytosis are triggered by high local calcium concentration during the action potential invasion. Ca^{2+} ions act in a co-operative way, as judged from the steep relationship between change in intracellular

calcium concentration ($[Ca^{2+}]_i$) and transmitter release, thus accounting for a considerable margin of safety for synaptic transmission (Dodge & Rahamimoff, 1967). Different lines of evidence suggest that synaptotagmins function as Ca^{2+} sensors in the final fusion step (Südhof, 1995). According to the classical model, during exocytosis, vesicles collapse completely into the plasma membrane (“total fusion”) and release neurotransmitter in the synaptic cleft. During this process Rab proteins dissociate from the vesicle membranes and may retard the activation of neighbouring vesicles, resulting in release site refractoriness (Geppert *et al.*, 1997). Therefore, empty vesicles internalise slowly (endocytosis) at sites distant from the active zones and translocate into the interior for endosomal fusion. New vesicles accumulate again neurotransmitter by means of an active transport driven by an electrochemical gradient created by a proton pump. Finally, filled vesicles translocate back to the active zones and the vesicle cycle ends. A few years ago, this cycle model has been revisited and an alternative fusion process has been proposed. It suggests a transient state of the vesicle fusion, known as “transient fusion” or “kiss and

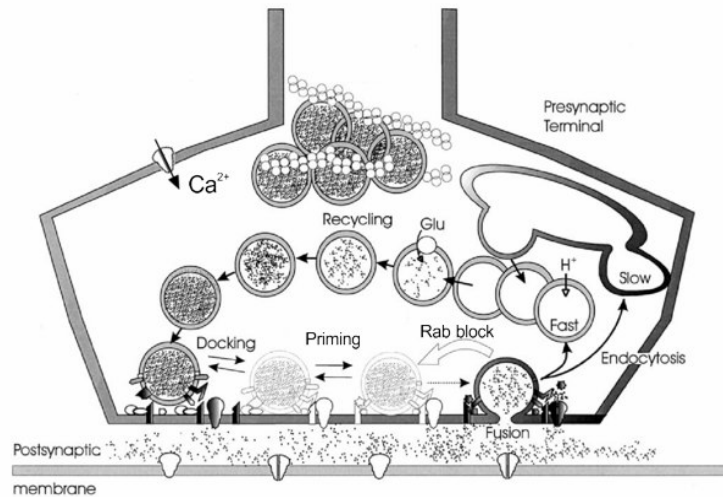


Figure 2. Main steps in neurotransmitter release at chemical synapses. A small part of synaptic vesicles approaches the plasma membrane and, through docking and priming processes, gets ready for being rapidly released. The influx of Ca^{2+} ions during action potential invasion triggers vesicle fusion. Thus, the neurotransmitter released diffuses across the narrow synaptic cleft and acts on postsynaptic receptors. Following or during fusion, Rab proteins dissociate from the vesicle and may in some way retard the activation of neighbouring vesicles (resulting in release site refractoriness). Synaptic vesicles are therefore recycled, in either slow or fast way, and may accumulate neurotransmitter again. (Modified from Thomson, 2000)

run”, a concept already proposed in the 1970s by Ceccarelli *et al.* (1973). According to this hypothesis, vesicles fuse with the plasma membrane by forming a transient fusion pore while preserving vesicle integrity. After detachment, vesicles can fuse again without any preceding endosomal fusion. The advantages are a rapid cycling between fusion and non-fusion state and reduced energy consumption. Applications of fluorescent and atomic force microscopy have provided evidence for the kiss and run model in non-neuronal and neuronal cells (Schneider, 2001).

Once neurotransmitter is released in the cleft, it diffuses to act mainly on ionotropic or metabotropic receptors that are clustered in an electron-dense thickening of the postsynaptic membrane, known as postsynaptic density. Then neurotransmitter is rapidly eliminated by diffusion, enzymatic degradation or by uptake into nerve terminals or glial cells. Ionotropic receptors are ion channels that open when they are bound by neurotransmitter molecules, allowing ions to flow within the cell membrane. This process changes the membrane potential of the postsynaptic neurone either in the positive (depolarisation) or in the negative direction (hyperpolarisation). When receptors are permeable to calcium ions, these cations can also activate intracellular processes. After opening, postsynaptic receptors normally desensitize, i.e. they remain in an “open state” without allowing ion influx, until they recover and restore their initial condition. Alternatively, the transmitter may bind to metabotropic receptors that are linked to ion channels through GTP-binding proteins (G-proteins).

An interesting approach to analyze the time course of transmitter concentration in the cleft deserves to be mentioned. This detection technique utilizes the non-equilibrium displacement of a competitive antagonist following the synaptic release of transmitter (Clements *et al.*, 1992; Clements, 1996; Tong & Jahr, 1994a,b; Barberis *et al.*, 2004). Displacement is a passive process whereby antagonist unbinds from receptors and is replaced by transmitter. Synaptic responses are elicited in the presence of a competitive antagonist, and the size of the reduction in amplitude provides information about the average transmitter timecourse at that synapse. A significant amount of antagonist unbinding must occur within the same timescale as clearance of transmitter, therefore a rapidly dissociating (low-affinity) competitive antagonist is required (a so-called “fast-off antagonist”). At equilibrium, antagonist molecules are constantly binding and unbinding,

and a fraction of receptors is vacant at any given moment. An instantaneous change to a high concentration of transmitter results in the rapid binding of transmitter to vacant receptors. As transmitter clearance continues, some antagonist molecules unbind from the receptors and are replaced by transmitter molecules (non-equilibrium displacement). Thus, the longer the transmitter is present, the more antagonist is displaced and the larger the response becomes. In this way, changes in amplitude of the postsynaptic response will depend not only on the concentration of the antagonist, but also on the amplitude and time course of the transmitter transient. In contrast, the block exerted by an antagonist with unbinding kinetics much slower than the synaptic pulse (a slowly dissociating competitive antagonist) does not depend on synaptic pulse concentration and time duration but only on the concentration of the antagonist, because during the synaptic pulse the antagonist cannot unbind from the receptor; in particular, if transmitter clearance is made faster or slower for any reason, the effectiveness of a slowly dissociating antagonist is unchanged and the modification cannot be detected.

2.2 Synaptic efficacy

The first step in the study of chemical synaptic transmission is the analysis of the efficacy of the synapse. By definition, the synaptic efficacy is the strength of synaptic transmission, measured by the average size of the postsynaptic response to stimulation of a presynaptic neuron (Faber *et al.*, 1998) and it was originally studied at the neuromuscular junction (NMJ).

The NMJ represents the standard model for studying synaptic transmission. At the beginning of the 1950s del Castillo and Katz (1954) proposed the quantal hypothesis of transmitter release, according to which neurotransmitter is packaged in discrete quantities of fixed size, called *quanta*, which are generally identified with synaptic vesicles. Thus, when a nerve impulse reaches the terminal, an integer number of *quanta* release their content in the synaptic cleft. In line with this idea, miniature currents, which can be recorded in the absence of action potential, are due to the release of a single *quantum*. Each release site operates in an all-or-none fashion, meaning that it can release either zero or one *quantum* and each *quantum* is released probabilistically and independently of the others. If the probability of release is uniform among the different sites, synaptic

transmission can be fit with a simple binomial model. Thus, in a synapse with N functional release sites and a probability p of release at each individual site, the probability that n *quanta* are released by a single action potential is:

$$P(n) = \frac{N!}{n!(N-n)!} p^n (1-p)^{N-n} \quad (\text{I.1})$$

While the probability of detecting no response (failure rate) is:

$$P(0) = (1-p)^N \quad (\text{I.2})$$

The mean number of *quanta* released, known as quantal content, is given by:

$$m = Np \quad (\text{I.3})$$

If Q represents the magnitude of the postsynaptic response to a single transmitter *quantum* (quantal size), the mean response I and its standard deviation σ are:

$$I = NpQ \quad (\text{I.4})$$

$$\sigma = Q\sqrt{Np(1-p)} \quad (\text{I.5})$$

Thus, the efficacy of a synaptic connection is the quantity written in eqn. I.4, and it depends on the synaptic parameters N , p and Q .

Interestingly the coefficient of variation (*CV*), defined as the ratio between the standard deviation and the mean, is independent of Q :

$$CV = \frac{\sigma}{I} = \sqrt{\frac{(1-p)}{Np}} \quad (\text{I.6})$$

In case of a very low probability of release ($p \ll 1$) and large N , the binomial distribution approximates the Poisson one and eqns. I.1-I.2-I.6 convert respectively into:

$$P(n) = \frac{e^{-m} m^n}{n!} \quad (\text{I.7})$$

$$P(0) = e^{-m} \quad (\text{I.8})$$

$$CV^2 = \frac{1}{m} \quad (\text{I.9})$$

Later on, the basic concepts of neurotransmitter release have been extended to central synaptic transmission, despite the obvious differences, both functional and morphological, that distinguish the two systems. For example, most of central synapses are characterised by a very small quantal size, with a change in conductance that is two

orders of magnitude smaller than that measured at the NMJ and is due to the opening of tens rather than thousands of postsynaptic receptors (but see calyx of Held; Borst *et al.*, 1995).

More importantly, at central synapses it is convenient to introduce a change in the simple picture depicted at the NMJ, in order to be able to account also for multivesicular release at a single release site (see paragraph 2.4). For this modality of transmission, the single sites are not constrained to operate in an all-or-none manner, and each active site can release a variable number of vesicles from the RRP as a consequence of a single action potential. For simplicity, it is convenient to focus on one single release site at a time, especially since the probability of release can vary a lot between different terminals at the same central synapses (Rosenmund *et al.*, 1993). The following considerations refer therefore to a central synapse with a single release site. In this condition, the case of univesicular release is very simple, since for each action potential just zero or one vesicle can be released, and the probability of having a postsynaptic response is identical to the probability that the vesicle be released. On the other hand, in the multivesicular case, formulas identical to the ones written above are valid, if now N is the number of vesicles of the RRP which can be independently released and p is the release probability for a single vesicle. The notable difference from the univesicular case, that is often mistaken also in the literature, is that now p is not any more equal to the probability of release of the synapse, which can be indicated with P_r ; consequently, the probability of having multiquantal responses depends on p and it has no relation with P_r (while many authors relate it to P_r^2 ; for example see Clements, 1996). If for example $N = 5$ and $p = 0.1$, using eqn. I.1 it is clear that over 100 stimulations of the synapse there will be in average 33 unit responses, 7 double-quantum responses, 1 triple response, zero quadruple and quintuple responses, 59 failures. Thus, p is very different from P_r , that is equal to 0.41; moreover, double release is predicted to happen with probability $10p^2(1-p)^3 = 0.0729$, which is very different from $P_r^2 = 0.1681$, and triple release with probability $10p^3(1-p)^2 = 0.0081$, and not with $P_r^3 = 0.068921$.

2.2.1 Modulation of synaptic efficacy

Changes in one or more of the synaptic parameters account for modifications in synaptic strength. Such modulation of synaptic efficacy is thought to be very important for the refinement of neural circuitry, information processing and storage. Thus, the possibility to find out the mechanisms and the sites of changes of synaptic strength is really important for understanding brain functions. Such changes and modulation are referred to as synaptic plasticity, and a detailed analysis of the mechanisms of this important phenomenon is beyond the purpose of this work. Briefly, synapses can undergo various kinds of synaptic plasticity, which can be sorted in different classes.

Short-term plasticity refers to use-dependent synaptic changes that are restricted to brief periods of time (reviewed in Zucker & Regehr, 2002). These processes are crucial for regulating temporal coding and information processing between neurones in the brain (Tsodyks & Markram, 1997), where, in fact, information is conveyed by spike train rather than by isolated action potentials. These modifications vary from synapse to synapse and in the same synapse according to its previous history (Debanne *et al.*, 1996; Markram & Tsodyks, 1996). Thus, most synapses in the CNS, including neocortex and hippocampus, undergo dynamic bidirectional regulations of their efficacy following activity-dependent processes. Increases in transmitter release by repeated stimulation fall into two categories: those that act over short interval (facilitation) and those that accumulate significantly during prolonged stimulation, augmentation and potentiation. These phenomena have been shown to be presynaptic in origin, with a strong correlation between elevation in $[Ca^{2+}]_i$ and enhancement of synaptic strength (Zucker & Regehr, 2002; Thomson, 2000). Another common form of short-term plasticity lasting from seconds to minutes is depression upon repeated use (Thomson & Deuchars, 1994; Nelson & Turrigiano, 1998). This may provide a dynamic gain control over a variety of presynaptic afferent firing action potentials at different rates (Markram & Tsodyks, 1996). Repeated use can either enhance or decrease synaptic efficacy, but in some cases multiple processes are present and the result is a combination of facilitation and depression. A particular example is obtained through the application of a paired-pulse protocol within a short time interval. In this case, the ratio between the mean amplitudes of the second response over the first one, known as paired-pulse ratio (PPR), is often inversely related to the initial release probability. This means that either paired-pulse

facilitation or paired-pulse depression can be observed in case of low or high release probability, respectively (Debanne *et al.*, 1996; Dobrunz & Stevens, 1997).

Finally, long-lasting activity dependent changes in synaptic efficacy are thought to play a fundamental role in the development of the neural circuitry, learning and memory (Stevens, 1998; Martin *et al.*, 2000). Long-term potentiation (LTP) refers to an increase in synaptic efficacy that can last for hours or even days, and it was first obtained by repetitive stimulation at synapses between perforant path fibres and granule cells in the DG of the hippocampus (Bliss & Lomo, 1973). LTP has been shown to occur in many other regions of the brain, but it has been mainly studied in the hippocampus and, in particular, at CA3-CA1 synapses (reviewed in Bliss & Collingridge, 1993; Larkman & Jack, 1995; Nicoll & Malenka, 1995; Malenka & Nicoll, 1999). Long-term depression (LTD), on the other hand, is a lasting activity-dependent decrease in synaptic efficacy that was at first described in CA1 neurons (Lynch *et al.*, 1977; for a review see Kemp & Bashir, 2001). It is widely accepted that LTD prevails in neonatal and young animals where it precedes the developmental onset of LTP (Dudek & Bear, 1993; Battistin & Cherubini, 1994).

2.3 Quantal analysis and estimation of quantal parameters

For a successful analysis of the synaptic activity it is therefore critically important to be able to obtain precise estimations of the quantal parameters N , p (indicating generically the release probability) and Q . It is clear that, while Q depends on both pre and postsynaptic mechanisms, N and p are controlled only by presynaptic factors. On the basis of the simple equations in paragraph 2.2, quantal analysis has been developed to find estimations of these parameters and/or to define the site of changes in case of modifications in synaptic efficacy (Katz, 1969; Korn & Faber, 1991; Faber *et al.*, 1998). At central synapses it is quite difficult to find appropriate experimental approaches and models for the application of quantal analysis, even though some authors have provided recipes for a 'proper' quantal analysis (see for example Korn & Faber, 1991). In many cases the distribution of miniature currents at central synapses is found surprisingly skewed (Bekkers *et al.*, 1990; Bekkers & Stevens; 1995), and more generally a great variability of the parameters is found both with experimental and simulation studies

(Rosenmund *et al.*, 1993; Bekkers, 1994; Auger & Marty, 1997; Auger & Marty, 2000; Franks *et al.*, 2003). This is due to different factors which can be sorted according to the various steps in the process of chemical synaptic transmission.

2.3.1 *Presynaptic issues*

Even if changes in Q and N may be involved in the modulation of synaptic strength and have always to be taken into account, the probability of release seems to be a major factor that influences the pattern of transmitter release (Thomson, 2000). A strong variability in p has been found when comparing both synapses from different preparations and the same kind of synapses. p can vary from less than 0.01 at specific cortical connections (Thomson *et al.*, 1995) up to 0.9 at the calyx of Held (von Gersdorff *et al.*, 1997) and a similar range of variability has been detected in the CA1 region of the hippocampus (Dobrunz & Stevens, 1997). It is still difficult to define p in an unambiguous and precise way, as a lot of different processes are involved in transmitter release. This particularity can probably account for the high variability in p values as well as for the many opportunities in controlling and modulating it. In general, p represents the probability that Ca^{2+} ions entering the nerve terminal because of a single action potential triggers the release of fusion-competent vesicles. Thus, we could imagine that different values of p are due to differences in local calcium affinity or binding at the level of Ca^{2+} sensors. Alternatively, the shape of the presynaptic action potential may be of fundamental importance for determining the strength of synapses, since the degree and the duration of depolarisation control the opening of voltage-gated Ca^{2+} channels, as well as the driving force for calcium influx itself (Sabatini & Regehr, 1997). Therefore, also the number, location and properties of calcium channels are important in modulating the shape and the size of the Ca^{2+} transients themselves. On the other hand, a differential expression of proteins involved in release or differences in their phosphorylation could account for further variability in the probability of release. The interplay between all these mechanisms determines p and a modification at any of these levels might affect synaptic strength (Thomson, 2000). Moreover, at hippocampal synapses the variability of p is found to be high even between different release sites of the same synapse (Rosenmund *et al.*, 1993) or between different stages of the postnatal development (Wasling *et al.*, 2004).

Finally, modulations of synaptic strength during synaptic plasticity may require presynaptic mechanisms to act as possible regulation sites for the modification of quantal size. One such site could be the vesicular neurotransmitter transporter, which, if subject to activity-dependent regulation, could link vesicle content to terminal activity. Another possible site of regulation is the fusion pore, the conductance of which has been observed to be quite small in small synaptic vesicles (19 pS) in relation to large dense-core vesicles. If the size of fusion pore conductance in CNS synapses occurs in similar ranges, alterations to fusion pore kinetics could provide meaningful regulatory mechanisms to determine the strength of synaptic connections (Liu, 2003).

2.3.2 *Time course of synaptic signalling*

After the release, the synaptic signal is propagated *via* the diffusion of the transmitter in the synaptic cleft. In this phase, the signal is subject to variability due to changes in delay times and agonist concentration (Liu *et al.*, 1999; Franks *et al.*, 2003). The time course of postsynaptic responses depends on the synchrony of transmitter release, on the time course of transmitter concentration in the cleft as well as on the gating properties of the receptors (Jonas, 2000). As previously described, evoked release of transmitter involves several steps; therefore it would not be surprising that the synaptic delay is somewhat variable from trial to trial at the same release site and between different release sites. The diffusion of neurotransmitter itself depends on several factors, such as the diffusion coefficient, the geometry of the cleft, the distribution and affinity of transmitter binding sites and the transporter uptake rate (Clements, 1996). It has been estimated that glutamate concentration during a synaptic event has a peak ranging between 1 and 5 mM and decays in a biphasic manner with time constants approximately 100 ms and 2 ms (Clements, 1996). The rising phase of postsynaptic signals is determined by the binding process between neurotransmitter molecules and receptors. Therefore it depends on the transmitter concentration time course and on the receptors opening rate. The decay phase, on the contrary, is mainly determined by the unbinding process, if desensitisation is considerably slow as in the case of nicotinic acetylcholine receptors. For example, no detectable AMPA receptor desensitisation has been revealed at hippocampal synapses (Hjelmstad *et al.*, 1999). The decay phase depends also on the kinetics of desensitisation

when desensitisation itself occurs at the time scale comparable to the one of transmitter concentration, as in the case of AMPA receptors at most glutamatergic synapses (Clements *et al.*, 1992; Jones & Westbrook, 1996; but see also Jonas, 2000).

2.3.3 Postsynaptic issues

An early interpretation suggested that the small quantal size at central synapses could be due to a small number of postsynaptic receptors. Thus, because of the high number of transmitter molecules released and because of the small volume of the synaptic cleft, glutamate would reach a concentration high enough to saturate all the receptors (Edwards *et al.*, 1990). According to this interpretation the skewed distribution of the minis could be due either to multiple quantal clusters of receptors on the postsynaptic membrane or to synapses consisting of multiple active zones (Edwards, 1995). Alternatively, the variability observed could be accomplished by differences in miniature amplitudes between different release sites (Edwards *et al.*, 1990; reviewed in Auger & Marty, 2000) or by fluctuations in the number of functional receptors or in their affinity for the transmitter. Obviously, receptor saturation has many important implications in synaptic physiology and in its possible modifications during synaptic plasticity (Scheuss *et al.*, 2002). Indeed, it seems that certain heterogeneity exists among different types of synapses. In the hippocampus, while high receptor saturation was initially described at certain connections (Edwards *et al.*, 1990; Clements *et al.*, 1992; Jonas *et al.*, 1993; Tang *et al.*, 1994), more recent studies exploiting different techniques have shown that variation in the concentration of the agonist is the main source of variability of the responses (Liu *et al.*, 1999; Hanse & Gustafsson, 2001a; Franks *et al.*, 2003) and that receptors are not saturated (Mainen *et al.*, 1999; Raghavachari & Lisman 2004; McAllister & Stevens 2000; Nimchinsky *et al.*, 2004; Conti & Lisman 2003). Moreover, an incomplete occupancy of AMPA receptors has been suggested by recordings of miniature excitatory postsynaptic currents from single synaptic boutons in hippocampal cultures (Forti *et al.*, 1997). It is worth noticing that saturation of postsynaptic receptors can lead to errors also in the estimation of N , since multi-site (and in general, multivesicular) release could give rise to a postsynaptic response that is not significantly different from a univesicular one. In fact, in the case of a simple functional

characterization of a synapse it is advisable to designate it not as a one-site or univesicular synapse, but rather as a ‘uniquantal’ synapse (Silver, 1998). Finally, a number of other sources of variability have been treated in experimental and modelling studies, including different number and stochastic properties of the postsynaptic receptors at the same or at different release sites (Auger & Marty, 1997; Auger & Marty, 2000; Franks *et al.*, 2003).

2.3.4 *Methods: classical approaches and novel ideas*

Starting from the pioneer work of del Castillo and Katz (1954), various approaches have been used to address the problems of quantal analysis. By convention, synaptic amplitude fluctuations are often visualized by measuring the amplitudes of several hundred evoked synaptic responses and plotting their distribution as a histogram. Several different techniques have been developed for interpreting synaptic amplitude fluctuations, and many of these focus on the amplitude histogram (reviewed by Bekkers, 1994; Redman, 1990; Bennett and Kearns, 2000). Moreover, in the case of a Poissonian model for the release, eqns. I.8 and I.9 have been used to obtain immediate estimates of the quantal content m from the number of failures or from the CV , respectively. The corresponding expressions allow these two methods to be applied to a binomial process (eqns. I.2 and I.6) just upon requirement of independent estimates of p , e.g., by comparing two conditions of release, such as high and low $[Ca^{2+}]$ (for details, see Martin, 1977). More often, because the binomial CV is independent of Q , it has been used as a tool for identifying the site of a change in synaptic strength, i.e., pre- versus postsynaptic (Faber and Korn, 1991).

However, some of these techniques rely on models of synaptic transmission that incorporate unrealistic simplifying assumptions, or have too many free parameters (Brown *et al.*, 1976; Barton and Cohen, 1977; Clements, 1991; Faber and Korn, 1991; Walmsley, 1995; Frerking and Wilson, 1996; Bekkers, 1994, 1995; Bekkers and Clements, 1999). Of particular concern are methods that search for ‘quantal’ peaks in the synaptic amplitude histogram (del Castillo and Katz, 1954; Redman, 1990; Bekkers, 1995; Bekkers and Clements, 1999). These methods assume that every vesicle of transmitter produces a postsynaptic response of approximately the same amplitude (the

‘quantal’ amplitude), and that the quantal amplitude is identical at all terminals or release sites, assumptions that are valid just at the NMJ. For central synapses, due to the variability of the responses discussed above, modifications of the original quantal hypothesis have been developed. They take into account the possibility of a non-uniform probability of release as well as the existence of both intra and intersite quantal variability, i.e. the variability in the quantal size at individual release site and between different release sites, respectively (Frerking & Wilson, 1996; Bennett & Kearns, 2000; Scheuss & Neher, 2001). In particular, methods which require fewer assumptions and are more robust to variability than previous approaches are the ones based on the analysis of the relationship between the mean and the variance of the responses (Clements, 2003), and the so-called multiple-probability fluctuation analysis (Silver, 2003). As described by Clements and Silver (2000), such methods also provide powerful tools for understanding the site of expression of synaptic plasticity (Silver *et al.*, 1998; Reid & Clements, 1999; Foster & Regehr, 2004).

Finally, some authors have pointed out recently a couple of different problems that must be acknowledged when dealing with quantal analysis of synaptic responses. In fact, it is not clear yet whether at small central synapses different release sites behave independently as observed at the NMJ. The analysis of the stochastic properties of miniature excitatory postsynaptic currents at individual hippocampal synapses has shown a clear divergence of the output of quanta from Poisson’s law (Abenavoli *et al.*, 2002). This result, together with the morphological observation of spontaneous pairs of omega profiles at active zones by fast freezing, suggests that functional release sites might be clustered. Moreover, impressive results suggest that spontaneously recycling vesicles and activity-dependent recycling vesicles originate from distinct pools with limited cross-talk with each other (Sara *et al.*, 2005), thus undermining the idea itself of an analysis of synaptic activity based on experiments with minis.

2.4 Univesicular versus multivesicular release

It was shown in the central nervous system that the number of release sites equals N , one of the parameters of the binomial law used in quantal analysis to describe the amplitude distribution of evoked synaptic currents (for a review see Redman, 1990). This identity

means that the maximal number of quantal peaks in amplitude distributions is inferior or equal to the number of release sites. In the extreme case where the connection involves a single release site, a single peak is observed. These observations together with electron microscopy structural data have been interpreted by Triller and Korn (1982) as indicating that only one vesicle can be released per release site after the arrival of an action potential (one site–one vesicle hypothesis). Nevertheless, as stressed by the same authors, near saturation of postsynaptic receptors by the neurotransmitter content of a single vesicle could provide an alternative to the single site–single vesicle hypothesis (Korn *et al.*, 1982). If postsynaptic receptors are close to saturation, multivesicular release would result in a small signal increment over univesicular release as only few additional receptors can be recruited. Single release sites would therefore generate single peak amplitude histograms in spite of multivesicular release. If on the other hand postsynaptic receptor occupancy is significant but far from saturation, multivesicular release will result in multiple peaks at decreasing intervals as the number of free postsynaptic receptors decreases after each vesicular release. In practice, occupancy values of 0.5 or higher will generate amplitude histograms that are virtually indistinguishable from single peak distributions. Furthermore, even if full saturation of postsynaptic receptors occurs, multivesicular release can in principle be demonstrated at single site synapses. Vesicular release is a time distributed process: synaptic current onsets are spread over a period of about 1 ms at room temperature (Katz & Miledi, 1965; Isaacson & Walmsley, 1995). Two successive exocytotic events should therefore result in a succession of a large and a small synaptic current, very much as in the case of two closely separated miniature events. Moreover, since the release probability is a function of time, early release events are more likely to be followed by a second release event than late ones. Thus multivesicular events will tend to have early latencies. Their rise times should be slowed down because of temporal summation of the rising phases of the underlying individual components. They will also have long durations, because larger and longer agonist pulses tend to prolong the decay time of the postsynaptic currents. Finally, they will have large amplitudes because of the partial summation of successive events (due to the fact that receptor occupancy is less than 1). Conversely, univesicular events will tend to be associated with longer latencies, fast rise times, short decay times and small amplitudes

(Raghavachari & Lisman, 2004). It is worth noticing that this observation about response amplitudes means that multivesicular release is more easily subject to postsynaptic saturation, especially if p is high; this implies that highly plastic synapses with the possibility of multivesicular release will have lower values of p , and that in general quantal size is determined by a fine balance of pre and postsynaptic factors (Liu, 2003). Using the tools described above, the application of fast-off antagonists, and even other techniques, multivesicular release was demonstrated at central synapses, for example at cerebellar synapses (Auger *et al.*, 1998; Auger & Marty, 2000; Wadiche & Jahr, 2001; Foster *et al.*, 2002).

The situation is more controversial at hippocampal synapses. For instance, at the CA3-CA1 synapses, proofs of univesicular release are reported both during the first week of development (Hanse & Gustafsson, 2001a,b) and in later periods (Stevens & Wang, 1995; Hjelmstad *et al.*, 1997). At this synapse, the non-saturation of postsynaptic receptors has been assessed with various techniques (Mainen *et al.*, 1999; Raghavachari & Lisman 2004; McAllister & Stevens 2000; Nimchinsky *et al.*, 2004; Conti & Lisman 2003).

Moreover, several lines of evidence suggest the involvement of a single functional release site at these connections for the first postnatal week, and the development of an increased number of release sites for each axon in the following weeks (Hsia *et al.*, 1998; Groc *et al.*, 2002). Interestingly, new studies using optical and electrophysiological methods have recently reported proofs of multivesicular release at CA1-CA3 synapses at late developmental stages (Oertner *et al.*, 2002; Conti & Lisman, 2003; Christie & Jahr, 2006), even though no evidence of multivesicular release has been reported at this synapse during the first week of development.

SECTION II

1. **Interneurons of the hippocampus: overview**

Since the early studies of Ramón y Cajal (1911) and Lorente de Nó (1934) describing the different neuronal varieties that make up the circuitry of the hippocampal cortex, it has been clear that a high level of heterogeneity is present in the morphology and connectivity of local circuit neurons, as opposed to principal neurons, which are much more uniform in their appearance.

The term interneuron was originally used to describe cells at the interface between input and output neurons in invertebrates. However, following the development of the concept of synaptic inhibition (Eccles, 1964), the word ‘interneuron’ progressively conveyed the unifying principle that inhibitory cells with short axons play an essential role in the regulation of local circuit excitability, in contrast to (excitatory) principal cells with long axons that project information to distant brain regions. Nevertheless, the continuous emergence of novel functional, biochemical and anatomical data has clearly shown that the concept of ‘interneuron’ is an oversimplification that needs to be readjusted to accommodate cellular types that would not strictly fit the definition. The debates over nomenclature have surfaced in more recent years, particularly when neurons with local axons were shown to establish asymmetrical (presumably excitatory) synapses; confusion also existed concerning what to call “interneurons” with axon collaterals that project to distant brain areas. These cases clearly indicated that the correspondence among Golgi’s short axon cells, the non pyramidal cells of Ramón y Cajal and Lorente de Nó, and the inhibitory interneurons described by Eccles and others was not at all straightforward. Therefore, it is not surprising that interneurons have been collectively referred to as ‘non-principal cells’ just because of the lack of a better unifying criterion. Albeit extremely vague, the term ‘non-principal neuron’ has the advantage of retaining the complexity of the real scenario and highlighting the difficulty in finding a positive common denominator that can encompass such a variety of neuronal types.

For the hippocampal formation, the term ‘non-principal cell’ was sufficiently simple and correct to designate neurons mostly involved in local synaptic circuits, but some of them, in addition to their local collaterals, may have an extra hippocampal or commissural

projection. On the other hand, neurons with well-established local excitatory output (e.g., mossy cells) are not considered interneurons, even if their axon remains restricted to the hippocampal formation. Given that most, if not all, non-principal cells use GABA as a transmitter (Freund & Buzsáki, 1996), the definition “GABAergic non-principal cells” appears to be the most adequate for hippocampal interneurons.

In the past few decades, the quest for a unifying criterion has radically turned into a more specific search for extended classification schemes, with the ideal goal of restraining the wide heterogeneity of interneurons to manageable subgroups. According to most authors

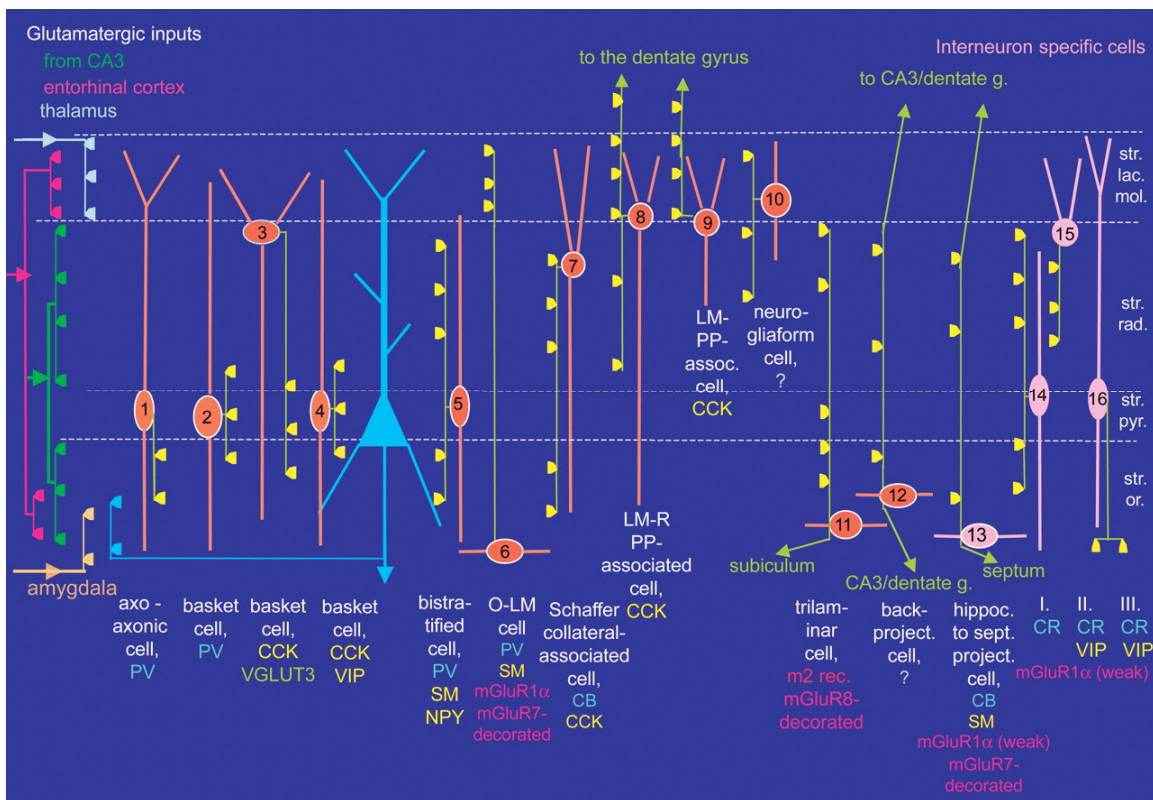


Figure 3. Interneurons in the CA1 area of the hippocampus. Somata and dendrites of interneurons innervating pyramidal cells are shown in orange, those innervating other interneurons are shown in pink. Axons are green and the main termination zone of GABAergic synapses are shown in yellow. Molecular cell markers in combination with the axonal patterns help the recognition and characterisation of each class. Further data may lead to lumping of some classes and to the identification of additional cell types. CB, calbindin; CR, calretinin; LM-PP, lacunosum-moleculare–perforant path; LM-R-PP, lacunosum-moleculare–radiatum–perforant path; m2, muscarinic receptor type 2; NPY, neuropeptide tyrosine; PV, parvalbumin; SM, somatostatin; VGLUT3, vesicular glutamate transporter 3. (From Somogyi & Klausberger, 2005)

(see for example McBain & Fisahn, 2001), to understand the role of well-defined populations of interneurons in a particular brain function, one must first understand the nature of the afferent synaptic drive (both excitatory and inhibitory). In addition, one must identify the precise roles of intrinsic voltage-gated conductances, the types and roles of interneuronal signalling, and the anatomical identity of the cell types embedded in the network of interest. Once equipped with this information, models and simulations based on the exact properties and function of identified synapses and cells in a well-characterized computational network can be constructed. This would allow asking precise questions about the roles of specific inhibitory interneurons in generating or modulating particular brain functions. However, a basic obstacle to performing such analysis, and to explaining why cortical neurons produce action potentials in a particular pattern, is the lack of knowledge of the identity and number of input neurons in the required detail. In most cortical areas many populations of input axons and several distinct populations of recipient neurons are mixed in space, making synaptic connections difficult to predict. As an example, the cortical area with the least heterogeneous neuronal population and the smallest number of extrinsic inputs is probably the hippocampal CA1 area, one reason for its popularity for studying the cortical network. The alignment of the somata and dendrites of pyramidal cells into defined layers and the laminar segregation of much of the extrinsic and intrinsic inputs provide the best chance for defining the synaptic relationships of distinct cell types and the basic cortical circuit. Nevertheless, even in this limited region it is not simple to unveil the complete organization of the inhibitory system (see Figure 3).

It is therefore convenient to undergo a detailed description of the approaches that have been most widely used in the quest for a precise classification of the hippocampal interneurons.

1.1 Towards a classification of the interneurons

One important problem that has always afflicted studies of interneuron function has been the inability to classify interneurons into neat sub-populations, identified for example with functional or anatomical tools. In contrast to the more homogeneous principal cell population, interneurons are exceptionally diverse in their morphological appearance and

functional properties. To date, there is no universally accepted taxonomy of cortical and, in particular, hippocampal interneurons. Classification schemes vary from many defined classes (Freund & Buzsáki, 1996; McBain & Fisahn, 2001; Maccaferri & Lacaille, 2003; Somogyi & Klausberger, 2005) to views that regard interneurons as a single group with virtually unlimited heterogeneity of its members (Mott *et al.*, 1997; Parra *et al.*, 1998).

In general, there is no agreement on the number and identity of neuronal species in the cerebral cortex. This is partly due to the lack of agreement on criteria of what is necessary to define a cell type, and consequently different authors use partial criteria or sets of non-overlapping data for studying the same or a mixture of several neuronal populations. The lack of adequate definition of cell types mainly results from the small number of cells and cortical areas studied in a comprehensive manner, despite the availability of long established methods of proven value. In other words, relative to the challenge of defining the likely number of cell types that occupy a distinct position in the spatio-temporal structure of the cortex, little effort has been devoted to defining them in a rigorous manner. In addition, some statistical variability is expected within a single population of cells in all measures, which may have profound biological significance (Aradi *et al.* 2002; Foldy *et al.* 2004), but at the same time may make the recognition of individual cells more difficult.

In the following sections, an overview will be provided of a number of different features which make the interneuronal family such a multifarious ensemble of cells (see Maccaferri & Lacaille, 2003). According to many authors, based on the whole range of measured parameters each cell would eventually fall into a tight cluster, the *cell type*, in this multidimensional space. Of course, in most cases only some of the measures will be available in a given experiment, and one of the important current tasks is to establish which partial measures are sufficient for the correct recognition of a class of cell, in one cortical area, across areas and across different species. As stated above, initial progress towards this goal is expected from simple cortical areas such as the hippocampal CA1 region (Somogyi & Klausberger, 2005; Figure 3).

1.1.1 Morphological classification

The hypothesis that neurones with different shapes have distinct roles in the cortex was implicit in the earliest studies of Ramón y Cajal and was later elaborated by many, most elegantly by Janos Szentagothai (1975). A further useful predictor for distinct roles was found in the differential and highly selective location of output synapses on target neurones (Ramón y Cajal, 1893; Szentagothai, 1975). The morphological appearance of interneurons is now regarded as a source of important information for their specific role in neuronal circuits. Indeed, their anatomy alone can provide intuitive insights into cell-type-specific contributions in an active network, by relating the somatodendritic location to the layer specificity of synaptic input and the axonal projections to the postsynaptic target domain.

The earliest studies, based on Golgi impregnations (Ramón y Cajal, 1893; Lorente de Nó, 1934), distinguished ~20 different types of interneurons in the hippocampus. Specific types of cell were assigned a simple descriptive term according to a striking feature of their axonal or dendritic processes (e.g. basket cell, horizontal cell and stellate cell). A significant improvement was the development of labelling techniques that allowed examination of the entire dendritic and axonal processes of single cells (Buhl *et al.*, 1994). To match the large number of interneuron types, an equally rich terminology was adopted. Specific cellular types were defined by a combination of classical terms (e.g. basket cells) and new descriptive terms that emphasized different aspects of interneuron anatomy (Gulyas *et al.*, 1993). For example, some terms highlighted the postsynaptic target domain (e.g. ‘axo–axonic cells’, which innervate the axon initial segment of the postsynaptic cell; Buhl *et al.*, 1994); others referred to the two specific layers containing the soma and the axonal processes (e.g. oriens–lacunosum moleculare, ‘O–LM cells’; Freund & Buzsáki, 1996; pyramidale–lacunosum moleculare, ‘P–LM cells’; Oliva *et al.*, 2000; oriens–oriens and radiatum, ‘O–bistratified cells’; Maccaferri *et al.*, 2000). In the case of long-projection interneurons, the origin and target brain regions were embedded in the terminology (e.g. hippocampo–septal neurons). Different systems emphasized the main axis of orientation of the interneuron dendritic tree (e.g. stellate cells, and vertical and horizontal cells located in stratum oriens) or, finally, the specific afferents onto pyramidal cells that overlap with the interneuron projections (e.g. Schaffer-collateral associated interneurons).

However, given the lack of a universally agreed anatomical nomenclature, different investigators have described the same type of interneuron using different descriptive terminology (e.g. horizontal cells in McBain *et al.*, 1994, and O-LM cells in Maccaferri *et al.*, 2000; vertical cells in McBain *et al.*, 1994, and basket or bistratified cells in Buhl *et al.*, 1994), leading to a strong need for a universally recognized interneuron vocabulary. Despite the usefulness and potential descriptive power of accurate morphological characterization, the role of an interneuron in an active brain network is ultimately and crucially shaped by its functional properties which, therefore, need to be included in its definition.

1.1.2 Neurochemical classification

The morphology of an interneuron does not define it; within a given morphological type, interneurons can show widely varying electrical or molecular properties. For example, the development of immunohistochemical tools has uncovered a tremendous number of neurochemical markers for interneurons, and although no single neuropeptide defines a specific interneuron type, some interneuron types tend to express specific combinations of neuropeptides.

First, interneurons were found to contain GABA (Storm-Mathisen *et al.*, 1983), as well as the GABA-synthesizing enzymes GAD65 and GAD67 (Ribak, 1978), providing evidence that local circuit cells in the hippocampus were inhibitory (Freund & Buzsáki, 1996). But, in addition, various populations of interneurons were found to contain different peptides (e.g. somatostatin, cholecystokinin (CCK) and substance P) or Ca²⁺-binding proteins (e.g. calbindin, parvalbumin and calretinin) (see for example Somogyi *et al.*, 1984; for a review see Freund & Buzsáki, 1996). This has resulted in a neurochemical classification that is based on the cell-specific presence of these markers, which are potentially expected to be functionally discriminating (Freund & Buzsáki, 1996). For example, the specific expression of parvalbumin, calbindin and calretinin appears to identify groups of interneurons with different geometry of dendritic architecture, postsynaptic target selection and synaptic input density (Gulyas *et al.*, 1999). However, different types of morphologically defined interneurons could co-exist and overlap in a single neurochemically identified subgroup. For example, somatostatin immunoreactivity has

been detected in O–LM, O–bistratified, P–LM and radiatum–lacunosum moleculare (R–LM) interneurons of the CA1 hippocampal subfield (Oliva *et al.*, 2000; Maccaferri *et al.*, 2000; Katona, 1999; Losonczy *et al.*, 2002). Similarly, parvalbumin is expressed in all cellular compartments of basket and axo–axonic cells (Kosaka *et al.*, 1987; Klausberger *et al.*, 2003). In addition, parvalbumin immunoreactivity has been shown in O–LM cells, although at lower levels and not in the synaptic terminals (Maccaferri *et al.*, 2000; Losonczy *et al.*, 2002).

Moreover, neurochemical markers can be differentially expressed in morphologically similar interneurons with different functional properties (e.g. parvalbumin- and CCK-expressing basket cells; Freund, 2003). Therefore, a combination of the two approaches, neurochemical and anatomical, might be required to distinguish selectively interneurons performing specific tasks in a circuit. Recent work *in vivo* using a combination of single-cell anatomy and neurochemical characterization has shown that three types of hippocampal interneurons, identified as parvalbumin-positive basket cells, axo–axonic cells and somatostatin-positive O–LM cells, display differences in firing pattern during various population discharge patterns (theta oscillations and sharp waves; Klausberger *et al.*, 2003). Although information is missing for additional interneuronal types, a strong degree of consistency was found within each class of cells, suggesting that these specific interneurons subtypes are selectively recruited and carry out distinct types of operation during rhythmic brain activity.

1.1.3 Functional classification

Characterizations based on function have proved to be even more problematic. Classical subdivisions were based solely on action potential firing patterns, with different distinctions due to different investigators (accommodating or non-accommodating, bursting, fast-spiking cells and regular-spiking cells; see Lacaille *et al.*, 1987; Traub *et al.*, 1987; Kawaguchi & Hama, 1988). Even more recently, interneurons have been divided according to their steady-state or initial responses to stimuli, as well as to the spontaneous firing pattern, obtaining for example a distinction between cells firing regularly, irregularly or in clusters (Parra *et al.*, 1998). These response types are useful markers, regardless of whether they define discrete classes (as opposed to a continuum).

However, the generation of action potentials results from the combined activity of numerous voltage-gated conductances overlapping in time, all of which have unique expression patterns throughout interneuron subpopulations and impart subtle characteristics to the action potential waveform. So, whereas this classification has been historically useful, it has only limited value given the ever-expanding repertoire of voltage-gated channels identified on inhibitory neurons.

Finally, recent studies on the properties of synapses have been made by identified afferent projections on specific interneuron subpopulations. In fact, classifications based on the nature of excitatory synaptic transmission have become increasingly common. In hippocampal circuits, repetitive activation of afferents either progressively increases or decreases the amplitudes of excitatory synaptic events. The list of synapses that show facilitation or depression has become increasingly extensive, primarily as a result of studies involving connected pairs of neurons. The usefulness of such a classification scheme for hippocampal interneurons can be questioned since a single axon may transmit information in a target-specific manner (Maccaferri *et al.*, 1998; Scanziani *et al.*, 1998).

2. Functional role of interneurons

Many fundamental principles of interneuron function have been originally defined using the hippocampus, specifically the dentate gyrus (Freund & Buzsáki, 1996). The local-circuit, GABA-releasing inhibitory interneurons in the hippocampus, as in the rest of the cortex, have traditionally been considered as the regulators of principal neuron excitatory activity. Recent evidence indicates that, in addition to that role, their network connectivity and the properties of their intrinsic voltage-gated currents are finely tuned to permit inhibitory interneurons to generate and control the rhythmic output of large populations of both principal cells and other populations of inhibitory interneurons, indicating a much more complex role for these cells than just providers of inhibition. For instance, GABAergic interneurons innervating the perisomatic region of pyramidal cells are now thought to control population discharge patterns, and thereby cognitive operations, in the whole cerebral cortex (Freund, 2003).

In particular it has been noted that, in contrast with the rather uniform population of principal cells in any of the hippocampal subfields, the afferent and efferent connectivity

of interneurons shows great variation (Ramón y Cajal, 1893, 1911; Lorente de Nó, 1934), thereby enabling them to carry out multiple tasks.

Within the hippocampal circuitry, interneurons receive afferent excitatory input from several intrinsic and extrinsic sources (Lacaille *et al.*, 1987; Kawaguchi & Hama, 1988; Freund & Buzsáki, 1996; Oliva *et al.*, 2000), and excitatory inputs have been shown to undergo various types of activity-dependent modulation (see Losonczy *et al.*, 2002, and references therein). For example, in the above mentioned work, Gulyas *et al.* (1999) also examined how the pattern of excitatory innervation varied among three different cell types containing parvalbumin, calretinin and calbindin. Whereas both parvalbumin and calretinin interneurons received synapses within all layers of the hippocampus, calbindin cells received input largely from Schaffer collateral afferents in stratum radiatum. The high input specificity of calbindin cells indicates that they may be activated primarily in a feed-forward manner. By contrast, parvalbumin and calretinin interneurons are activated both in a feed-forward manner by Schaffer collaterals and by entorhinal fibres and thalamic afferents from the nucleus reunions, as well as in a feed-back manner by local CA1 recurrent collaterals.

In the following paragraphs, the efferent connections of hippocampal interneurons will be examined, by presenting the different kinds of interneuronal activity. Both chemical and electrical synapses will be introduced since interneurons communicate with target cells and among them *via* these two types of synaptic connections.

2.1 Chemical synaptic activity

The dendrites, cell bodies, and the axon initial segment of every principal cell in cortical structures are innervated by inhibitory interneurons. As stated above, the terminals of interneurons release the inhibitory transmitter GABA and may also release peptides that colocalize with GABA in many types of interneurons. The complex issue of GABA-mediated transmission has been reviewed extensively (see for example Mody *et al.*, 1994).

Peptides themselves can modulate GABAergic activity, even though their physiologic role in the operations of the hippocampal formation has remained elusive. One major difficulty is that all experiments to date test the pharmacological effects of peptides on

neuronal excitability, passive membrane properties, and/or transmitter release by pharmacological means rather than by physiological activation of interneurons. Furthermore, bath application or even pressure ejection of the peptide may act on multiple sites, some of which may exert an opposite effect on the measured experimental variable. Another typical interpretational problem is a mismatch between the axon terminals of the peptide-containing interneurons and the intrahippocampal distribution of receptors for the same type of peptide. However, it is known that several peptides exert a relatively selective action on the release of GABA from the presynaptic terminals of interneurons (Freund & Buzsáki, 1996). Assuming that peptides are not released without GABA, the peptide will most effectively regulate the release of GABA from the terminals of its parental interneuron on the basis of spatial proximity. Such an effect may be viewed as a variant of autoregulation (see paragraph 2.1.1). Because some interneurons with dendritic targets may not possess presynaptic GABA_B receptors (Lambert and Wilson, 1993), an interesting possibility is that autoregulation of GABA release in those neurons may be carried out by a coreleased peptide. It is worth noticing that the axon collaterals of most peptide containing interneurons target the dendritic domains of principal cells. It is also possible that high-frequency firing or certain discharge patterns are a prerequisite for peptide release; therefore, presynaptic regulation of GABA release may be discharge pattern dependent.

2.1.1 Postsynaptic actions on the principal cells

In general, the stimulation of afferent fibres elicits biphasic IPSPs in principal cells. The early phase of this event is due to the activation of GABA_A receptors while the late phase is due to the activation of GABA_B receptors. GABA, released from presynaptic nerve terminals binds to synaptic GABA_A receptors facing the presynaptic release site and induces an early inhibitory postsynaptic potential. The membrane hyperpolarisation and the associated increase in membrane conductance lower the threshold for action potential generation leading to inhibition of cell firing. Activation of GABA_A receptors also shunts excitatory synaptic currents. The late phase of the IPSP is mediated by K⁺ ions flowing through channels linked by G-proteins to GABA_B receptors. Initially, questions were posed regarding the modes of interneuron-mediated inhibition of principal cells and

among interneurons themselves. For example, it is unclear if separate groups of inhibitory cells are responsible for activating postsynaptic GABA_A and GABA_B receptors; however, at least in the hippocampus, spontaneously occurring GABA_B-mediated synaptic events have been never found.

GABA receptors are located at pre- and postsynaptic sites. Chloride-dependent GABA_A-receptor-mediated synaptic inhibition is similar in these two locations, while metabotropic GABA_B receptors cause presynaptic inhibition by suppressing calcium influx and reducing transmitter release. In this way, GABA can be important also in presynaptic control and modulations of transmitter release (Owens & Kriegstein, 2002). It is interesting to notice that in the hippocampus presynaptic GABA_B receptor function is already present perinatally, but postsynaptic receptor function is delayed until about one week later (Gaiarsa *et al.*, 1995; McLean *et al.*, 1996).

An early hypothesis suggested that dendritic inhibition is mediated by GABA_B receptors, probably activated by GABA released by a separate group of interneurons (Alger & Nicoll, 1982; Segal, 1990). In support of this hypothesis, IPSPs with similar kinetics to the GABA_B-receptor-mediated responses are produced by activation of interneurons in stratum lacunosum-moleculare (Lacaille & Schwartzkroin, 1988). However, the slow rise time of somatic IPSPs in postsynaptic pyramidal cells may simply reflect electrotonic filtering by the dendrites (Soltesz & Mody, 1994). Furthermore, other experiments that have involved pharmacological manipulations show that dendritic inhibition brought about by intracellular activation of the presynaptic interneuron is mediated by GABA_A receptors (Buhl *et al.*, 1994, 1995).

Overall, different GABAergic interneurons can affect hippocampal principal cells with inhibition, shunting, and even excitation in the presence of particular conditions for the reversal potential of chloride (Freund & Buzsáki, 1996). It is clear that fast ‘phasic’ synapses synchronize the activity of principal cell ensembles and contribute to the generation of high-frequency oscillatory activity in interneuron networks (Cobb *et al.*, 1995; Buzsáki & Draguhn, 2004), whereas slow ‘tonic’ inhibition may set the gain or offset of the input-output relations of postsynaptic target cells (Holt & Koch, 1997; Mitchell & Silver, 2003).

More recently, the mapping of axonal arbours to specific domains across the dendritic trees of their targets has provided important clues to the specific functional roles carried out by various interneuron subtypes (Buhl *et al.*, 1994; Halasy *et al.*, 1996; Miles *et al.*, 1996; Maccaferri *et al.*, 2000; Klausberger *et al.*, 2002). For example, interneurons that innervate pyramidal cell somata regulate the local generation of Na⁺-dependent action potentials (Miles *et al.*, 1996). By contrast, inhibition arriving at dendritic locations influences dendritic voltage-gated currents, shunts excitatory inputs at sites distal to the soma (Callaway & Ross, 1995; Hoffman *et al.*, 1997), and regulates dendritic Ca²⁺-dependent action potentials (Miles *et al.*, 1996). In brief, somatic GABA synapses control action potential discharge, whereas dendritic GABA synapses control local electrogenesis and synaptic plasticity. Results unveiling distinct functional roles have also been obtained by comparing interneuron subtypes distinguished from a molecular point of view (Hefft & Jonas, 2005). Of course, this division of labour is excessively rigid and exceptions to this classification probably exist (Maccaferri *et al.*, 2000; McBain, 2000).

2.1.2 Synaptic plasticity

It is worth mentioning that interneurons undergo activity-dependent forms of synaptic plasticity different from those commonly found in principal cells (Maccaferri & McBain, 1996; McBain *et al.*, 1999). Calcium entry *via* Ca²⁺-permeable AMPA receptors, present on various hippocampal interneurons is crucial for the induction of long-term potentiation in these cell types. Ca²⁺-permeable AMPA receptor channels are tonically blocked (from inside) by endogenous polyamines and the relief from this blockade is both use- and voltage-dependent. This mechanism of activation endows Ca²⁺-permeable AMPA receptor synapses with a new postsynaptic mechanism for short-term enhancement of synaptic gain. Short-term facilitation is greatest at depolarized potentials and acts to boost sub threshold EPSPs to trigger action potentials despite the reduced driving force. A novel form of long-term plasticity also exists at interneuron Ca²⁺-permeable AMPA synapses. High-frequency stimulation of associational inputs onto CA3 stratum radiatum interneurons or of mossy fibre inputs onto stratum lucidum interneurons induces a form of NMDA-independent long-term depression termed interneuron LTD (iLTD; McMahon & Kauer, 1997). Interestingly, identical patterns of stimuli delivered to mossy fibre axons

resulted in opposing long-term changes in synaptic efficacy at principal synapses compared with interneuron synapses (long-term potentiation versus iLTD, respectively). This differential plasticity is likely to shift the excitation–inhibition balance in favour of excitation at mossy fibre–CA3 connections (McMahon & Kauer, 1997; Laezza *et al.*, 1999; Toth *et al.*, 2000).

2.2 Networks of interneurons

One of the main challenges of neuroscience is to understand how complex behaviours of the brain emerge from its cellular constituents. Interneurons differ from each other not only in intrinsic biophysical properties, morphological and molecular biological features, but also in their connectivity. Complex wiring affects the contribution of interneurons to network performance and many authors suggest that connectivity is a useful approach for examining how complex functions (e.g. oscillations) emerge from elementary features (e.g. inhibitory connections; Buzsáki *et al.*, 2004).

2.2.1 Gap junctions between interneurons

Gap junctions are clusters of channels that connect the interiors of adjoining cells and mediate electrical coupling and transfer of small molecules. In the initial electron microscopic description, the extracellular space between the adjoining cells appeared reduced to a narrow gap, and the channels crossing the gap were not well resolved (Revel and Karnovsky, 1967). Thus, the term gap junction derives from a structural characteristic not obviously related to function. The gap distinguishes these junctions from “tight junctions” or “zonulae occludentes”, where the intercellular space between adjoining cells appears completely occluded (but see Tang and Goodenough, 2003). The large internal diameter (1.2–2 nm) of many gap junction channels allows not only flow of electric current, largely carried by K⁺ ions, but also exchange of small metabolites and intracellular signalling molecules. In general, gap junctions may subserve metabolic coupling and chemical communication as well as electrical one, and they are thought to play an important role in brain development, morphogenesis, and pattern formation (Bennett *et al.*, 1991; Bruzzone *et al.*, 1996; Dermietzel *et al.*, 1989; Goodenough *et al.*, 1996).

The structural proteins comprising gap junctional channels, called connexins (Cx), form a multigene family whose members are distinguished according to their predicted molecular mass in kDa (e.g. Cx32, Cx43; Willecke *et al.*, 2002). The family of connexin genes comprises 21 members in the human and 20 in the mouse genome, 19 of which can be considered as orthologue pairs on the basis of their sequence. Intercellular channels span two plasma membranes and result from the association of two half channels, called connexons, contributed separately by each of the two participating cells. Each connexon, in turn, is a hexameric assembly of connexin subunits. Intercellular channels are defined as homotypic, when the two connexons have the same molecular composition, or heterotypic, when the connexons differ (Hormuzdi *et al.*, 2004). Connexins have evolved a code of compatibility that permits only selective interactions between connexons, so that the establishment of electrical coupling is also dependent on the pattern of connexin expression between neighboring cells (Bruzzone *et al.*, 1996). It is known that mice with targeted deletion of any one of a number of connexins still exhibit relatively normal structure and function, suggesting either redundancy or relative unimportance (Deans *et al.*, 2001; Guldenagel *et al.*, 2001; Buhl *et al.*, 2003).

Evidence that inhibitory interneurons of the hippocampus are interconnected by electrical synapses is persuasive. Dendrodendritic gap junctions between interneurons are frequently seen in areas CA1 and CA3 (Kosaka & Hama, 1985) and in the dentate gyrus (Kosaka, 1983). Several types of gap junction-coupled interneurons have been identified (Katsumaru *et al.*, 1988; Fukuda & Kosaka, 2000), and dye coupling has been observed between inhibitory cells of the hilus (Strata *et al.*, 1997) and of the CA1 region (Michelson & Wong 1994). Paired-interneuron recordings have shown electrical coupling directly, and single-cell RT-PCR has revealed mRNA encoding for connexin 36 (Cx36) (Venance *et al.*, 2000). Furthermore, although electrical coupling between pairs of interneurons was abundant in the CA3 and in the dentate areas of wild-type mice, it was absent in cells of Cx36 knockout mice (Hormuzdi *et al.*, 2001).

The functions of electrical coupling between hippocampal interneurons are not yet well understood. Many studies have focused on the possibility that gap junctions play a role in generating or modulating synchronous oscillations or seizure-like activity. Measurements in Cx36 knockout mice have implicated electrical synapses in the generation of gamma-

frequency rhythms (see paragraph 2.2.3; Figure 4), but not of fast ripples or slower theta rhythms (Hormuzdi *et al.*, 2001; Traub *et al.*, 2002; Buhl *et al.*, 2003); however the role of gap junctions is found to be important also in high-frequency oscillations (Draguhn *et al.*, 1998). It should also be considered that, if single neurons must “choose” between chemically mediated excitation and inhibition, gap junctions permit GABAergic cells to be also excitatory and to synchronize with others more precisely than possible with inhibition alone.

2.2.2 *Inhibition in networks of coupled neurons*

Inhibition is critical in shaping response properties in single cells as well as in assisting cooperativity in large cell populations. Inhibitory interneurons in cortical structures provide stability to the activity of the principal cell populations by feedback and feed-forward inhibition (Freund & Buzsáki, 1996). Groups of interneurons tonically or phasically hyperpolarize and/or increase membrane conductance (“shunting”) in the perisomatic and/or dendritic regions of neurons and thereby decrease the efficacy of excitatory afferents in discharging their principal cell targets. Activation of hippocampal interneurons may be brought about by extra hippocampal inputs, by intra hippocampal inputs afferent to interneurons (both feed-forward), or by principal cells of the same hippocampal region (recurrent or feedback). In the feed-forward regulatory system, afferent volleys directly activate the inhibitory neuron (first event) that in turn reduces the probability of firing of the principal cells (second event). In the feedback system, an excitatory input discharges the principal cells, whose excitatory output is fed back to the inhibitory cell(s) through recurrent axon collaterals (Andersen *et al.*, 1964). The inhibitory interneuron(s) then may discharge and inhibit a group of principal cells, including those that initially activated the interneuron(s). In short, the directions of firing rate changes of local principal cells and inhibitory interneurons are the same in the feedback systems but opposite in the feed-forward scheme (Buzsáki, 1984).

Interestingly it was seen that, although inhibition and disinaptic disinhibition are useful concepts in the description of physiological effects of interneurons, application of usual Boolean logic often fails to provide correct predictions in systems where interneurons are interconnected with each other (Freund & Buzsáki, 1996). It is clear from both

experimental and simulation studies that in networks of inhibitory cells, independent of whether members are connected unidirectionally or mutually, oscillatory activity often emerges (Bragin *et al.*, 1995; Whittington *et al.*, 1995; Traub *et al.*, 1996; Bartos *et al.*, 2002; Sohal & Huguenard, 2005; Vida *et al.*, 2006), and the rules that govern the timing of action potentials and the frequency changes of the participating cells can no longer be inferred from the simple logic of inhibition and disinhibition.

2.2.3 Network activity and oscillations

Interneurons of the hippocampus are able to synchronize principal cells (see Cobb *et al.*, 1995). Moreover, they can phase the output of principal neurons giving rise to oscillatory

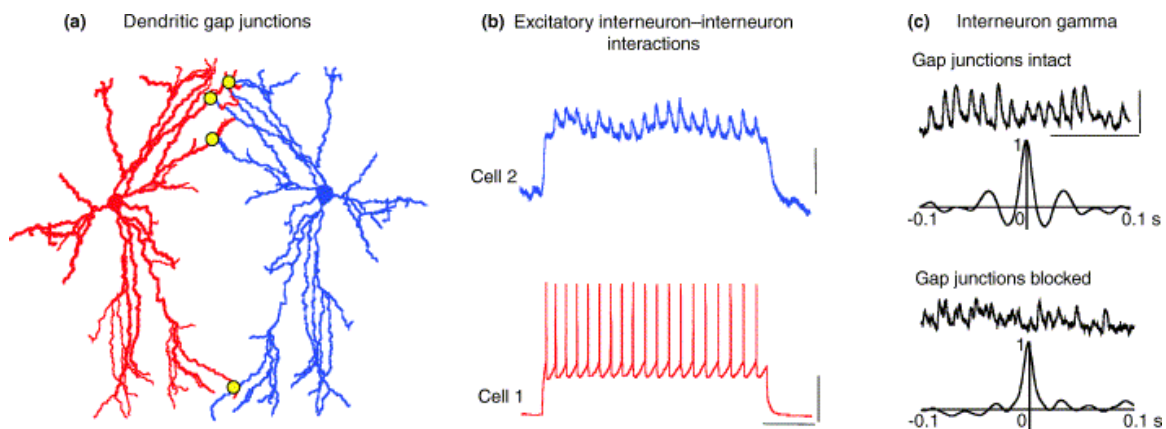


Figure 4. Gap junctions between interneurons stabilize interneuron network gamma oscillations. (a) The putative organization of dendro–dendritic gap junctions between fast-spiking interneurons. The dendritic field of a basket cell is used to show representative gap junctions between distal dendritic compartments (yellow circles). (b) Electrical coupling between interneurons using dendritic gap junctions allows excitatory interneuron interactions, whereby tonic depolarization is shared between cells and a low-pass-filtered correlate of action potentials in an active interneuron can be seen in the coupled interneuron. Gap-junction coupling provides a mechanism by which changes in membrane potential can be passed throughout the interneuron network, thus ‘smoothing’ the postsynaptic effects of any input heterogeneity. Scale bars: 2 mV, 40 mV and 100 ms. (c) Using pyramidal cell recordings to sample the output from interneurons (as inhibitory postsynaptic current (IPSC) trains) during interneuron-network gamma rhythms reveals a strong dependence on gap junction coupling. The upper trace shows a gamma frequency IPSC train in response to glutamate pressure ejection with fast excitatory synaptic transmission blocked. The lower trace shows the response in the same cell with gap junction conductance reduced by 0.2 mM carbenoxolone. Graphs show autocorrelations to illustrate changes in rhythmicity and local temporal coherence. Scale bars, 0.3 nA and 200 ms. (From Whittington & Traub, 2003)

network activity in different frequency bands (Whittington & Traub, 2003; Buzsáki & Draguhn, 2004; Traub *et al.*, 2004). There is in fact compelling evidence that hippocampal interneurons have a pivotal role in driving inhibition-based rhythms, such as gamma (30–80 Hz) and theta (5–12 Hz) frequency network oscillations (Whittington *et al.*, 1995; Fisahn *et al.*, 1998; Chapman & Lacaille, 1999a,b; Hormuzdi *et al.*, 2001; Gillies *et al.*, 2002; Klausberger *et al.*, 2003, 2004; see Figure 4). In vitro models of rhythms of cognitive relevance, such as gamma and theta rhythms, and sharp-wave-associated ripple oscillations (140–200 Hz), demonstrate an absolute requirement for phasic inhibitory synaptic transmission (see Whittington & Traub, 2003). Such rhythms represent different behavioural states and can occur transiently (~1s duration), or persistently (lasting for many hours). In the latter case, stable patterns of interneuron output, and their postsynaptic consequences for pyramidal cell membrane potential occur despite known constraints of synaptic habituation and potentiation. In particular, synchronous gamma-frequency oscillations represent a temporally coherent activity and are thought to be important in cortical information processing (Gray & Singer, 1989; Jones & Barth, 1997; Ritz & Sejnowski, 1997; Fries *et al.*, 2001). One of their putative roles may be the synchronization of groups of spatially segregated cortical neurons at sites that can be many millimetres apart (Gray *et al.*, 1989). Synchronous activity is ideally suited to provide a mechanism for the functional ‘binding’ of sensory features. Gamma frequency oscillations have been observed in a variety of brain structures (Singer & Gray, 1995), amongst them the hippocampus, which has a key role in memory formation (Morris *et al.*, 1982; Zola-Morgan & Squire, 1993), and shows oscillatory activity in the theta/gamma frequency band during specific behavioural states (Buzsáki *et al.*, 1983; Soltesz & Deschenes, 1993; Sik *et al.*, 1995; Singer & Gray, 1995; Penttonen *et al.*, 1998).

Some authors have recently investigated how interneurons can fire phase-locked to oscillations, such as theta or sharp-wave-associated ripple oscillations. During these rhythms, various subfamilies of interneurons are able to fire with fixed frequencies at a characteristic time on the phase of theta or high-frequency waves. The firing patterns of individual cells of the same class are remarkably stereotyped and provide unique signatures for each class (Klausberger *et al.*, 2003, 2004, 2005). Moreover, it is

reasonable to assume that the anatomical heterogeneity of hippocampal interneurons is reflected in their functional diversity (as discussed in paragraph 2.2.1) in particular during different forms of network activity. Thus, many studies have attempted a correlation of structure and function, and in particular, the way in which oscillatory input affects the activity of individual interneurons in the active network. For example, the different passive and active membrane properties of interneuronal subtypes can give them a role in the generation and maintenance of oscillations in different frequency ranges (see Figure 5; Pike *et al.*, 2000; Whittington & Traub, 2003; Schreiber *et al.*, 2004). Moreover, the diverse targeting properties of interneurons or their different neurochemical specification may determine their differential involvement in the generation of various kinds of hippocampal oscillatory network activity, also leading the hippocampal network to

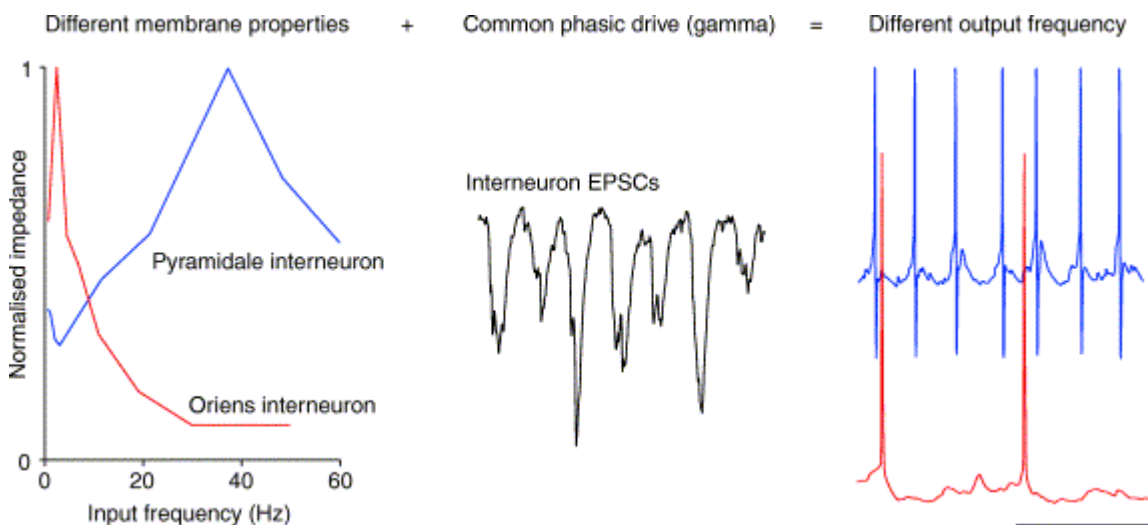


Figure 5. Different intrinsic membrane properties of interneurons generate different outputs from a common excitatory synaptic network drive. Impedance profiles from hippocampal basket cells of *stratum pyramidale* (blue) and *stratum oriens* interneurons (red) reveal strong frequency dependence. Fast-spiking interneurons such as basket cells have peak impedance for inputs at gamma frequencies, whereas slow-spiking oriens interneurons have peak impedance for inputs at theta frequencies. During gamma oscillations in vitro, different interneuron subclasses receive remarkably similar rhythmic excitatory postsynaptic currents (EPSCs). The interaction between the common network input and the specific intrinsic properties of fast-spiking and slow-spiking interneurons leads to a different frequency of interneuron output, closely correlated with the frequency of peak impedance. Thus, a single frequency mode of principal cell output can generate multiple frequencies of feedback inhibitory input. Scale bars, 5 mV and 200 ms. (From Whittington & Traub, 2003)

generate ‘nested’ rhythms concurrently occurring in the theta and gamma frequency bands (Klausberger *et al.*, 2003, 2004, 2005; Gloveli *et al.*, 2005).

In general, various paradigms have been identified which enable to evoke network oscillations in the hippocampus *in vitro*, and their properties have been studied extensively (for a complete review see Traub *et al.*, 2004).

3. Molecular and genetic variety of the interneurons

In the recent years, the development of novel techniques, including single-cell reverse-transcriptase polymerase chain reaction (RT-PCR), *in vivo* labelling and other molecular biological methods, as well as use of transgenic animals, has allowed interneurons to be probed from new and different angles (Meyer *et al.*, 2002; Blatow *et al.*, 2003; for a review see Monyer & Markram, 2004).

For example, the first combined patch-clamp RT-PCR study showed differences in ion channels in pyramidal neurons and interneurons (Martina *et al.* 1998). More interestingly, in the neocortex, it has been recently described how the electrical diversity arises from active properties (ion-channel combinations) and passive properties (the morphology of the neuron). The ion-channel genes that are expressed by an interneuron correlate with its electrophysiological properties, and ion-channel expression seems to fall into three clusters, which map around the three calcium-binding proteins (parvalbumin, calbindin and calretinin) that are expressed in separate populations of interneurons (Markram *et al.*, 2004). On the other hand, knockout mice have helped to understand why the expression of particular proteins in GABAergic interneurons is relevant at the network level (Deans *et al.*, 2001; Hormuzdi *et al.*, 2001), and in general transgenic mice are being widely used for specifically investigating the properties of interneuronal subfamilies (Oliva *et al.*, 2000; Meyer *et al.*, 2002).

3.1 Correlating molecular and functional studies: new ideas for a classification

The interesting question to be answered is if these powerful tools can be used to shed light on the debate whether hippocampal interneurons are subdivided in definite classes, or they constitute a continuum of different neurons. In general, at the anatomical level, cortical interneurons are generally accepted as being in distinct classes, not because of

any objective analyses, but because of more obvious functional specializations indicated by their different domain-targeting tendencies. At the molecular level, the issue is simpler because some markers are expressed only by certain interneuron types. However, it should be stressed that no one marker points unambiguously towards only one anatomical or electrical type of interneuron; the expression pattern of four or five markers might be required for a proper analysis. At the electrical level, the diversity might seem arbitrary, but this is probably due to the lack of defined functions for the different behaviours. The class-versus-continuum issue at all levels will probably only be resolved objectively at the level of gene expression. In the neocortex it has already been shown that the correlation between expression profiles and electrical phenotypes, the constraints in co-expression profiles and the ‘flip’ of entire expression profiles to form opposite electrical phenotypes all indicate that only a few transcription factors, expressed in different combinations, might give rise to a finite number of distinct classes of interneurons (Toledo-Rodriguez *et al.*, 2004, 2005). So, most interneurons probably belong to distinct electrical, morphological and molecular classes. The observed diversity is several orders of magnitude smaller than expected for a continuum of electrical types using more than 100 ion-channel genes, indicating powerful constraints on diversity. Understanding these constraints, also with the aid of molecular and genetic tools, will be crucial for resolving the class-versus-continuum debate for hippocampal interneurons.

AIM OF THE STUDY

In the investigation of the functionality of the nervous system, a precise analysis of how neurons communicate with each other holds a critical importance. Aim of the present study was to go deeper in characterising synaptic transmission in the hippocampus, mainly focusing on quantal transmission at single synapses and on different signalling properties throughout the hippocampal network. In order to take advantage of my theoretical background, I addressed this question in two ways, from both analytic and experimental point of view.

Firstly, I developed an analytic model of chemical transmission at CA3-CA1 synapses, which uses simple hypotheses on quantal release from the presynaptic terminal to provide useful predictions on some quantal parameters, and on the mode of transmitter release. The model was validated with experimental data that we obtained in previous work (not included in this thesis) by recording postsynaptic responses in single CA1 pyramidal cells to minimal stimulation of afferent fibres.

Secondly, I investigated the intrinsic and signalling properties of a subset of hippocampal interneurons, which are EGFP-positive in a particular strand of transgenic mice. Since with minimal stimulation methods it is difficult to make sure that the same single presynaptic axon is activated trial after trial, I decided to perform paired recordings from interconnected cells. To this aim I set up organotypic hippocampal slice cultures. This preparation has the advantage of maintaining morphological and functional features similar to those of native hippocampus even if flattened close to a monolayer. Moreover, the connectivity between neurons is enhanced, making it easier to find interconnected cells in double patch experiments. With this approach, I first characterized the population of EGFP-positive somatostatin-containing interneurons of the *stratum oriens* of CA1 using single whole-cell patch clamp experiments, focusing on active and passive membrane properties and firing patterns of these neurons. Later, I performed double patch experiments to record either the simultaneous activity of couples of EGFP-positive interneurons in the population, or the activity of one interneuron and one principal cell of the CA1. In particular, I analyzed the different types of synaptic signalling, and I also collaborated in developing a simple model of this inhibitory network.

METHODS AND RESULTS

- **Multivesicular release at CA3-CA1 synapses: see enclosed paper**

**Multivesicular release at developing Schaffer collateral-CA1 synapses:
an analytic approach to describe experimental data.**

Journal of Neurophysiology (2006) Jul; 96(1):15-26.

Federico Ricci-Tersenghi, Federico Minneci, Elisabetta Sola, Enrico Cherubini and Laura
Maggi

Multivesicular Release at Developing Schaffer Collateral–CA1 Synapses: An Analytic Approach to Describe Experimental Data

F. Ricci-Tersenghi,¹ F. Minneci,³ E. Sola,³ E. Cherubini,³ and L. Maggi^{2,3}

¹Dipartimento di Fisica and ²Dipartimento di Fisiologia Umana e Farmacologia, University La Sapienza, Rome; and ³Neuroscience Programme, International School for Advanced Studies, Trieste, Italy

Submitted 11 November 2005; accepted in final form 3 April 2006

Ricci-Tersenghi, F., F. Minneci, E. Sola, E. Cherubini, and L. Maggi. Multivesicular release at developing Schaffer collateral–CA1 synapses: an analytic approach to describe experimental data. *J Neurophysiol* 96: 15–26, 2006. First published April 5, 2006; doi:10.1152/jn.01202.2005. We developed and analytically solved a simple and general stochastic model to distinguish the univesicular from the multivesicular mode of glutamate release. The model solution gives analytical mathematical expressions for average values of quantities that can be measured experimentally. Comparison of these quantities with the experimental measures allows one to discriminate the release mode and to determine the most probable values of model parameters. The model has been validated at glutamatergic CA3–CA1 synapses in the hippocampus from newborn (P1–P5 old) rats. Our results strongly support a multivesicular type of release process requiring a variable pool of immediately releasable vesicles. Moreover, computing quantities that are functions of the model parameters, the mean amplitude of the synaptic response to the release of a single vesicle (q) was estimated to be 5–10 pA, in very good agreement with experimental findings. In addition a multivesicular type of release was supported by the following experimental evidences: 1) a high variability of the amplitude of successes, with a coefficient of variation ranging from 0.12 to 0.73; 2) an average potency ratio a_2/a_1 between the second and first response to a pair of stimuli >1 ; and 3) changes in the potency of the synaptic response to the first stimulus when the release probability was modified by increasing or decreasing the extracellular calcium concentration. Our results indicate that at Schaffer collateral–CA1 synapses of the neonatal rat hippocampus a single action potential may induce the release of more than one vesicle from the same release site.

INTRODUCTION

According to the quantal theory, the strength of a synaptic connection is defined as the product of the probability of transmitter release, the number of release sites, and the size of the postsynaptic response to a single transmitter quantum (Katz 1969). These parameters, which are crucial for information processing in the brain, are determined both presynaptically through the amount of neurotransmitter released and postsynaptically through the number and the gating properties of available receptors. Differences between these parameters account for the large variability of synaptic responses that can be observed in central neurons. Such variability represents an intrinsic property of synaptic transmission and can be detected at both excitatory and inhibitory synapses (Forti et al. 1997; Frerking et al. 1995; Kirischuk et al. 1999; Liu and Tsien 1995).

Address for reprint requests and other correspondence: L. Maggi, Dipartimento di Fisiologia Umana e Farmacologia, University “La Sapienza,” Piazzale A. Moro 5, 00185 Rome, Italy (E-mail: maggilaura@gmail.com).

On the postsynaptic site the degree of receptor saturation set the conditions by which the synapses can “sense” the amount of neurotransmitter released. Different techniques have revealed that most synapses work in nonsaturating conditions, although the degree of receptor saturation varies enormously between different synapses (Auger and Marty 1997; Barberis et al. 2004; Frerking et al. 1995; Liu et al. 1999; Mainen et al. 1999; McAllister and Stevens 2000; Umekiya et al. 1999).

On the presynaptic site the number of functional active zones per connection and the release probability per active zone are important issues in determining the amount of neurotransmitter released. The number of primed vesicles released at a single release site per action potential may vary from one (univesicular release) to several (multivesicular release) (Silver 2003).

In the case of univesicular release the released vesicle would inhibit within microseconds the release of other docked vesicles (Redman 1990; Regehr and Stevens 2001). This type of synapse has been observed at excitatory connections between CA3 pyramidal cells and interneurons in the hippocampus (Arancio et al. 1994; Gulyas et al. 1993) and between mossy fibers and granule cells in the cerebellum (Silver et al. 1996). These connections are characterized by a low coefficient of variation ($CV = SD/mean$) of the amplitude of synaptic currents whose distribution can be fitted by a Gaussian function.

In the case of multivesicular release, multiple vesicles are released at the same active zone by one action potential. In support of this model is the observation that at least at some glutamatergic synapses the concentration of glutamate in the synaptic cleft changes in relation with the probability of release at a single release site (Oertner et al. 2002; Wadiche and Jahr 2001). In comparison with the univesicular release, the multivesicular one is associated with a larger CV of the amplitude of responses whose distribution cannot be fitted by a Gaussian function. This type of connection has been well characterized at interneuron–interneuron synapses, climbing fiber–Purkinje cell and mossy fiber–granule cell synapses in the cerebellum (Auger et al. 1998; Wall and Usowicz 1998), and in the hippocampus (Conti and Lisman 2003; Oertner et al. 2002; Tong and Jahr 1994).

At hippocampal Schaffer collateral–CA1 connections several lines of evidence suggest the involvement of a single functional release site (Hanse and Gustafsson 2002; Hsia et al. 1998). However, the morphological characterization of these synapses, i.e., an active zone with several docked vesicles

The costs of publication of this article were defrayed in part by the payment of page charges. The article must therefore be hereby marked “advertisement” in accordance with 18 U.S.C. Section 1734 solely to indicate this fact.

apposed to the postsynaptic density (Harris and Sultan 1995; Schikorski and Stevens 1997; Shepherd and Harris 1998), has provided the anatomical basis for multivesicular release. Indeed, as expected for simultaneous release of multiquanta, minimal stimulation of afferent inputs has revealed synaptic currents exhibiting a high CV value and a skewed amplitude distribution histogram (Conti and Lisman 2003; Hessler et al. 1993; Hsia et al. 1998; Huang and Stevens 1997; Maggi et al. 2004; Oertner et al. 2002).

Here we have developed and solved a simple and general analytic model to distinguish univesicular from multivesicular mode of transmitter release. The model has been validated experimentally at Schaffer collateral–CA1 synapses in neonatal animals using paired pulses and minimal stimulation of afferent inputs. From this it appears that multivesicular release is the mode by which most synapses operate at developmental CA3–CA1 connections.

METHODS

Slice preparation

Transverse hippocampal slices (300–400 μm thick) from P1–P5 Wistar rats were prepared as previously described (Maggi et al. 2004). The procedure was in accordance with the regulations of the Italian Animal Welfare Act and was approved by the local authority veterinary service. Briefly, animals were decapitated after being anesthetized with an intraperitoneal injection of urethane (2 g/kg). The brain was quickly removed from the skull and placed in ice-cold artificial cerebrospinal fluid (ACSF) containing (in mM): NaCl 130, KCl 3.5, NaH_2PO_4 1.2, NaHCO_3 25, MgCl_2 1.3, CaCl_2 2, glucose 11, saturated

with 95% O_2 –5% CO_2 (pH 7.3–7.4). After 1 h, an individual slice was transferred to the recording chamber where it was continuously superfused with oxygenated ACSF at a rate of 2–3 ml/min at 30°C.

Electrophysiological recordings

α -Amino-3-hydroxy-5-methyl-4-isoxazolepropionic acid (AMPA)–mediated excitatory postsynaptic currents (EPSCs) evoked by minimal stimulation of the Schaffer collateral were recorded at -60 mV from individual CA1 pyramidal neurons using the patch-clamp technique in whole cell configuration. Patch pipettes were filled with a solution containing (in mM): Cs-methanesulfonate 125, CsCl 10, HEPES 10, EGTA 0.6–2, MgATP 2, NaGTP 0.3 (resistance 5 M Ω). Bicuculline methiodide (5 μM) and tetrodotoxin (TTX, 10 nM) were added to the bath solution to block γ -aminobutyric acid type A (GABA_A) receptors and reduce polysynaptic activity, respectively. The Schaffer collateral was stimulated with bipolar twisted NiCr-insulated electrodes placed in stratum radiatum. Paired (50-ms, 100- μs duration) stimuli (at 0.25 Hz; Fig. 1) were adjusted to evoke minimal EPSCs, which were intermingled with transmission failures. In all analyzed cells, the stimulus intensity was in the range of 3.5–10 V, corresponding to 2.3–6.7 μA . According to the technique described by Jonas et al. (1993) and Allen and Stevens (1994) the stimulation intensity was decreased until only a single axon was activated. This was achieved when the mean amplitude of the postsynaptic currents and failure probability remained constant over a range of stimulus intensities near threshold for detecting a response. The example of Fig. 1C shows average traces of synaptic currents recorded from a CA1 pyramidal cell in response to different stimulation intensities. An abrupt increase in the mean peak amplitude of synaptic currents was observed when the stimulus intensity was changed from 4.5 to 5 V. The amplitude of responses remained constant for stimu-

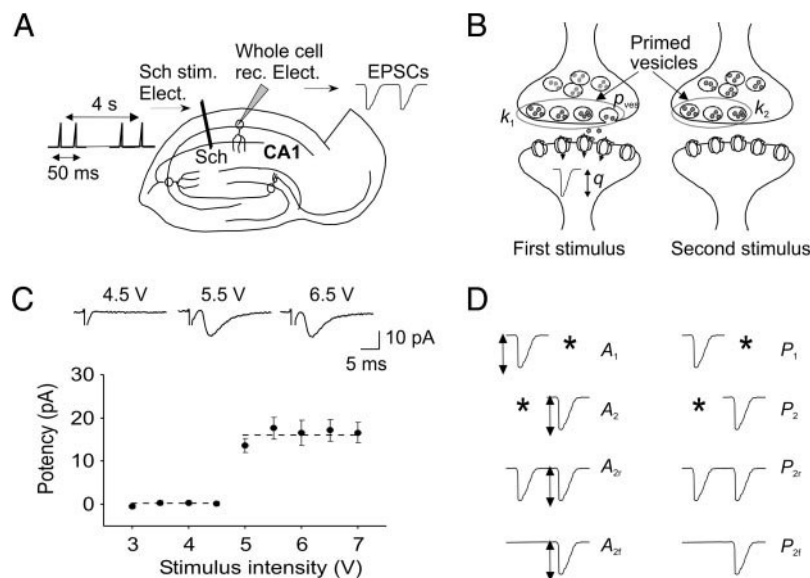


FIG. 1. Methods. A: schematic diagram of a hippocampal slice showing the classical 3-synaptic pathway, the stimulating, and the recording electrodes. Schaffer collateral (Sch) was activated at 0.25 Hz with a pair of stimuli delivered at 50-ms interval (left). Schaffer collateral stimulation evoked in CA1 pyramidal neurons (held at -60 mV) α -Amino-3-hydroxy-5-methyl-4-isoxazolepropionic acid (AMPA)–mediated excitatory postsynaptic currents (EPSCs, right). B: schematic representation of a glutamatergic synapse depicted before the first (left) and the second (right) paired stimuli. Each presynaptic vesicle (circle) containing the neurotransmitter (in gray) has a characteristic probability of release p_{ves} , k is the variable representing the number of primed vesicles in the ready releasable pool and q (mean quantal size) is the mean amplitude of the synaptic current obtained by activation of postsynaptic receptors by glutamate released from a single vesicle. C, top: EPSCs evoked by minimal stimulation of Schaffer collateral. Different stimulus intensities were used to evoke synaptic currents in a CA1 pyramidal cell at P3. Each trace is the average of 15–20 responses. Holding potential was -60 mV. Bottom: plot of the peak amplitude of synaptic currents against different stimulus intensities. Note the all-or-none appearance of synaptic currents with increasing stimulus intensities. Error bars indicate SE. Dashed lines connect the mean values of individual points within the same groups. D, left: A_1 and A_2 are the mean amplitude currents elicited by 2 pulses at 50-ms interval; A_{2r} and A_{2f} represent the mean amplitude currents to the second pulse given a response or a failure on the first stimulus, respectively. D, right: P_1 and P_2 are the probability of transmitter release after the first or second pulse; P_{2r} and P_{2f} are the probability of transmitter release on the second pulse given a response or a failure to the first one, respectively.

lations ≤ 7 V. This all-or-none behavior suggests that only a single fiber was stimulated. When the stimulation intensity was turned down, the probability of failures in synaptic transmission was 1. In 10 cells we have also measured the latency of individual EPSCs. The distribution of latencies was unimodal and narrow with an average SD of 0.47 ms (ranging from 0.25 to 0.67 ms).

Transmitter failures were estimated by visual discrimination. In a set of experiments to control the adequacy of the visual selection we used the method described by Nicholls and Wallace (1978), consisting in doubling the responses with positive amplitude (see also Gasparini et al. 2000). A similarity and a high correlation between the two methods were obtained ($r = 0.95$; $P < 0.0001$).

To see whether changing the $[Ca^{2+}/Mg^{2+}]_o$ ratio can affect pre-synaptic axon excitability, field excitatory postsynaptic potentials (fEPSPs) were recorded with a glass microelectrode filled with NaCl (2 mM) placed in stratum radiatum of the CA1 area. fEPSPs were evoked by stimulation of the Schaffer collateral with bipolar twisted NiCr insulated wires.

Drugs were applied to the bath by a three-way tap system. Drugs used were tetrodotoxin (TTX, Affinity Research Products, Exeter, UK) and bicuculline methiodide (Sigma, Milan, Italy).

If not otherwise stated, data are expressed as means \pm SE. Statistical comparisons were made with χ^2 test. The errors on all the quantities that are expressed as a ratio between two measurable values (e.g., P_{2r}/P_{2f} , a_2/a_1 , q) or as a more complex function of measurable quantities (e.g., CV) have been computed with the Jackknife method (Shao and Tu 1995).

Data acquisition and analysis

Data acquisition was done using the LTP114 software package for evoked responses (courtesy of W. W. Anderson, Bristol University, UK). Current signals were transferred to a computer after digitization with an A/D converter (Digidata 1200, Axon Instruments, Foster City, CA). Data were sampled at 20 kHz and filtered with a cutoff frequency of 2 kHz. Evoked EPSCs were analyzed with the AxoGraph 4.6 Program and Pclamp 9 software (Axon Instruments).

The coefficient of variation (CV) of successful responses (>100 stimuli) was calculated as follows: $CV = (SD_{\text{successes}}^2 - SD_{\text{failures}}^2)^{0.5} / \text{mean success amplitude}$, where SD represents the standard deviation.

We distinguished between the average response amplitude (A), where the average was computed over all trials including failures and the average response potency (a), where the average was computed only over successes (Stevens and Wang 1995). In the paired-pulse experiment, a_1 and a_2 represent the potency of the first and of the second pulse, respectively; a'_1 represents the potency of the first synaptic current after changing external calcium concentration.

The model

Our purpose was to develop and solve in a fully analytical way a model that allows one to distinguish univesicular from multivesicular release. With simple mathematical passages we computed quantities that are functions of the model parameters; comparison of these quantities with those obtained experimentally allowed estimating which model better describes the experimental data.

Model definitions

We defined A_1 and A_2 as the mean amplitude currents elicited by two pulses at 50-ms interval; P_1 and P_2 as the probability of transmitter release after the first or second pulse; A_{2r} and A_{2f} as the mean amplitude current to the second pulse given a response or a failure to the first stimulus, respectively; P_{2r} and P_{2f} as the probability of transmitter release to the second pulse given a response or a failure to the first one, respectively; the mean quantal size q as the mean

amplitude of the synaptic current after the release of a single vesicle; k as the variable counting the number of primed vesicles (i.e., the number of vesicles in the ready releasable pool); and p_{ves} as the probability of release of each single vesicle (Fig. 1).

We allowed the number of primed vesicles to change from trial to trial, and thus k is a random variable with probability distribution function $Q(k)$.

Model assumptions

We made the following assumptions:

- All vesicles have the same release probability p_{ves} .
- Postsynaptic receptors are not saturated.
- Postsynaptic receptors do not desensitize.
- Synaptic responses sum linearly.
- No new vesicles become primed in the time interval of 50 ms.

We have assumed that all primed vesicles have the same p_{ves} . However, p_{ves} associated with the first and second pulses, at least at CA3–CA1 synapses, can differ because of the residual calcium and for this reason we used two independent parameters: $p_{\text{ves}1}$ and $p_{\text{ves}2}$ (Atluri and Regehr 1996; Kamiya and Zucker 1994; Sakaba and Neher 2001).

Although the degree of glutamate receptors saturation varies among different synapses, at Schaffer collateral–CA1 synapses they are far from saturation, allowing the effective summation of many quanta (Conti and Lisman 2003; Mainen et al. 1999; McAllister and Stevens 2000; Nimchinsky et al. 2004; Raghavachari and Lisman 2004). Moreover, no detectable AMPA receptor desensitization in response to synaptic release of glutamate has been revealed (Hjelmstad et al. 1999).

The assumptions of receptor desensitization and saturation would eventually lead to an underestimation of the number of released vesicles and to an overestimation of the quantal content.

Regarding the last assumption, it is known that refilling of the vesicle pool occurs in two ways: by recruiting new vesicles from the recycling pool (RP) to the ready releasable pool (RRP) (Rizzoli and Betz 2005), a process that has a timescale τ of about 30 s (Pyle et al. 2000) and by endocytosis of the RRP of vesicles after the first pulse. This last process takes place with a timescale $\tau \approx 1$ s (Dobrunz and Stevens 1997; Pyle et al. 2000; for review see Rizzoli and Betz 2005). Therefore it is unlikely that refilling may occur within 50 ms.

Distributions of primed vesicles

The experimental determination of $Q(k)$, i.e., the probability of having k primed vesicles before the first pulse, is very difficult and would require counting many times the number of ready releasable vesicles at the same synapse. At present, although attempts have been made to estimate the typical number of primed vesicles at active zones in the pyramidal cells of the hippocampus, their distribution $Q(k)$ over time is unknown. Depending on the different preparations and methods the estimated number of primed vesicles varies between 2 and 10 (Dobrunz and Stevens 1997; Hanse and Gustafsson 2001b; Oertner et al. 2002; Schikorski and Stevens 2001; Zhai et al. 2001; for review see Rizzoli and Betz 2005). Therefore in our model, when required, the mean λ of $Q(k)$ has been fixed equal to 2, 5, or 10.

We stress that our analytical computations are done in full generality for any $Q(k)$: once an experimental determination of $Q(k)$ will be available, it can be plugged into the equations (which are written explicitly in the APPENDIX).

Because the exact shape of $Q(k)$ is unknown, we prefer to discuss the results obtained with the following distributions.

- Fixed number of primed vesicles: $Q(k) = \delta(k, \lambda)$, where the

Kronecker delta distribution $\delta(k, \lambda)$ takes the value 1 for $k = \lambda$ and 0 otherwise.

- Variable number of primed vesicles following a Poisson distribution: $Q(k) = \exp(-\lambda)\lambda^k/k!$, where $k! = 1 \times 2 \times 3 \times \dots \times k$ is the factorial of k .

The first distribution describes the case where there are no fluctuations from trial to trial in the number of primed vesicles; whereas the second distribution takes into account variations in the number of primed vesicles. Both of these distributions depend on a single parameter, the mean λ .

We do not explicitly discuss another distribution, which is often used in the literature, the binomial distribution of mean λ and maximum number N

$$Q(k) = \binom{N}{k} \left(\frac{\lambda}{N}\right)^k \left(1 - \frac{\lambda}{N}\right)^{N-k} \quad \text{with} \quad \binom{N}{k} \equiv \frac{N!}{k!(N-k)!}$$

There are several reasons beyond this choice. 1) Presenting general results varying both λ and N would be too complicated (and perhaps confusing). 2) The experimental determination of N , representing the largest number of primed vesicles that can be found at one synapse, requires roughly as many measures as the determination of the whole $Q(k)$. 3) The binomial distribution can be very well approximated by a Poisson distribution if N is much larger than the mean λ or if N is not perfectly conserved from trial to trial (i.e., eventual fluctuations in N make the binomial look like a Poisson distribution).

So we believe that if N is small the exact distribution can be easily determined, whereas if N is large (and so much larger than λ , which is a small number) the Poisson distribution is fairly accurate and there is no need for the extra parameter N . An example would better illustrate our last assertion. In Fig. 2 we show three distributions with a mean $\lambda = 5$: a Poissonian and two binomials with $n = 20$ and $n = 40$. As it appears from the figure, the distributions are very similar and the small differences are certainly much smaller than the uncertainty on the real shape of $Q(k)$. To be more quantitative, we have estimated the number of measures required for discriminating among these distributions by performing the following virtual (numerical) experiment: we have generated a set of M measures of k , by extracting random integers from a binomial distribution with mean $\lambda = 5$ and $n = 20$; then we have made the histogram of these numbers and have fitted it with a Poisson distribution. It turns out that the fit with a Poisson distribution is unacceptable ($P < 0.001$) only if $M > 850$, a huge number of measures.

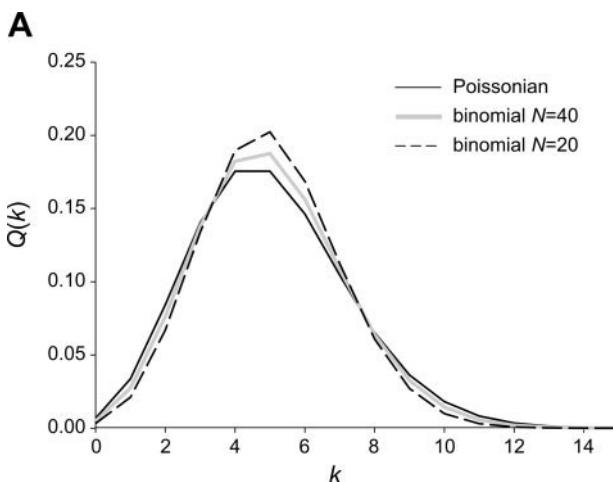


FIG. 2. Poisson and binomial distributions with the same mean are very similar. Comparison between a Poisson distribution of mean 5 and binomial distributions with the same mean and 2 different n values ($n = 20$ and $n = 40$). Although the random variable k can take only integer values, distributions are drawn with continuous lines for readability reasons.

Analytical resolution

Let us derive the equations linking the distribution of primed vesicles, $Q(k)$, and the probability that a vesicle releases its neurotransmitter content after the first stimulus, p_{ves1} , to A_1 and P_1 values, measured experimentally.

For k primed vesicles, the probability of having no response at all equals $(1 - p_{\text{ves1}})^k$, which is the probability that none of the k vesicles releases its content. Here we assume that primed vesicles behave independently. This assumption is not valid when specific mechanisms can limit the number of released vesicles per site.

Because the number of primed vesicles varies from trial to trial, when the paired-pulses are repeated many times the probability of having no response on the first stimulus is

$$1 - P_1 = \sum_{k=0}^{\infty} Q(k)(1 - p_{\text{ves1}})^k \quad (1)$$

Explicit expressions for this probability are $P_1 = 1 - (1 - p_{\text{ves1}})^\lambda$ for a fixed number distribution and $P_1 = 1 - e^{-\lambda p_{\text{ves1}}}$ for a Poisson distribution. Although the derivation of the first expression is simple (k always takes the value λ), to obtain the second one it is necessary to remember the power expansion of the exponential function: $e^x = \sum_{k=0}^{\infty} x^k/k!$

In a very similar way we can compute the mean amplitude, A_1 , assuming that each released vesicle gives a current with amplitude q . The mean amplitude is given by q multiplied by the number of released vesicles, which is a random variable fluctuating from trial to trial. There are two sources of stochasticity in the process: 1) the number k of primed vesicles, which is distributed according to the distribution $Q(k)$; and 2) the number of primed vesicles m actually released, which depends on k and the released probability p_{ves1} . The mean amplitude is given by the following expression

$$A_1 = q \sum_k Q(k) \sum_{m=0}^k m \binom{k}{m} p_{\text{ves1}}^m (1 - p_{\text{ves1}})^{k-m}$$

where the first sum takes the average over the number of primed vesicles, whereas the second sum gives the mean number of released vesicles when there are k primed vesicles and each of them can be released independently with probability p_{ves1} . The previous expression can be simplified with some elementary algebra to

$$A_1 = q p_{\text{ves1}} \sum_k k Q(k) = q p_{\text{ves1}} \langle k \rangle_1 = q p_{\text{ves1}} \lambda \quad (2)$$

where $\langle k \rangle_1$ is the mean number of primed vesicles when the first stimulus is given, fixed to λ . If the quantal size varies from vesicle to vesicle our expressions are perfectly valid because q is the mean current induced by a single vesicle release. In contrast, methods based on the analysis of amplitude distribution are influenced by fluctuations in the quantal size (e.g., peaks become broader and very hard to interpolate). Working only with mean values allows one to infer accurate results even for noisy data, as long as the number of trials is large enough to have small uncertainties on the mean values. Using this analytical method it is possible to reduce the number of collected data to 100–200 trials per synapse.

The most interesting part of the model is the response to the second stimulus. Indeed, according to the assumption that no new vesicle is recruited in the RRP within 50 ms, we expect that the number of primed vesicles to the second stimulus depends on the intensity of the response to the first stimulus. In particular, if there is no response to the first stimulus, then the number of primed vesicles to the second is unchanged, whereas in the case of a response to the first stimulus the number of primed vesicles is reduced. To simplify our analysis we group all possible outcomes on the first stimulus in two categories: failures (f) or successes (r). The number of primed vesicles to the

second stimulus still varies from trial to trial, but now its probability distribution depends on the outcome of the first stimulus. We call the distribution $Q_{2f}(k)$ in the case of failure to the first pulse and $Q_{2r}(k)$ in the case of successes.

$Q_{2f}(k)$ can be computed as

$$Q_{2f}(k) = \frac{Q(k)(1 - p_{ves1})^k}{1 - P_1}$$

The numerator is the probability of having k primed vesicles to the first stimulus, $Q(k)$, multiplied by the probability than none of the k vesicles is released. The denominator is the normalization factor and equals the probability of having no response to the first stimulus. We have computed the expression for $Q_{2r}(k)$ as well (see the APPENDIX for detailed computation).

Once the probability distributions of primed vesicles to the second stimulus are known, the mean release probability and the mean amplitude to the second stimulus are derived

$$P_{2f} = 1 - \sum_k Q_{2f}(k)(1 - p_{ves2})^k \quad P_{2r} = 1 - \sum_k Q_{2r}(k)(1 - p_{ves2})^k$$

$$A_{2f} = qp_{ves2} \sum_k kQ_{2f}(k) = qp_{ves2}\langle k \rangle_{2f} \quad A_{2r} = qp_{ves2} \sum_k kQ_{2r}(k) = qp_{ves2}\langle k \rangle_{2r}$$

These expressions are identical to Eqs. 1 and 2, the only difference being the probability distribution of primed vesicles, $Q_{2f}(k)$ and $Q_{2r}(k)$, and the probability that each of the vesicles is released to the second stimulus, p_{ves2} . In principle, p_{ves2} may depend on whether there is a response to the first stimulus; however, to keep the number of parameters in our model as small as possible a single probability was used.

Considering all events to the second stimulus, irrespective of the response to the first one, the release probability and the mean current amplitude are given by

$$P_2 = P_1P_{2r} + (1 - P_1)P_{2f} \quad A_2 = P_1A_{2r} + (1 - P_1)A_{2f}$$

Summarizing, we have analytic expressions for all the quantities measured in paired-pulse experiments: $P_1, P_{2f}, P_{2r}, P_2, A_1, A_{2f}, A_{2r},$ and A_2 . Parameters entering these analytical expressions (to be determined from experimental measurements) are the distribution of primed vesicles $Q(k)$, the release probability for a single vesicle, p_{ves1} and p_{ves2} , and the mean current induced by the release of one vesicle, q .

Combining in a convenient way the expressions for mean values, the following simple equality can be obtained

$$\frac{A_2}{A_1} = \frac{qp_{ves2}\langle k \rangle_2}{qp_{ves1}\langle k \rangle_1} = \frac{(1 - p_{ves1})p_{ves2}}{p_{ves1}} \quad (3)$$

The last expression has been obtained by using the relation $\langle k \rangle_2 = (1 - p_{ves1})\langle k \rangle_1$, which gives the mean number of primed vesicles to the second stimulus as a function of p_{ves1} and $\langle k \rangle_1$, where $\langle k \rangle_1$ is the mean number of primed vesicles to the first stimulus. It is clear from Eq. 3 that $Q(k)$ and q are no longer present. If experimentally $A_2 > A_1$, this means that facilitation is taking place at the synapses under study and the release to the second stimulus is enhanced ($p_{ves2} > p_{ves1}$).

Univesicular versus multivesicular

In the previous section the release of each primed vesicles has been assumed to be an independent event. Nevertheless, this assumption is not valid in the case of univesicular release. In the case of univesicular release each active site can release at most one vesicle per stimulus. This mechanism implies a clear dependency among vesicles: if a vesicle is released all the remaining vesicles cannot be released, and so they are not independent. In our univesicular release model each vesicle can be released with the same probability, p_{ves1} , but, as soon as one vesicle is released, the probability of the remaining vesicles to be released is zero. On the contrary, in the multivesicular model vesicles release independently.

When the ratio P_{2r}/P_{2f} is plotted parametrically as a function of P_1 , it allows one to discriminate univesicular from multivesicular release (see Hanse and Gustafsson 2002). At variance with Hanse's work, in which the release model has been analyzed with Monte Carlo simulations, in the present study analytic expressions for both the ratio P_{2r}/P_{2f} and P_1 were derived and plotted parametrically without any approximation. The general expression is complicated (see the APPENDIX for more detailed computation). In Fig. 3, the P_{2r}/P_{2f} relation as a function of P_1 for the Poisson and a fixed number distribution is represented graphically. In this figure, continuous lines refer to the Poissonian distributions, whereas dashed lines refer to fixed N ones. From the plots it can be concluded that the method for discriminating univesicular from multivesicular release does indeed work. For fixed number distributions the curve is <1 for any given value of P_1 and any release mechanism. For the Poissonian distribution, a multivesicular release produces a horizontal line equal to 1, whereas the univesicular release produces an upward-bending curve. It should be stressed that in this case the most relevant region in the graph is that corresponding to a larger P_1 value. Predictions for the P_{2r}/P_{2f} relation as a function of P_1 obtained with different $Q(k)$ values are represented in Fig. 3, A and B. In particular, although Fig. 3A has been obtained

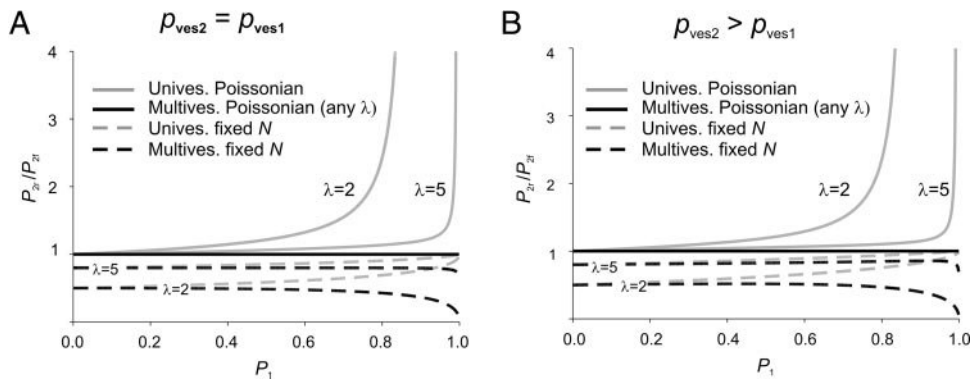


FIG. 3. Dependency of the P_{2r}/P_{2f} ratio on P_1 allows discriminating univesicular from multivesicular release. P_{2r}/P_{2f} ratio, computed from the analytical model, is plotted against the release probability (P_1). Continuous lines refer to the Poissonian distributions, whereas dashed lines refer to the fixed N ones. A: distribution with $p_{ves2} = p_{ves1}$. Note that for fixed number distributions the curve is always <1 ; for the Poissonian distribution, a multivesicular release produces a horizontal line equal to 1, whereas the univesicular release produces an upward-bending curve. B: distribution with $p_{ves2} > p_{ves1}$, where $p_{ves2} = \alpha p_{ves1} + (1 - \alpha)p_{ves1}^2$ and $\alpha = 1.5(p_{ves2}$ is 50% more than p_{ves1} in the low P_1 region). Note that for $\alpha < 1.5$ the P_{2r}/P_{2f} relation would look still more similar to A.

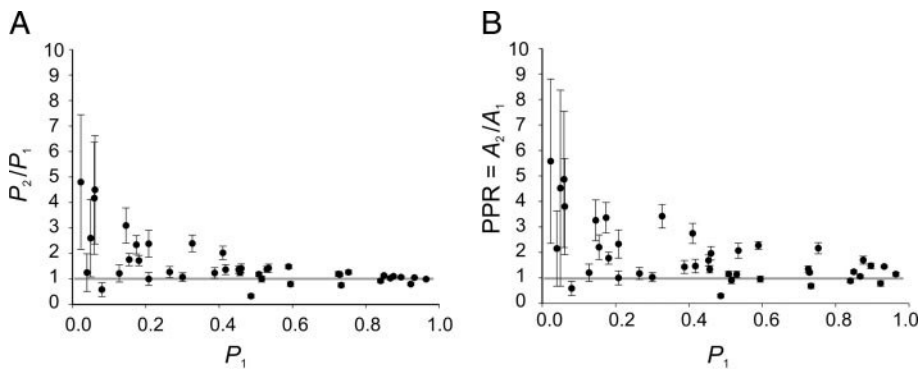


FIG. 4. Facilitation occurs at CA3–CA1 connection. Synaptic currents evoked in CA1 pyramidal cells by paired stimuli (50 ms apart) delivered to the Schaffer collateral in hippocampal slices obtained from P1 to P5 old rats. *A*: release probability is plotted as a function of P_1 ($n = 41$). Note that the majority of cells responds more to the second than to the first stimulus ($P_2 > P_1$). *B*: plot of the paired-pulse ratio (PPR) as a function of P_1 . Note that the PPR is >1 , although facilitation is more evident at low P_1 values.

by fixing $p_{ves2} = p_{ves1}$, Fig. 3*B* has been obtained with $p_{ves2} > p_{ves1}$, just for showing that there are no relevant qualitative changes in the shape of the functions. To our knowledge, the full correlation between p_{ves2} and p_{ves1} is not known, although we always observed a facilitation. To verify the effect of a larger p_{ves2} on the P_{2r}/P_{2f} relation, we can consider a simple and reasonable function (a second-order polynomial) with p_{ves2} ranging between 0 and 1, and linearly correlated with p_{ves1} for low values of this variable, i.e., $p_{ves2} = \alpha p_{ves1} + (1 - \alpha)p_{ves1}^2$. No major qualitative differences between the distributions with $p_{ves2} = p_{ves1}$ and $p_{ves2} > p_{ves1}$ can be observed.

Analysis of experimental data

Synaptic currents evoked by minimal stimulation of the Schaffer collateral were analyzed in 41 CA1 pyramidal neurons in hippocampal slices obtained from P1 to P5 old rats. In Fig. 4 the ratio of the release probabilities (*A*) and the paired-pulse ratio (PPR, *B*) as a function of P_1 have been plotted. It is clear that the majority of cells responded more to the second stimulus than to the first ($P_2 > P_1$, Fig. 4*A*) and that the PPR was >1 (Fig. 4*B*). However, these effects were more pronounced for low P_1 values. Given that the number of primed vesicles to the second stimulus is on average smaller than or equal to the first one, using Eq. 3 we can conclude that $p_{ves2} > p_{ves1}$ and a

facilitation process is taking place. Note that all the cells with $P_1 = 0$ and $P_1 = 1$ were excluded from the analysis because for these two values of P_1 the probability of P_{2r} and P_{2f} cannot be properly defined.

The main purpose for developing the analytical model was the possibility of discriminating among different release mechanisms—univesicular versus multivesicular—by comparing the experimental data with the analytical prediction reported in Fig. 3. In Fig. 5*A* the ratio P_{2r}/P_{2f} has been plotted as a function of P_1 . It is clear that data are mainly on the $P_{2r}/P_{2f} = 1$ line, suggesting that the number of primed vesicles is not fixed from trial to trial (for fixed number of primed vesicles the ratio P_{2r}/P_{2f} is <1 ; see Fig. 3). To facilitate the comparison with analytical results, the curves obtained for the Poisson distribution $Q(k)$ with mean λ were superimposed to data points: in the multivesicular case the ratio P_{2r}/P_{2f} was equal to 1, whereas in the univesicular case the curve always increases steeply when P_1 approached 1 and its exact value was dependent on λ . In Fig. 5*A* the curves for λ values equal to 2, 5, and 10 are represented. To check whether the univesicular mechanism could be compatible with the experimental data, we performed a statistical analysis for many values of λ (recall that λ is an undetermined parameter of the model because it cannot be measured directly from the data). We also fitted the data to the multivesicular Poissonian hypothesis, i.e., the straight line $P_{2r}/P_{2f} = 1$. This always turned out to be the better fit with respect to

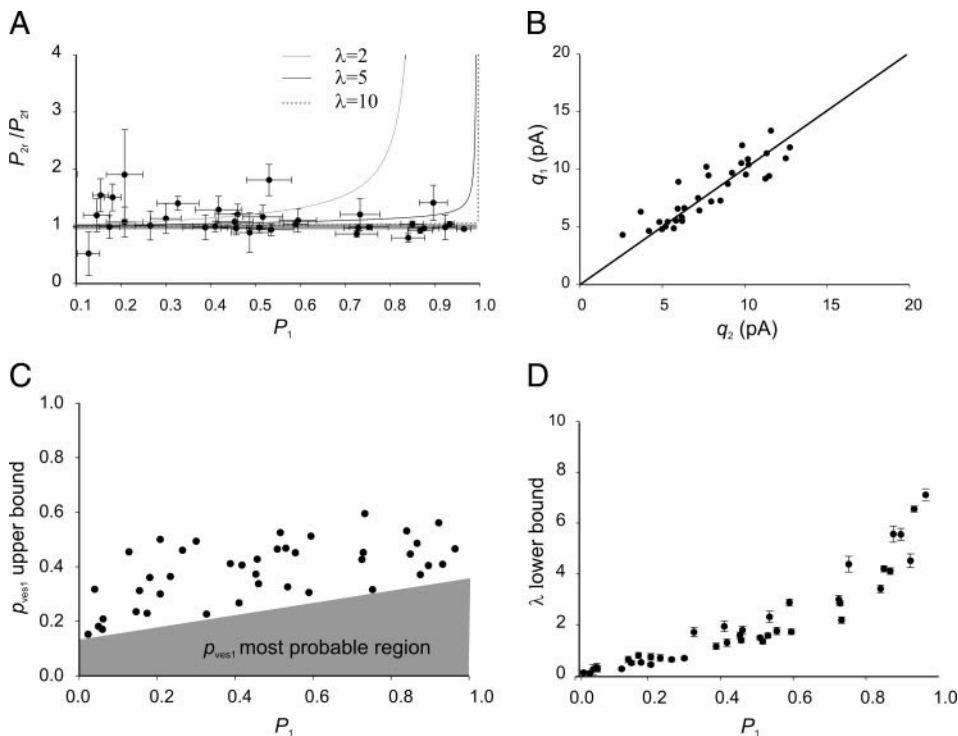


FIG. 5. Multivesicular release at CA3–CA1 connections. *A*: correlation between P_1 and the release dependency during paired-pulse activation. P_{2r}/P_{2f} ratio is plotted over P_1 values ($n = 36$, cells with $P_1 > 0.1$). Curves for the Poissonian distribution with release independency (multivesicular, horizontal gray line, i.e., P_{2r}/P_{2f} ratio=1) or release dependency (univesicular, upward-bending continuous line, with $\lambda = 2$, $\lambda = 5$, and $\lambda = 10$, as indicated) are superimposed to the data points. Note that experimental data can be fitted by a straight line. *B*: plot of the estimation of the q value obtained by computing Eq. 4 with the data related to the first (q_1) or the second (q_2) stimulus in a pair ($n = 34$). Note that points are on the bisecting line, indicating that the 2 estimations are compatible. *C*: upper bound for p_{ves1} is plotted as a function of P_1 ($n = 41$). Most probable values for p_{ves1} are in the gray region. *D*: lower bound for λ is plotted against P_1 values ($n = 41$).

all the other models for any value of λ . We performed χ^2 analysis and the resulting P values are the following: multivesicular Poissonian model $P = 0.13$, univesicular Poissonian model $P \ll 10^{-6}$ ($\lambda = 5$) and $P < 0.05$ ($\lambda = 10$), univesicular fixed N model $P < 0.05$ ($\lambda = 10$) and $P = 1.1 \times 10^{-5}$ ($\lambda = 5$).

Note that few experimental points (those above the $P_{2r}/P_{2f} = 1$ line) could be interpreted as being attributed to a univesicular mechanism. Indeed, we are not asserting that all cells follow the multivesicular mode of release, but certainly the vast majority is concentrated on the $P_{2r}/P_{2f} = 1$ line, which is naturally interpreted as evidence for multivesicular release. Moreover cells with very low release probability ($P_1 < 0.1$), have a very large statistical error (resulting from the small number of successes), and thus they give no significant contribution to the data analysis and were excluded.

From the analysis of the ratio P_{2r}/P_{2f} versus P_1 it appears that the most likely model of transmitter release at immature CA3-CA1 connections is the multivesicular one with a Poisson distribution of primed vesicles with mean λ . Thus in the rest of the analysis we compared this model to the experimental data. We started by making explicit for this model the formulas previously written in the general case; distributions of primed vesicles, release probabilities, and mean amplitudes are given by the following expressions (see the APPENDIX for a detailed derivation)

$$Q(k) = e^{-\lambda} \frac{\lambda^k}{k!} \quad Q_{2r}(k) = Q_{2f}(k) = e^{-\lambda(1-p_{ves1})} \frac{[\lambda(1-p_{ves1})]^k}{k!}$$

$$P_1 = 1 - e^{-\lambda p_{ves1}} \quad P_2 = P_{2r} = P_{2f} = 1 - e^{-\lambda(1-p_{ves1})p_{ves2}}$$

$$A_1 = q\lambda p_{ves1} \quad A_2 = A_{2r} = A_{2f} = q\lambda(1-p_{ves1})p_{ves2}$$

Note that in this model it is possible to check whether the response failure to the first stimulus depends on activation failure (failure of the action potential to invade the axon terminal) because in the presence of a real transmission failure the amplitude of A_{2r} and A_{2f} should be the same. From our experimental data the A_{2r}/A_{2f} value was equal to 1.09 ± 0.05 ($n = 36, P_1 > 0.1$), implying that the lack of successes to the first pulse were real transmitter failures and not activation failures.

Combining the expressions for $P_1, P_2, A_1,$ and A_2 we could compute the quantal size q in two equivalent ways

$$q = \frac{A_1}{-\ln(1-P_1)} = \frac{A_2}{-\ln(1-P_2)} \quad (4)$$

Note that the second equality can also be used as a consistency check of the model. An estimation of q in response to the first stimulus (q_1) versus that obtained in response to the second one (q_2) is given in Fig. 5B. Data points are spread around the bisecting line, as expected from the model (from the paired Student's t -test, the q_1 and q_2 distributions

turned out to be similar: $P = 0.2$). This observation suggests that desensitization of receptors is very small; otherwise, q_2 would be systematically smaller than q_1 . On average, we obtained a q_1 value of 7.8 ± 0.5 pA and a q_2 value of 8.0 ± 0.4 pA ($n = 34$). Because of the model assumption on linear summation of the responses, these estimations could be slightly smaller than the real average values.

Although from the experimental measures it is not possible to make direct estimates of $p_{ves1}, p_{ves2},$ and λ , we can still use the model to put an upper bound on p_{ves1} and a lower bound on λ . The following inequalities show how to derive these bounds

$$\frac{A_2}{A_1} = \frac{(1-p_{ves1})p_{ves2}}{p_{ves1}} \leq \frac{1-p_{ves1}}{p_{ves1}} \Rightarrow p_{ves1} \leq \frac{A_1}{A_1 + A_2}$$

$$P_1 = 1 - e^{-\lambda p_{ves1}} \Rightarrow \lambda = \frac{-\ln(1-P_1)}{p_{ves1}} \geq -\ln(1-P_1) \frac{A_1 + A_2}{A_1}$$

The upper bound on p_{ves1} and the lower bound on λ are shown in Fig. 5, C and D, respectively. Although these are only bound, they give a strong hint about the dependency on the release probability P_1 of model parameters: p_{ves1} increases roughly linearly with P_1 and stays well below 1, whereas λ increases much more steeply with P_1 , especially in the high release probability region. As predicted from the relation $P_1 = 1 - e^{-\lambda p_{ves1}}$, λ has to become very large to obtain high release probabilities. It is important to notice that λ lower bounds are of the same order of experimental estimation of the number of primed vesicles (see INTRODUCTION).

Given that the distribution of released vesicles is Poissonian, we can analytically compute the coefficient of variation (CV) as a function of the release probability P

$$CV = \sqrt{P \left[1 - \frac{1}{\ln(1-P)} \right] - 1} \quad (5)$$

In this expression we did not use any subscript because the result is general and holds both on the first and the second stimulus as long as the distribution of primed vesicles is Poissonian.

The CV analytic curve is illustrated with a continuous line in the graph below the individual traces of Fig. 6A. Note that this curve is an exact prediction of the model and thus has no fitting parameter.

Further experimental evidence for multivesicular release

HIGH VARIABILITY OF COEFFICIENT OF VARIATION (CV). In the uniquantal models of synaptic transmission, the variability of the amplitude of successes, measured by the CV of these amplitudes, is very low (in the order of 0.2), whereas in the multiquantal models the CV is significantly larger (>0.4) (Auger and Marty 2000; Conti and Lisman 2003; Forti et al. 1997; Mainem et al. 1999; McAllister and

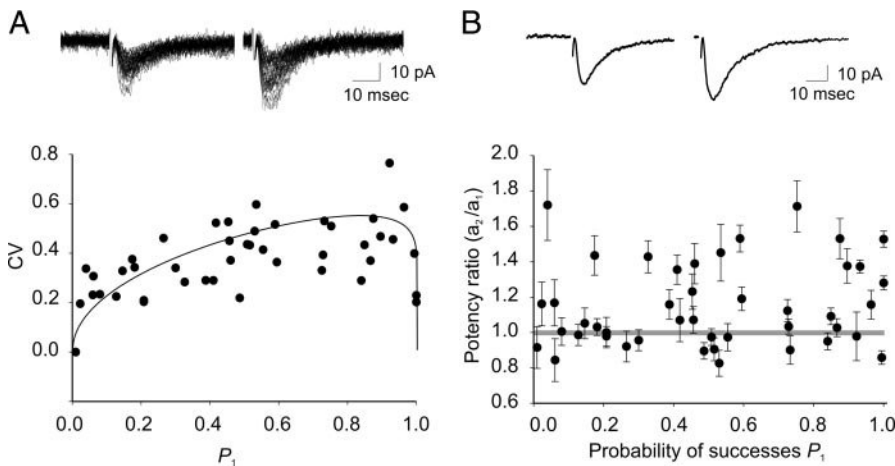


FIG. 6. Dependency of the coefficient of variation (CV) from P_1 . A, top: example of superimposed individual traces ($n = 50$) from a single cell showing successes to the first (left) and the second stimulus (right). Bottom: CV values of the response amplitudes obtained from 44 cells are plotted vs. P_1 values. Note that the CV is highly variable. Superimposed to the plot (full line) is the analytic curve obtained from the model $CV = \sqrt{P \{1 - [1/\ln(1-P)]\} - 1}$ (Eq. 5). Note that this curve is the exact prediction of the model and there are no fitting parameters. B, top: average of successful responses (potency) from the same cell shown in A. Bottom: a_2/a_1 ratio is plotted vs. P_1 values ($n = 44$ cells). Note that there is no correlation between the potency ratio (a_2/a_1) and the P_1 values.

Stevens 2000; Oertner et al. 2002; Striker et al. 1996; Umekiya et al. 1999)

We performed the analysis of the CV on our data, collected at individual CA3–CA1 synapses, to assess whether the amplitude of successes showed large trial-to-trial variation or whether the responses were stereotyped. The CV was on average 0.35 ± 0.14 , varying from 0.12 to 0.73 ($n = 44$). This variability supports the multivesicular mode of neurotransmitter release. The *top traces* of Fig. 6A represent an example of synaptic currents (only successes; $n = 50$) evoked in a CA1 principal cell in response to a paired-pulse protocol. It is clear from the figure that a certain degree of variability between individual currents exists. In the graph below the CV individual cells ($n = 44$) are plotted against P_1 . These CV values are clearly not P_1 independent (data interpolation with a horizontal line is not acceptable: $P \ll 10^{-6}$). On the contrary, their dependency on P_1 seems to be in good qualitative agreement with the analytic prediction from the Poisson model, shown with a line in Fig. 6A.

AVERAGE RESPONSE AMPLITUDE TO THE FIRST (a_1) AND SECOND PULSE (a_2) ARE DIFFERENT. The amplitude of the success to a single stimulus is defined potency (a). In the case of univesicular release changes in the probability of release should not affect the potency. This means, for example, that the potency ratio a_2/a_1 between the second and the first response to a pair of stimuli (50 ms apart), should be equal to 1 (Stevens and Wang 1995). This condition is necessary, but not sufficient, i.e., cells with $a_2/a_1 \neq 1$ cannot have univesicular release (unless we take into account receptor desensitization), whereas cells with $a_2/a_1 = 1$ may have a multivesicular release; indeed, for low release probabilities, the multivesicular mechanism typically releases just one vesicle, making the discrimination very difficult.

In a first set of experiments using the paired-pulse protocol, the potency ratio was measured in each cell and the results are shown in Fig. 6B. Among the $n = 44$ cells analyzed, 21 have a potency ratio statistically different from 1 ($P < 0.05$), suggesting a multivesicular release. It is interesting to note that the remaining 23 cells, those with a_2/a_1 close to 1, are concentrated in the region of small success probabilities (11 of the 23 have $P_1 \leq 0.2$), making it impossible to establish the release mechanism.

Moreover if all cells had a univesicular release the average value of a_2/a_1 should be equal to 1; the mean value of our data is 1.15, which is statistically different from 1 ($P < 0.01$), again excluding the univesicular mode of release.

Finally note that no correlation between the a_2/a_1 values and the P_1 was found (Fig. 6B). It is known that glutamate released from a neighboring synapse can diffuse to postsynaptic receptors (“spillover”; Asztely et al. 1997; Diamond 2001) and may contribute to potency facilitation ($a_2/a_1 > 1$). In our experiments, trials with failures to both first and second stimuli were indistinguishable from the baseline, indicating that spillover from neighboring active synapses it is unlikely to occur and to affect our measurements. Moreover, in our experimental conditions spillover was partially prevented by the enhanced glutamate uptake occurring at more physiological temperature (33°C; Asztely et al. 1997).

Changes in extracellular calcium concentration affect the potency and the postsynaptic amplitude distribution

In a second set of experiments we modified the probability of glutamate release by increasing or decreasing the external calcium concentration. In particular we changed the $[Ca^{2+}/Mg^{2+}]_o$ ratio from 2/1.3 to 4/1 or 1/2, respectively. To see whether changing the $[Ca^{2+}/Mg^{2+}]_o$ ratio alters the excitability of axon terminals, in additional experiments we measured the amplitude of afferent volleys and field EPSPs evoked in stratum radiatum by stimulation of the Schaffer collateral, before and after changing the $[Ca^{2+}/Mg^{2+}]_o$ ratio from 2/1.3 to 4/1. On three hippocampal slices from P3 to P4 old rats, the amplitude of the afferent volley changed from $57 \pm 21 \mu V$ (2/1.3

ratio) to $54 \pm 16 \mu V$ (4/1 ratio), indicating that axon excitability was not modified. The amplitude of the corresponding field EPSP changed from 76 ± 5 to $100 \pm 16 \mu V$. We then measured the potency ratio (a'_1/a_1) of the first synaptic current after and before changing the external calcium concentration. In the case of low $[Ca^{2+}/Mg^{2+}]_o$ the a'_1/a_1 value was 0.73 ± 0.06 ($n = 8$, $P < 0.01$), whereas in the case of high $[Ca^{2+}/Mg^{2+}]_o$ the a'_1/a_1 value was 1.28 ± 0.14 ($n = 7$, $P < 0.05$).

These findings indicate that a multivesicular modality of release at individual CA1 synapses is likely to occur.

Representative examples of synaptic currents evoked in CA1 pyramidal neurons by Schaffer collateral stimulation in low or high calcium containing medium are illustrated in Fig. 7. As shown in the average traces (from $n = 50$ successes plus failures) of Fig. 7A, lowering the $[Ca^{2+}/Mg^{2+}]_o$ ratio from 2/1.3 to 1/2 produced a decrease in the mean amplitude response to the first pulse and an increase in the paired-pulse ratio. The graphs below the traces show that the reduction in $[Ca^{2+}/Mg^{2+}]_o$ caused an increase in the number of transmitter failures (in gray) to the first response and a decrease in the skewness of the successes distribution (in white). On the contrary, increasing the $[Ca^{2+}/Mg^{2+}]_o$ ratio from 2/1.3 to 4/1 enhanced the mean amplitude of the first response (average of 50 failures and successes) and decreased the paired-pulse ratio. This effect was associated with a reduction in the number of failures to the first stimulus and an increase in the skewness of distribution of successes (Fig. 7B). These findings cannot be explained by the univesicular mode of glutamate release.

DISCUSSION

Synaptic transmission consists of a series of highly coordinated functional steps during which synaptic vesicles are tethered to the active zones on presynaptic nerve endings, primed and fused in a Ca^{2+} -dependent way with the plasma membrane to release the neurotransmitter into the synaptic cleft. One interesting and not fully clarified aspect of transmitter release is whether vesicles can be released in an independent way, i.e., if at active sites vesicles can be released in an “univesicular” (at most one vesicle released per stimulus) or in a “multivesicular” fashion.

We have developed and analytically solved a model that allows one to distinguish between the release of one or more vesicles. In the case that more than one vesicle is released, the model cannot distinguish between single-site/multivesicular or multisite/univesicular type of release. Thus to correctly use the model and to extract useful information, it is crucial to have the experimental indication that data are collected from a single axon stimulation. In this study, the model has been experimentally validated in the immature hippocampus at Schaffer collateral–CA1 synapses known to bear only a single release site (Hsia et al. 1998). Moreover, in our case, evidence has been provided that a single Schaffer collateral input was activated (i.e., the potency of EPSCs remained constant over a range of stimulus intensities after the threshold for detecting a response, and the latencies of individual synaptic responses exhibited a unimodal distribution with a small SD). Although we cannot completely exclude that at least in some cases more than one fiber was activated, on the whole the results of our analysis strongly favor a multivesicular type of release.

In the model we have taken into account parameters such as the number of vesicles in the ready releasable pool and the probability of release of each vesicle. We then computed quantities that are functions of the model parameters, such as

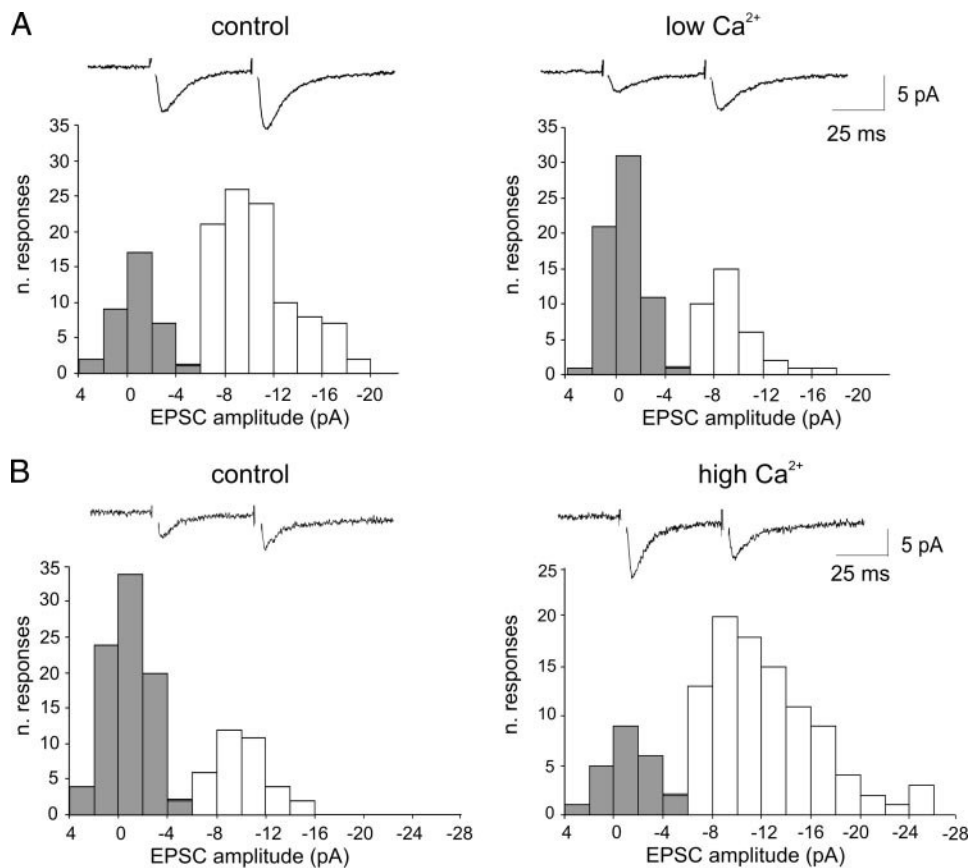


FIG. 7. Changes in extracellular calcium modify amplitude distribution of EPSCs. Amplitude distribution of the EPSCs evoked in control conditions and after switching to a low (1 mM calcium, 2 mM magnesium, *A*) or to a high calcium containing solution (4 mM calcium, 1 mM magnesium, *B*). Insets above the graphs represent average traces ($n = 50$, successes plus failures). Note the decrease or increase of the skewness of the amplitude distribution of synaptic events after switching to a low or high calcium containing solutions, respectively. Columns in gray refer to transmitter failures; columns in white refer to successes. Note that in the $-4/-6$ pA bin both columns are represented.

the release probability and the amplitude of postsynaptic current ($P_1, P_{2f}, P_{2r}, P_2, A_1, A_{2f}, A_{2r}, A_2$), and analyzed the relation between the ratio P_{2r}/P_{2f} and the probability of release P_1 . Comparison of these quantities with those obtained experimentally in paired-pulse experiments allowed us to estimate which model better describes the experimental data. From this comparison it appears that the multivesicular mode of release is the most probable mechanism by which immature CA3–CA1 connections operate.

The analytical method developed is very general and presents some useful properties. First, it deals with simple average quantities that can be easily measured at each synapse. Working with only mean values allows one to infer accurate results even for noisy data, as long as the number of trials is large enough to have small uncertainties on the mean values. Using this analytical method it is possible to reduce the number of collected data to <100 trials per synapse. Interesting information can be achieved when the analysis is extended to many synapses with a large range of release probabilities. Moreover it is possible to estimate the mean amplitude of synaptic response to the release of a single vesicle (q), an upper bound for the probability of release of a single vesicles (p_{ves}), and a lower bound for the mean value of primed vesicles (λ). The estimated value of q (5–10 pA) to both the first and the second stimulus (q_1 and q_2) computed in two equivalent ways (see RESULTS) is in good agreement with that obtained with different experimental approaches and theoretical prediction (5 pA: Conti and Lisman 2003; 10 pA: Raghavachari and Lisman 2004; 10 pA: Magee and Cook 2000).

One important assumption in the model is that postsynaptic receptors are not saturated (see INTRODUCTION), implying that quantal responses can summate. This assumption is supported by recent work indicating that transmission at single CA1 synapses can be multiquantal: in particular, quantal response seems to involve the opening of only a small fraction of channels and multiple quanta summate to produce a wide range of currents of different amplitudes (Conti and Lisman 2003; Hsia et al. 1998; Huang and Stevens 1997; Mainen et al. 1999; Oertner et al. 2002; Raghavachari and Lisman 2004). Another assumption in the model is the absence of AMPA receptor desensitization. Data concerning this issue are rather controversial. Whereas in outside-out patches pulled from CA1 principal cells, extrasynaptic AMPA receptor desensitization occurs when the patch is exposed to brief pulses of glutamate (Arai and Lynch 1996; Colquhoun et al. 1992), synaptic receptors do not seem to be affected, as suggested by experiments with minimal and paired-pulse stimulation (Hjelmstad et al. 1999).

In principle, it could be possible to introduce in the model a nonlinearity in the sum of the responses and a desensitization factor (by specific nonlinear functions). Indeed, we decided to keep the model simpler (no desensitization and linear summation) because uncertainty on such nonlinear functions would make model predictions less reliable. Further work is needed to identify these hypothetical nonlinear functions.

Fitting our experimental data with the model provides strong evidence that at immature rat CA3–CA1 connections synaptic transmission is multiquantal. Further support in favor of this hypothesis is given by: 1) the high variability in the amplitude

of successes, with a coefficient of variation (CV) ranging from 0.12 to 0.73; 2) the potency ratio $a_2/a_1 > 1$; and 3) changes in the potency to the first stimulus in relation to different release probability as suggested by the experiments with low or high calcium.

At CA3–CA1 synapses, quantal responses with low (Bolshakov and Siegelbaum 1995; Larkman et al. 1991; Liao et al. 1992; Stricker et al. 1996) or high CV values (Conti and Lisman 2003; Maggi et al. 2004; Raghavachari and Lisman 2004) have been reported. In agreement with the present experiments, similar CV values (ranging from 0.2 to 0.7) have been detected at Schaffer collateral–CA1 connections of the hippocampus from immature animals (Hanse and Gustafsson 2001a). However, in contrast with the present findings, the large quantal variability observed by Hanse and Gustafsson (2001a) was interpreted as based on nonsaturated AMPA responses fluctuating as a function of the amount of transmitter released from each vesicle.

Moreover, some discrepancies regarding potency modulation by factors that modify release probability compatible either with the univesicular (Hanse and Gustafsson 2001a; Stevens and Wang 1994) or with the multivesicular mode of release (Oertner et al. 2002) can be attributed to the different experimental conditions, including variations in the age of the animals, the temperature of the experiment, and the technique used (imaging vs. electrophysiology).

In conclusion, although we cannot exclude the possibility that, at least in a few cases univesicular release may also occur in our experiments, the present data indicate that in the majority of cases at immature Schaffer collateral–CA1 synapses an action potential is able to evoke from a single release site multiquanta events, each of them being far from saturation. It is noteworthy that the analytical model we developed and solved represents a very general method that could be successfully used for studying the release mechanisms at any given synapse.

APPENDIX

Herein we report the most technical aspects of our computation. We use the same notation as in the main text, i.e., $Q(k)$ is the probability of having k primed vesicles before the first stimulus.

In the univesicular mode of release only one vesicle may be released in each trial; given k primed vesicles, we have that $(1 - p_{\text{ves}})^k$ is the probability that none is released and $1 - (1 - p_{\text{ves}})^k$ is the probability that just one vesicle is released.

In the multivesicular mode of release each primed vesicle may be released independently; given k primed vesicles, the probability that exactly m are released is given by the expression

$$\binom{k}{m} p_{\text{ves}}^m (1 - p_{\text{ves}})^{k-m}$$

where the binomial coefficient is

$$\binom{k}{m} \equiv \frac{k!}{m!(k-m)!}$$

First of all we write some expressions that are valid for a generic $Q(k)$.

The release probability on the first stimulus P_1 is given by the expression

$$P_1 = 1 - \sum_{k=0}^{\infty} Q(k)(1 - p_{\text{ves1}})^k$$

This expression is valid for both release mechanisms, univesicular and multivesicular.

In case of failure on the first stimulus, the distribution of primed vesicles on the second stimulus is given by the expression

$$Q_{2f}(k) = \frac{Q(k)(1 - p_{\text{ves1}})^k}{1 - P_1}$$

which is valid for both release mechanisms. On the contrary, if a release took place on the first stimulus, then the probability of having k primed vesicles before the second stimulus does depend on the release mechanism; in the univesicular case it is given by the expression

$$Q_{2r}(k) = Q(k+1) \frac{1 - (1 - p_{\text{ves1}})^{k+1}}{P_1}$$

where the denominator is nothing but the normalization factor; in the multivesicular one it is given by the expression

$$Q_{2r}(k) = \frac{1}{P_1} \sum_{j=k+1}^{\infty} Q(j) \binom{j}{k} p_{\text{ves1}}^{j-k} (1 - p_{\text{ves1}})^k$$

The probabilistic interpretation of this expression is straightforward: the probability of having still k primed vesicles after a release occurred on the first stimulus is given by the sum of the probabilities that $j > k$ primed vesicles were present on the first stimulus times the probability that exactly $(j - k)$ were released and k remained. The sum is then multiplied by the normalization factor $1/P_1$.

Given the distributions $Q_{2f}(k)$ and $Q_{2r}(k)$, the release probabilities on the second stimulus are simply given by the expressions

$$P_{2f} = 1 - \sum_{k=0}^{\infty} Q_{2f}(k)(1 - p_{\text{ves2}})^k \quad P_{2r} = 1 - \sum_{k=0}^{\infty} Q_{2r}(k)(1 - p_{\text{ves2}})^k$$

Substituting $Q_{2f}(k)$ and $Q_{2r}(k)$ with the expressions previously derived and doing some algebraic simplifications, we finally obtain

$$P_{2f} = 1 - \frac{\sum_{k=0}^{\infty} Q(k)(1 - p_{\text{ves1}})^k (1 - p_{\text{ves2}})^k}{\sum_{k=0}^{\infty} Q(k)(1 - p_{\text{ves1}})^k}$$

$$P_{2r} = 1 - \frac{1}{P_1} \sum_{k=0}^{\infty} Q(k+1) [1 - (1 - p_{\text{ves1}})^{k+1}] (1 - p_{\text{ves2}})^k \quad (\text{uni})$$

$$P_{2r} = 1 - \frac{1}{P_1} \sum_{k=0}^{\infty} Q(k) \times \{ [p_{\text{ves1}} + (1 - p_{\text{ves1}})(1 - p_{\text{ves2}})]^k - (1 - p_{\text{ves1}})^k (1 - p_{\text{ves2}})^k \} \quad (\text{multi})$$

In the following we fix some explicit forms for $Q(k)$ and we write the ratio P_{2r}/P_{2f} as a function of P_1 . In principle such a ratio may depend on both p_{ves1} and p_{ves2} , so we have to choose a functional relation between these two parameters to be able to express the ratio as a function of P_1 only. A reasonable choice is given by the function

$$p_{\text{ves2}} = f(p_{\text{ves1}}) \equiv \alpha p_{\text{ves1}} - (\alpha - 1) p_{\text{ves1}}^2$$

with $\alpha \geq 1$, which implies facilitation ($p_{\text{ves2}} \geq p_{\text{ves1}}$) and $p_{\text{ves2}} = \alpha p_{\text{ves1}}$, for small p_{ves1} .

In Fig. 3 the ratio P_{2r}/P_{2f} is plotted as a function of P_1 for $\alpha = 1$ and $\alpha = 1.5$ to highlight the small dependency on α . Hereafter we write the explicit expressions for $\alpha = 1$.

If k does not vary from trial to trial, then $Q(k) = \delta(k - \lambda)$, and we have in the univesicular case

$$\frac{P_{2r}}{P_{2f}} = \frac{1 - (1 - P_1)^{1-1/\alpha}}{P_1}$$

and in the multivesicular case

$$\frac{P_{2r}}{P_{2f}} = \frac{1 - P_1 + P_1^2 - [1 - (1 - P_1)^{1/\alpha} + (1 - P_1)^{2/\alpha}]^\alpha}{P_1^2}$$

If k varies following a Poisson distribution, $Q(k) = \exp(-\lambda)\lambda^k/k!$, then we have in the univesicular case

$$\frac{P_{2r}}{P_{2f}} = \frac{1}{1 - (1 - P_1)^{1+(1/\alpha)\ln(1-P_1)}} - \frac{1 - P_1}{P_1 \left[1 + \frac{1}{\lambda} \ln(1 - P_1) \right]}$$

and $P_{2r}/P_{2f} = 1$ in the multivesicular case.

We finally prove that for a Poisson distribution and a multivesicular mode of release the equality $Q_{2r}(k) = Q_{2f}(k)$ holds, implying that $A_{2r} = A_{2f}$. Substituting the expression $Q(k) = \exp(-\lambda)\lambda^k/k!$ in the second, third, and fifth equations of this APPENDIX we arrive at

$$\begin{aligned} P_1 &= 1 - \sum_{k=0}^{\infty} Q(k)(1 - p_{ves1})^k = 1 - e^{-\lambda} \sum_{k=0}^{\infty} \frac{\lambda^k}{k!} (1 - p_{ves1})^k \\ &= 1 - e^{-\lambda} e^{\lambda(1-p_{ves1})} = 1 - e^{-\lambda p_{ves1}} \\ Q_{2f}(k) &= \frac{Q(k)(1 - p_{ves1})^k}{1 - P_1} = e^{-\lambda} \frac{\lambda^k (1 - p_{ves1})^k}{k! e^{-\lambda p_{ves1}}} \\ &= e^{-\lambda(1-p_{ves1})} \frac{[\lambda(1 - p_{ves1})]^k}{k!} \\ Q_{2r}(k) &= \frac{1}{P_1} \sum_{j=k+1}^{\infty} Q(j) \binom{j}{k} p_{ves1}^{j-k} (1 - p_{ves1})^k \\ &= \frac{e^{-\lambda}}{1 - e^{-\lambda p_{ves1}}} \sum_{j=k+1}^{\infty} \frac{\lambda^j}{j!} \binom{j}{k} p_{ves1}^{j-k} (1 - p_{ves1})^k \\ &= \frac{e^{-\lambda}}{1 - e^{-\lambda p_{ves1}}} \frac{\lambda^k (1 - p_{ves1})^k}{k!} \sum_{j=k+1}^{\infty} \frac{\lambda^{j-k}}{(j-k)!} p_{ves1}^{j-k} \\ &= \frac{e^{-\lambda}}{1 - e^{-\lambda p_{ves1}}} \frac{\lambda^k (1 - p_{ves1})^k}{k!} (e^{\lambda p_{ves1}} - 1) \\ &= e^{-\lambda} \frac{\lambda^k (1 - p_{ves1})^k}{k!} e^{\lambda p_{ves1}} \\ &= e^{-\lambda(1-p_{ves1})} \frac{[\lambda(1 - p_{ves1})]^k}{k!} \end{aligned}$$

In conclusion, for the multivesicular model with a Poisson distribution of mean λ , the distribution of primed vesicles on the second stimulus is Poisson with mean $\lambda(1 - p_{ves1})$ independently from the response to the first stimulus.

ACKNOWLEDGMENTS

We thank L. Lagostena for participating in some experiments. L. Maggi kindly thanks Prof. F. Eusebi for support during the completion of this work.

GRANTS

This work was partially supported by Ministero Istruzione Universit  a e Ricerca Grant COFI 2003 to E. Cherubini. L. Maggi was partially supported by

a European Molecular Biology Organization long-term fellowship grant. E. Sola was partially supported by a Novartis fellowship. F. Ricci-Tersenghi was partially supported by EC 6FP IST Project EVERGROW.

REFERENCES

Allen C and Stevens CF. An evaluation of causes for unreliability of synaptic transmission. *Proc Natl Acad Sci USA* 91: 10380–10383, 1994.

Arai A and Lynch G. Response to repetitive stimulation of AMPA receptors in patches excised from fields CA1 and CA3 of the hippocampus. *Brain Res* 716: 202–206, 1996.

Arancio O, Korn H, Gulyas A, Freund T, and Miles R. Excitatory synaptic connections onto rat hippocampal inhibitory cells may involve a single transmitter release site. *J Physiol* 481: 395–405, 1994.

Asztely F, Erdemli G, and Kullmann DM. Extrasynaptic glutamate spillover in the hippocampus: dependence on temperature and the role of active glutamate uptake. *Neuron* 18: 281–293, 1997.

Atluri PP and Regehr WG. Determinants of the time course of facilitation at the granule cell to Purkinje cell synapse. *J Neurosci* 16: 5661–5671, 1996.

Auger C, Kondo S, and Marty A. Multivesicular release at single functional synaptic sites in cerebellar stellate and basket cells. *J Neurosci* 18: 4532–4547, 1998.

Auger C and Marty A. Heterogeneity of functional synaptic parameters among single release sites. *Neuron* 19: 139–150, 1997.

Auger C and Marty A. Quantal currents at single-site central synapses [Review]. *J Physiol* 526: 3–11, 2000.

Barberis A and Petrini EM, and Cherubini E. Presynaptic source of quantal size variability at GABAergic synapses in rat hippocampal neurons in culture. *Eur J Neurosci* 20: 1803–1810, 2004.

Bolshakov VY and Siegelbaum SA. Regulation of hippocampal transmitter release during development and long-term potentiation. *Science* 69: 1730–1734, 1995.

Colquhoun D, Jonas P, and Sakmann B. Action of brief pulses of glutamate on AMPA/kainate receptors in patches from different neurones of rat hippocampal slices. *J Physiol* 458: 261–287, 1992.

Conti R and Lisman J. The high variance of AMPA receptor- and NMDA receptor-mediated responses at single hippocampal synapses: evidence for multiquantal release. *Proc Natl Acad Sci USA* 100: 4885–4890, 2003.

Diamond JS. Neuronal glutamate transporters limit activation of NMDA receptors by neurotransmitter spillover on CA1 pyramidal cells. *J Neurosci* 21: 8328–8338, 2001.

Dobrunz LE and Stevens CF. Heterogeneity of release probability, facilitation, and depletion at central synapses. *Neuron* 18: 995–1008, 1997.

Forti L, Bossi M, Bergamaschi A, Villa A, and Malgaroli A. Loose-patch recordings of single quanta at individual hippocampal synapses. *Nature* 388: 874–878, 1997.

Frerking M, Borges S, and Wilson M. Variation in GABA mini amplitude is the consequence of variation in transmitter concentration. *Neuron* 15: 885–895, 1995.

Gasparini S, Saviane C, Voronin LL, and Cherubini E. Silent synapses in the developing hippocampus: lack of functional AMPA receptors or low probability of glutamate release? *Proc Natl Acad Sci USA* 15: 97: 9741–9746, 2000.

Gulyas AI, Miles R, Sik A, Toth K, Tamamaki N, and Freund TF. Hippocampal pyramidal cells excite inhibitory neurons through a single release site. *Nature* 366: 683–687, 1993.

Hanse E and Gustafsson B. Quantal variability at glutamatergic synapses in area CA1 of the rat neonatal hippocampus. *J Physiol* 531: 467–480, 2001a.

Hanse E and Gustafsson B. Vesicle release probability and pre-primed pool at glutamatergic synapses in area CA1 of the rat neonatal hippocampus. *J Physiol* 531: 481–493, 2001b.

Hanse E and Gustafsson B. Release dependence to a paired stimulus at a synaptic release site with a small variable pool of immediately releasable vesicles. *J Neurosci* 22: 4381–4387, 2002.

Harris KM and Sultan P. Variation in the number, location and size of synaptic vesicles provides an anatomical basis for the nonuniform probability of release at hippocampal CA1 synapses. *Neuropharmacology* 34: 1387–1389, 1995.

Hessler NA, Shirke AM, and Malinow R. The probability of transmitter release at a mammalian central synapse. *Nature* 366: 569–572, 1993.

Hjelmstad GO, Isaac JT, Nicoll RA, and Malenka RC. Lack of AMPA receptor desensitization during basal synaptic transmission in the hippocampal slice. *J Neurophysiol* 81: 3096–3099, 1999.

Hsia AY, Malenka RC, and Nicoll RA. Development of excitatory circuitry in the hippocampus. *J Neurophysiol* 79: 2013–2024, 1998.

- Huang EP and Stevens CF.** Estimating the distribution of synaptic reliabilities. *J Neurophysiol* 78: 2870–2880, 1997.
- Jonas P, Major G, and Sakmann B.** Quantal components of unitary EPSCs at the mossy fibre synapse on CA3 pyramidal cells of rat hippocampus. *J Physiol* 472: 615–663, 1993.
- Kamiya H and Zucker RS.** Residual Ca^{2+} and short-term synaptic plasticity. *Nature* 371: 603–606, 1994.
- Katz B.** *The Release of Neural Transmitter Substances.* Sherrington Lectures No. 10. Liverpool, UK: Liverpool Univ. Press, 1969.
- Kirischuk S, Veselovsky N, and Grantyn R.** Relationship between presynaptic calcium transients and postsynaptic currents at single gamma-aminobutyric acid (GABA)ergic boutons. *Proc Natl Acad Sci USA* 96: 7520–7525, 1999.
- Larkman A, Stratford K, and Jack J.** Quantal analysis of excitatory synaptic action and depression in hippocampal slices. *Nature* 350: 344–347, 1991.
- Liao D, Jones A, and Malinow R.** Direct measurement of quantal changes underlying long-term potentiation in CA1 hippocampus. *Neuron* 9: 1089–1097, 1992.
- Liu G, Choi S, and Tsien RW.** Variability of neurotransmitter concentration and nonsaturation of postsynaptic AMPA receptors at synapses in hippocampal cultures and slices. *Neuron* 22: 395–409, 1999.
- Liu G and Tsien RW.** Synaptic transmission at single visualized hippocampal boutons. *Neuropharmacology* 34: 1407–1421, 1995.
- Magee JC and Cook EP.** Somatic EPSP amplitude is independent of synapse location in hippocampal pyramidal neurons. *Nat Neurosci* 3: 895–903, 2000.
- Maggi L, Sola E, Minneci F, Le Magueresse C, Changeux JP, and Cherubini E.** Persistent decrease in synaptic efficacy induced by nicotine at Schaffer collateral–CA1 synapses in the immature rat hippocampus. *J Physiol* 559: 863–874, 2004.
- Mainen ZF, Malinow R, and Svoboda K.** Synaptic calcium transients in single spines indicate that NMDA receptors are not saturated. *Nature* 399: 151–155, 1999.
- McAllister AK and Stevens CF.** Nonsaturation of AMPA and NMDA receptors at hippocampal synapses. *Proc Natl Acad Sci USA* 97: 6173–6178, 2000.
- Nicholls J and Wallace BG.** Quantal analysis of transmitter release at an inhibitory synapse in the central nervous system of the leech. *J Physiol* 281: 171–185, 1978.
- Nimchinsky EA, Yasuda R, Oertner TG, and Svoboda K.** The number of glutamate receptors opened by synaptic stimulation in single hippocampal spines. *J Neurosci* 24: 2054–2064, 2004.
- Oertner TG, Sabatini BL, Nimchinsky EA, and Svoboda K.** Facilitation at single synapses probed with optical quantal analysis. *Nat Neurosci* 5: 657–664, 2002.
- Pyle JL, Kavalali ET, Piedras-Renteria ES, and Tsien RW.** Rapid reuse of readily releasable pool vesicles at hippocampal synapses. *Neuron* 28: 221–231, 2000.
- Raghavachari S and Lisman JE.** Properties of quantal transmission at CA1 synapses. *J Neurophysiol* 92: 2456–2467, 2004.
- Redman S.** Quantal analysis of synaptic potentials in neurons of the central nervous system. *Physiol Rev* 70: 165–198, 1990.
- Regehr WG and Stevens CF.** Physiology of synaptic transmission and short-term plasticity. In: *Synapses*, edited by Cowan WM, Sudhof TC, and Stevens CF. Baltimore, MD: Johns Hopkins Univ. Press, 2001, p. 135–175.
- Rizzoli SO and Betz WJ.** Synaptic vesicle pools [Review]. *Nat Rev Neurosci* 6: 57–69, 2005.
- Sakaba T and Neher E.** Quantitative relationship between transmitter release and calcium current at the calyx of held synapse. *J Neurosci* 21: 462–476, 2001.
- Schikorski T and Stevens CF.** Quantitative ultrastructural analysis of hippocampal excitatory synapses. *J Neurosci* 17: 5858–5867, 1997.
- Schikorski T and Stevens CF.** Morphological correlates of functionally defined synaptic vesicle populations. *Nat Neurosci* 4: 391–395, 2001.
- Shao J and Tu D.** *The Jackknife and Bootstrap.* Springer Series in Statistics. New York: Springer-Verlag, 1995.
- Shepherd GM and Harris KM.** Three-dimensional structure and composition of CA3→CA1 axons in rat hippocampal slices: implications for presynaptic connectivity and compartmentalization. *J Neurosci* 18: 8300–8310, 1998.
- Silver RA.** Estimation of nonuniform quantal parameters with multiple-probability fluctuation analysis: theory, application and limitations. *J Neurosci Methods* 130: 127–141, 2003.
- Silver RA, Cull-Candy SG, and Takahashi T.** Non-NMDA glutamate receptor occupancy and open probability at a rat cerebellar synapse with single and multiple release sites. *J Physiol* 494: 231–250, 1996.
- Stevens CF and Wang Y.** Facilitation and depression at single central synapses. *Neuron* 14: 795–802, 1995.
- Stricker C, Field AC, and Redman SJ.** Statistical analysis of amplitude fluctuations in EPSCs evoked in rat CA1 pyramidal neurones in vitro. *J Physiol* 490: 419–441, 1996.
- Tong G and Jahr CE.** Block of glutamate transporters potentiates postsynaptic excitation. *Neuron* 13: 1195–1203, 1994.
- Umemiya M, Senda M, and Murphy TH.** Behaviour of NMDA and AMPA receptor-mediated miniature EPSCs at rat cortical neuron synapses identified by calcium imaging. *J Physiol* 521: 113–122, 1999.
- Wadiche JI and Jahr CE.** Multivesicular release at climbing fiber–Purkinje cell synapses. *Neuron* 32: 301–313, 2001.
- Wall MJ and Usowicz MM.** Development of the quantal properties of evoked and spontaneous synaptic currents at a brain synapse. *Nat Neurosci* 1: 675–682, 1998.
- Zhai RG, Vardinon-Friedman H, Cases-Langhoff C, Becker B, Gundelfinger ED, Ziv NE, and Garner CC.** Assembling the presynaptic active zone: a characterization of an active one precursor vesicle. *Neuron* 29: 131–143, 2001.

- **Signalling properties of *stratum oriens* interneurons of the hippocampus: see enclosed paper**

**Signalling properties of *stratum oriens* interneurons of the hippocampus
of transgenic mice expressing EGFP in a subset of somatostatin-
containing cells**

In preparation

Federico Minneci, Mahyar Janahmadi, Natasa Dragicevic, Daniela Avossa, Michele
Migliore and Enrico Cherubini

Introduction

The hippocampal circuit is characterized by a large variety of distinct locally connected GABAergic cell types (Ramón y Cajal, 1911; Freund & Buzsáki, 1996) which, by releasing GABA on principal cells and interneurons, exert a powerful control on network excitability and are responsible for the oscillatory behaviour crucial for information processing in the brain. GABAergic interneurons selectively innervate different domains of pyramidal cells, thus providing the main source of feedback and feed-forward inhibition (Freund & Buzsáki, 1996; Miles *et al.* 1996). Due to their extensive dendritic and axonal arborisation, GABAergic interneurons can phase the output of principal cells giving rise to a coherent oscillatory activity (Klausberger *et al.* 2003; Klausberger *et al.* 2004; Somogyi & Klausberger, 2005), which occurs at different frequencies (Buzsáki, 2002; Whittington & Traub, 2003). Although some oscillations can be reproduced *in vitro*, they occur mainly *in vivo* during particular behavioural states of the animal (Buzsáki, 2002; Buzsáki & Draguhn, 2004). Oscillations have been implicated in encoding, consolidation and retrieval of information in the hippocampus (Freund & Buzsáki, 1996). Oscillatory rhythms are facilitated by the intrinsic properties of GABA releasing cells (Maccaferri & McBain, 1996) and by their electrical coupling *via* gap junctions (Hestrin & Galarreta, 2005). Different interneuron ensembles, each one comprising interneurons with similar characteristics, would define multiple functional networks (Blatow *et al.* 2003; Hestrin & Galarreta, 2005).

GABAergic interneurons have been differently classified according to their morphological, neurochemical and physiological characteristics, which include the intrinsic firing, network properties and activity dependent synaptic plasticity processes. In particular, in the CA1 area of the hippocampus, at least 16 different types of interneurons have been characterized on the basis of their selective targets (Somogyi & Klausberger, 2005).

More recently, transgenic techniques have been used to identify subsets of interneurons expressing enhanced green fluorescent protein (EGFP) in cells containing particular peptides or calcium binding proteins (Monyer & Markram, 2004). Using this approach, Oliva *et al.* (2000) have generated transgenic mice expressing EGFP in a subpopulation of interneurons containing somatostatin (GIN mice). According to these authors, the vast

majority of EGFP positive cells present in *stratum oriens* of the CA1 area projects to *stratum lacunosum-moleculare* (O-LM; Oliva *et al.* 2000). O-LM interneurons have been thoroughly investigated (Lacaille *et al.* 1987; Lacaille & Williams, 1990; McBain *et al.* 1994; Maccaferri & McBain, 1996; Maccaferri *et al.* 2000; Maccaferri & Lacaille, 2003; Maccaferri, 2005). They constitute a large proportion of *stratum oriens* horizontal neurons with soma and dendrites lying in *stratum oriens* and axons projecting to distal dendrites of CA1 pyramidal cells in *stratum lacunosum-moleculare*, the region that receives entorhinal cortex inputs (Maccaferri, 2005). They are driven by axon collaterals of CA1 principal cells (Lacaille *et al.* 1987; Blasco-Ibanez & Freund, 1995; Maccaferri & McBain, 1995; Ali & Thomson, 1998; Losonczy *et al.* 2002; Pouille & Scanziani, 2004) to such extent that synaptic plasticity on principal cells can be passively propagated to interneurons (Maccaferri & McBain, 1995; 1996).

Here, pair recordings from interconnected EGFP-positive cells in *stratum oriens* or interneurons and principal cells have been used to further characterize the functional properties of this type of interneurons in hippocampal slice cultures obtained from GIN mice (Oliva *et al.* 2000). We found that EGFP-positive interneurons in *stratum oriens* of GIN mice constitute a heterogeneous population of cells which are interconnected through electrical synapses. The dynamic interaction between electrically coupled interneurons with different firing properties can differentially affect target cells and act as a powerful filter which may be crucial for information processing within the hippocampal network.

Methods

Hippocampal slice cultures

Experiments were performed on hippocampal slices in culture. Hippocampal slices were obtained from post-natal day 8 (P8) EGFP-positive mice (GIN mice: Jackson Laboratories, Maine, USA; Oliva *et al.* 2000), following the procedure previously described by Stoppini *et al.* (1991). All experiments were carried out in accordance with the European Community Council Directive of 24 November 1986 (86/609EEC) and were approved by local authority veterinary service. Briefly, animals were decapitated after being anaesthetized with an i.p. injection of urethane (2 g/Kg) and the brains were quickly removed from the skull and placed in ice-cold dissection medium consisting of modified Eagle's medium (MEM, Invitrogen, Milan, Italy) containing HEPES (25 mM, Sigma, Milan, Italy), Tris base (10 mM), D-glucose (10 mM), MgCl₂ (3 mM) and penicillin-streptomycin (100 µg/ml, Invitrogen). Tissue slices (400 µm thick) containing the hippocampus and the entorhinal cortex were obtained using the McIlwain tissue chopper. Slices were placed on 30 mm cell culture inserts (Millicell-CM, Millipore, USA) and maintained in culture at the interface between air and culture medium in a CO₂ incubator at 37° C. Culture medium consisted of MEM containing 20% horse serum (Invitrogen), HEPES (25 mM), D-glucose (25 mM), MgCl₂ (2.5 mM), ascorbic acid (0.5 mM), insulin 0.5 mg/ml (Sigma) and penicillin-streptomycin (100 µg/ml). Cultures were maintained for up to 4 weeks.

Electrophysiological recordings

After 1 to 3 weeks in culture, slices, which had flattened to a thickness of about 150 µm, were transferred to a recording chamber under an upright microscope equipped with both fluorescence and IR-DIC video microscopy. The culture in the recording chamber was continuously perfused (2-4 ml/min) at 33-35 °C with a solution containing (mM): NaCl 150, KCl 3, CaCl₂ 2, MgCl₂ 1, Hepes 10, glucose 12 (pH 7.3, adjusted with NaOH). EGFP-positive interneurons in the *stratum oriens* of CA1 were visually identified using a 60X objective by switching between fluorescence and IR-DIC video microscopy. CA1 pyramidal cells were identified both visually by IR-DIC video microscopy and on the basis of their firing properties (i.e. their ability to accommodate in response to long

depolarising current pulses). In some cases (n=20), EGFP-positive interneurons were labelled with neurobiotin (0.2 %; Vector Laboratories, Burlingame, CA, USA) for later morphological identification. EGFP-positive interneurons were also morphologically identified by electroporation according to a previously described method (Lohmann *et al.* 2005; n=8), using patch pipettes containing sulforhodamine B (dissolved in methanol at 1 mg/ml). Whole-cell patch-clamp recordings (in current and voltage clamp mode) were performed from EGFP-positive interneurons in stratum oriens and/or CA1 principal cells using a Multiclamp 700A amplifier (Molecular Devices, Union City, CA, USA). Patch electrodes were pulled from borosilicate glass capillaries (Hingenberg, Malsfeld, Germany). They had a resistance of 5–7 M Ω when filled with the intracellular solution. For single patch experiments the intracellular solution contained (in mM): KMeSO₄ 135, KCl 10, Hepes 10, MgCl₂ 1, Na₂ATP 2, Na₂GTP 0.4 (solution 1). For pair recordings it contained (in mM): K-gluconate 135, KCl 5, Na₂HPO₄ 10, EGTA 0.5, MgATP 4, MgGTP 0.3 (solution 2). The pH was adjusted to 7.3 with KOH. The reversal potential for Cl⁻ was -65 mV for solution 1 and -87 mV for solution 2. The stability of the patch was checked by monitoring the input and series resistances during the experiment, and cells exhibiting changes bigger than 20% were excluded from the analysis. Membrane potential values were corrected for a liquid junction potential of 12 mV (solution 1) and 17 mV (solution 2). Excitatory and inhibitory postsynaptic currents (EPSCs and IPSCs) were recorded from a holding potential of -65 mV.

Drugs were applied to the bath *via* a three-way tap system. The following drugs were used: tetrodotoxin (Latoxan, Valence, France); sulforhodamine B (sodium salt), carbenoxolone (disodium salt) and bicuculline methiodide (Sigma); ZD7288, DL-2-amino-5-phosphonopentanoic acid (D-AP5) and 6,7-dinitroquinoxaline-2,3-dione (DNQX) (Tocris Bioscience, Bristol, UK). DNQX was dissolved in dimethylsulphoxide (DMSO). The final concentration of DMSO in the bathing solution was 0.1%.

Data acquisition and analysis

Data were transferred to a computer after digitization with an A/D converter (Digidata 1322, Molecular Devices). Data acquisition (digitized at 20 kHz and filtered at 2 kHz) was performed with pClamp 9.2 software (Molecular Devices). Input resistance and

capacitance of the cells were measured online with the Membrane Test feature of the pClamp software. Data were analyzed with Clampfit 9.2 (Molecular Devices). Single spikes were evoked in current clamp mode by short (5 ms) depolarizing current pulses. Hyperpolarizing electrotonic potentials were obtained by injecting 400 ms long hyperpolarizing current pulses. Voltage-dependent membrane oscillations and firing patterns were studied by injecting long (800 ms) depolarizing current pulses of variable amplitude. Power spectra were constructed from single traces, using the Power Spectrum feature of Clampfit 9.2 (Molecular Devices) with a rectangular window and a sample number of 4096 which corresponds to a spectral resolution of 2.44 Hz. Interspike interval (ISI) histograms were constructed using a custom-written programme in Matlab 7.1 (MathWorks, Natick, MA, USA). Impedance measurements were obtained by injecting long (10 s) sinusoidal current pulses at various frequencies (0.5, 1, 2, 5, 10, 20, 50, 100 Hz) in current clamp mode and calculating the ratio of the amplitude of the voltage response over the amplitude of the injected current waveform.

In pair recordings from interconnected EGFP-positive cells the coupling coefficient was calculated as the ratio of the amplitude of the electrotonic potential in one cell over the amplitude of the electrotonic potential in the other cell. At glutamatergic synapses, trains of 10 spikes were evoked at a definite frequency (20 Hz, 50 Hz or 100 Hz) in the presynaptic neuron (at least 20 consecutive sweeps for each frequency). The probability of successes was calculated as the number of postsynaptic responses over the total number of presynaptic spikes. Failures were visually identified. For each frequency, the potency ratio was calculated as the ratio of the mean potency of synaptic responses to the 10th spike within the trains over the mean potency of the responses to the 1st spike.

Data are presented as the mean \pm S.E.M. Comparisons between active and passive membrane properties were done using the unpaired t-test. Comparisons for differences in the probability and potency ratio were assessed by ANOVA followed by post hoc multiple comparison Tukey test. The differences were considered significant for $p < 0.05$.

Immunocytochemical experiments

Mice were anesthetized using diethylether and perfused transcardially with phosphate buffer saline (PBS), followed by PBS containing 4% paraformaldehyde (Sigma). Brains

were removed from the skull and stored in the same fixative overnight, at 4° C. The day after, brains were placed into a solution containing 30% sucrose in PBS. Coronal brain slices (50 µm-thick) were cut using a freezing sliding microtome and stored in PBS for further use. Sections containing the hippocampus were incubated overnight at 4° C in the following primary antibodies diluted in blocking buffer (3% normal goat serum, 0.3 % Triton X-100 and 3% bovine serum albumin): rabbit polyclonal anti-somatostatin 28 (1:700, AB 1752, Chemicon, Temecula, CA, USA); rabbit polyclonal anti-neuropeptide Y (1:1000, AB 10980, AbCam, Cambridge, UK); rabbit polyclonal anti-metabotropic glutamate receptor (1:100, AB 27199, AbCam); mouse monoclonal anti-parvalbumin (1:700, MAB 1572, Chemicon); rabbit polyclonal anti-GFP (1:1000, kindly provided by Dr. Kevin Ainger, Adriacell, Trieste, Italy). Brain sections were rinsed in PBS and incubated for 90 min at room temperature with the following secondary antibodies: Alexa Fluor 594 goat anti-rabbit, Alexa Fluor 594 goat anti-mouse and Alexa Fluor 488 goat anti-rabbit (Molecular Probes, Eugene, OR, USA, 1:350 diluted in blocking buffer). Sections were subsequently rinsed and wet-mounted using glycerol / pH 8.6 PBS (9:1) containing 2.5 % 1,4diazabicyclo-(2,2,2)-octane (Sigma), in order to prevent fluorescence fading. Slides were viewed using a Zeiss Axioskop (Germany) microscope equipped with a CCD camera. Images were exported and further processed using Adobe Photoshop and Corel Draw.

Modelling

All the simulations were carried out with the NEURON simulation program (Hines & Carnevale, 1997, v5.8) using its variable time step feature. The complete model and simulation files are available for public download under the ModelDB section of the Senselab database (<http://senselab.med.yale.edu>).

The morphology of the interneuron was based on a 3D reconstruction of a real cell (O-LM; Saraga *et al.* 2003), and it was downloaded from the public ModelDB archive. The same, uniform, passive properties were used for all compartments ($\tau_m = 25$ ms, $R_m = 25$ k Ω ·cm², $R_a = 150$ Ω ·cm). Resting potential was set at -65 mV and temperature at 34°C. We found that the basic firing behaviour of the cells described in this paper (regular and clustered) can be appropriately modelled using only a Na⁺ conductance and two fast and

slowly inactivating K^+ conductances. Since detailed information on the channels' subunits composition and distribution for the specific kind of neurons described in this work is not available, we decided to implement our model using the minimum number of active conductances that can reproduce the main properties of our cells. For this reason, to reproduce an action potential we used a Na^+ conductance from CA1 hippocampal pyramidal neurons (Migliore *et al.* 1999) and a fast inactivating K^+ channel from mitral cells in the olfactory bulb (K_f ; Wang *et al.* 1996). To obtain clusters of action potentials, we inserted in all compartments a slowly inactivating K^+ current (K_s) that has been proposed to be responsible for this effect in putatively GABAergic neurons in the nucleus basalis (Wang, 2002). We found that only slight modifications of the original kinetic parameters of the Na^+ and K_s conductances (a +15 mV shift of the activation/inactivation for Na^+ , and a steeper activation for K_s) were sufficient to qualitatively match all of our experimental traces under different current clamp conditions.

The current generated by a gap junction (GJ) was modelled as $I_{GJ} = g_{gap} \cdot (v_{post} - v_{pre})$, where g_{gap} , v_{post} , and v_{pre} , are the GJ conductance, the post- and the pre-synaptic membrane potentials, respectively. There is no indication from experiments on the dendritic location and total conductance. In our model, a 1.5 nS GJ connecting two identical model neurons at $\sim 120 \mu m$ from soma resulted in somatic voltage deflections very close to those recorded experimentally.

Results

Identification of EGFP-positive interneurons in stratum oriens

In agreement with Oliva *et al.* (2000), in acute hippocampal slices from P8 GIN mice, the vast majority of EGFP-positive interneurons were confined to *stratum oriens* (SO) and *stratum radiatum* (SR) of the CA1 and CA3 hippocampal regions and in the *hilus* (Figure 1A). Some of these cells exhibited the characteristics of O-LM interneurons with oval cell bodies and horizontal dendrites running in *stratum oriens* parallel to *stratum pyramidale* (Figure 1a). As previously shown (Stoppini *et al.* 1991), after 2-3 weeks, cultured slices maintained the characteristic architecture of acute hippocampal slices (De Simoni *et al.* 2003). In addition, several EGFP-positive cells could be identified displaying a morphology similar to that observed in acute slices (Figure 1B-D). In the

present study we examined only those interneurons with somata localized in *stratum oriens* of the CA1 area. A closer view of two EGFP-positive cells in stratum oriens, obtained with single-cell electroporation, shows overlapping extensive dendritic arborisations (Figure 1C). As explained in detail in a later section, dendritic arborisations were often establishing electrical connections. Figure 1D shows two electrically connected interneurons (as confirmed by electrophysiological data) labelled with neurobiotin.

EGFP-positive interneurons in *stratum oriens* were also identified according to their neurochemical markers. Thus, as shown in Figure 1E, every EGFP-positive cell was immunopositive for the neuropeptide somatostatin. However, somatostatin-positive neurons which were not expressing EGFP could be also identified (Oliva *et al.* 2000; Halabisky *et al.* 2006; see asterisk in Figure 1E). EGFP-positive cells also expressed the splice variant of the metabotropic glutamate receptor 1 α (Figure 1F). On the contrary, only few EGFP-positive cells were immunoreactive for the neuropeptide Y (NPY; Figure 1G) and none of them were immunopositive for parvalbumin (data not shown). In summary, the immunocytochemical characterization of EGFP-positive cells in *stratum oriens* was similar in all respects to that of previously identified O-LM interneurons (McBain *et al.* 1994; Katona *et al.* 1999; Maccaferri *et al.* 2000; Losonczy *et al.* 2002; Klausberger *et al.* 2003).

Passive and active membrane properties of O-LM interneurons

Whole cell recordings in current or voltage clamp mode were performed from 203 EGFP-positive *stratum oriens* interneurons having a resting membrane potential ranging from –61 mV to –79 mV (on average -70.5 ± 1.0 mV; n=30) and a membrane input resistance (measured from voltage responses to current pulses of different intensities) ranging from 90 M Ω to 798 M Ω (on average 246 ± 26 M Ω ; n=30). Cell capacitance varied between 56 pF and 180 pF (on average 110 ± 5 pF; n=30). The high capacitance values observed in some cells (often associated with low input resistance) probably reflects the larger dendritic arborisation of some interneurons after few weeks in culture (De Simoni *et al.* 2003). The passive membrane properties of these neurons are summarized in Table I. The majority of these cells did not fire spontaneously. Short (5 ms) depolarizing current

pulses induced action potentials with mean amplitude of 77.9 ± 1.4 mV and spike threshold of -51.9 ± 0.5 mV ($n=30$; Table I). Spike repolarization was relatively fast (spike width at half amplitude was 0.84 ± 0.03 ms; $n=30$) and was often followed by a large after-hyperpolarization. Injection of hyperpolarizing current pulses of different amplitude from the resting membrane potential revealed, in all cells examined, a sag in the electrotonic potential (Figure 2A, left), which varied in amplitude between one cell to another and was followed by a rebound depolarization occasionally giving rise to an action potential. The sag was abolished by ZD7288 (100 μ M) indicating that the time-dependent inwardly rectifying cationic current I_h was responsible for it (Figure 2A, right). Another prominent feature found in a minority of tested interneurons (20%) was the presence of active conductances observed when the membrane was depolarized from rest and synaptic transmission was blocked with D-AP5 (50 μ M), DNQX (20 μ M) and bicuculline (10 μ M). Thus, sustained depolarizing current pulses (800 ms), subthreshold for spike activation, revealed voltage-dependent membrane oscillations superimposed on the top of the electrotonic potential (Figure 2B, left). Further depolarization of the membrane induced repetitive high frequency firing. These oscillations were readily blocked by tetrodotoxin (1 μ M), indicating that voltage-dependent sodium channels were essential for their generation (Figure 2B, right). As shown in the example of Figure 2C the power spectrum of oscillations had a peak around 40 Hz.

Stratum oriens interneurons exhibit different firing patterns

Long depolarizing current pulses (800 ms duration) were used to characterize the firing patterns of EGFP-positive interneurons that did not fire spontaneously. In agreement with Parra *et al.* (1998) we found that, at the same membrane potential, cells fired with at least three distinct firing patterns which remained constant over time: regular, irregular and clustered (Figure 3). In regular firing cells, the interspike interval was constant for the entire duration of the pulse and the repolarization following each action potential directly initiated the next spike. In irregular firing neurons, the interspike interval was variable and spike repolarization was often followed by a variable delay before the occurrence of the next spike. In clustered cells, brief trains of spikes occurring at regular intervals were separated by silent periods of variable duration, usually exhibiting voltage dependent

oscillations (see preceding paragraph). Irregular firing cells occurred more frequently (48%) than clustered and regular firing neurons that were observed in 22% and 30% of the cases, respectively. For each individual cell the interspike interval was usually calculated from 10 sweeps obtained at the same membrane potential. As illustrated in Figure 3, each cell type exhibited characteristic interspike interval distributions. In order to see whether a particular firing pattern could be converted into another by membrane depolarization, current steps of increasing amplitude were applied to individual cells. Increasing membrane depolarization did not significantly alter the firing patterns (Figure 4). However, in all neurons examined (n=90), an increase in amplitude of the depolarizing current steps produced an enhancement of the instantaneous interspike or intercluster frequency. Thus, it seems likely that each individual cell possesses a particular set of voltage-dependent conductances responsible for their firing. This would in turn regulate neuronal signalling between EGFP-positive interneurons or between interneurons and principal cells.

It is worth noticing that, with the exception of clustered cells exhibiting lower values of input resistance, no correlation was found between different firing patterns and passive membrane properties of the cells (Table I).

Resonance properties of EGFP-positive interneurons in stratum oriens

One characteristic feature of interneurons is to exhibit coherent oscillations at different frequencies (Whittington & Traub, 2003). Distinct types of interneurons display an enhancement of the voltage responses to subthreshold oscillatory inputs (resonance) at different frequencies. This accounts for different frequency preferences of the firing output. In order to investigate their resonance properties, sinusoidal currents at frequencies ranging from 0.5 to 100 Hz were injected into EGFP-positive interneurons held in current clamp conditions under threshold for generating action potentials (Figure 5). The impedance of the membrane was calculated and plotted as a function of the stimulus frequency (Figure 5C, left). The maximal value of the impedance, corresponding to resonance, was always (n=7) in the frequency range of 1-5 Hz. A plot of the impedance normalised to the value at 0.5 Hz, averaged for 7 interneurons, is shown in Figure 5C (right). These data indicate that the resonance properties of the EGFP-positive

interneurons in *stratum oriens* are similar to those found for O-LM interneurons (Pike *et al.* 2000).

Stratum oriens interneurons are electrically coupled via gap junctions

Pair recordings from EGFP-positive cells localized in *stratum oriens* revealed the presence of electrical synapses in 47% of cases (8/17). Electrically coupled cells were located at least two cell diameters apart (~ 50 μm) indicating that gap junctions were not directly connecting the soma of the patched cells. Figure 6A shows simultaneous current clamp recordings from two cells one of which (cell 1) was firing spontaneously at 20 Hz. Each action potential in cell 1 was associated with a small electrotonic pre-potential (a so-called “spikelet”) in cell 2. Electrotonic transmission was reciprocal in all recordings. The electrotonic coupling persisted in the presence of the AMPA, NMDA and GABA_A receptor antagonists DNQX, D-AP5 and bicuculline, respectively, but was abolished by the selective gap junction blocker carbenoxolone (200 μM , n=3; Figure 6B). In previous work from cortical interneurons it was shown that electrical coupling coexisted with chemical synaptic transmission (Galarreta & Hestrin, 1999). Although we can not exclude that at least in some of the present cases synaptic potentials or currents could be “masked” by the large electrotonic responses, EGFP-positive interneurons appeared to be connected preferentially *via* gap junctions. Thus, we failed to detect inhibitory connections between electrically coupled interneurons even in the presence of carbenoxolone or when several traces (up to 30 sweeps) were averaged. Interestingly, blocking the electrical coupling with carbenoxolone induced the appearance of barrages of spontaneous glutamatergic synaptic responses (Figure 6C), suggesting that uncoupling removes the strong inhibitory action of the interneuronal network on principal cells.

Electrical coupling between EGFP-positive cells in *stratum oriens* was independent of the firing patterns of individual neurons. In the representative sample of Figure 7A, a steady depolarizing current step in cell 2 produced an irregular firing. This was associated in cell 1 with “spikelets” that under voltage clamp conditions were seen as fast inward currents followed by slower outward currents reflecting the after-hyperpolarization occurring after each action potential. Current injection in cell 1 produced regularly firing action potentials that were time-locked in cell 2 with inward spikelet-like currents.

Moreover, in all cells tested, a hyperpolarizing current pulse applied to one cell produced a simultaneous electrotonic potential in the second cell that was smaller in amplitude (Figure 7B). Changes in membrane potential of two coupled cells produced by injecting current in one of them were used to measure the coupling coefficient (Hestrin & Galarreta, 2005). On average, this was 0.21 ± 0.07 (n=5). Interestingly, in a pair of interconnected cells in which the coupling coefficient was particularly high (0.47), spontaneous firing in one neuron was able to trigger action potentials in the second one. A careful examination of the traces shown on Figure 8A revealed that, when two spontaneous action potentials in cell 1 were sufficiently close in time, the corresponding spikelets summated giving rise to an action potential in cell 2 which was time locked with the second spike. In addition, spikelets in one cell could influence the firing of the other cell and *vice versa*. When cell 1 was depolarized to fire action potentials at high frequency (in the gamma range), cell 2 displayed time locked spikelets which summated to give rise to action potentials occurring at lower frequency (in the theta range). Depolarization of cell 2 produced a similar effect in cell 1 (Figure 8B).

Therefore, strong electrical coupling acting as a powerful low-pass filter may contribute to alter the output of individual cells from gamma to theta frequency discharges, thus providing a mechanism for modifying synaptic weights and the temporal coding of neuronal ensembles.

Synaptic connectivity between principal cells and interneurons

Pair recordings from interconnected EGFP-positive interneurons in *stratum oriens* and principal cells allowed identification of their reciprocal connections. In the presence of DNQX (20 μ M) and D-AP5 (50 μ M), action potentials in interneurons evoked IPSCs in CA1 pyramidal cells (held at -65 mV). At this holding potential the synaptic currents were outward (see Methods). In spite many efforts, this type of connection was found only in few cases (3 out of 45). This may be attributed to the distal location of the synapses under investigation. Consistent with electrotonic filtering, synaptic currents were very small in amplitude (on average 2.6 ± 0.3 pA) and exhibited slow kinetics. In one case they could be seen only after averaging twenty sweeps (see also Lacaille *et al.* 1987 and Maccaferri *et al.* 2000). This precluded the possibility to perform any further

analysis on individual responses. When a paired pulse protocol was used, the peak amplitude of the second IPSC (evoked by a presynaptic spike occurring 50 ms after the first one) was unchanged or slightly reduced. Action potentials evoked in the presynaptic neuron at 20 Hz induced in pyramidal cells synaptic currents (Figure 9A) that exhibited short-term depression.

In contrast, excitatory connections between principal cells and EGFP-positive interneurons in *stratum oriens* were easily detectable (17/55; Figure 9B). Interneurons in *stratum oriens* are known to receive a strong excitatory input from CA1 pyramidal cells (Lacaille *et al.* 1987; Ali & Thomson, 1998; Losonczy *et al.* 2002), which is known to be further enhanced in cultured slices (De Simoni *et al.* 2003). In seventeen successful pair recordings from principal cells and interneurons, action potentials in principal cells evoked in interneurons EPSCs that, at a holding potential of -65 mV, were inward and were intermingled with transmission failures. These EPSCs were mediated by AMPA receptors since they were readily blocked by DNQX (20 μ M; data not shown). In double pulses experiments, the probability of successes to the first action potential varied from 0.17 to 0.91 (on average 0.45 ± 0.08 ; $n=10$). In agreement with previous data (Ali & Thomson, 1998), the second EPSC (occurring 50 ms after the first one) was always facilitated. The PPR calculated as the ratio between the amplitude of the second EPSC over that of the first one was 1.5 ± 0.2 ($n= 10$).

The ability of the excitatory synapses to follow trains of action potentials at different frequencies was studied in ten pairs on interconnected cells. Excitatory synaptic currents were evoked in interneurons by trains of 10 presynaptic spikes occurring at 20 Hz (repeated at least 20 times). EPSCs evoked by trains of presynaptic action potentials at 50 and 100 Hz were also recorded with the same protocol. As shown in the representative sample of Figure 9C, the synaptic responses were able to follow the presynaptic spikes at all frequencies. Moreover, in contrast with the inhibitory currents in principal cells, EPSCs in interneurons exhibited short-term facilitation. Both the overall probability of successes and the ratio of the average potency of the 10th response over the first one were used to measure the efficiency of these synapses at the 3 different frequencies tested. The plots of Figure 9D clearly demonstrate that, on average, the probability of successes and the potency ratio were significantly higher at 50 Hz than at 20 Hz ($p<0.01$ and $p<0.05$

respectively). At 100 Hz the probability of successes was not significantly different from that observed at 50 Hz, while the potency ratio was significantly ($p < 0.001$) reduced. The combination of these two frequency-dependent effects makes synapses between principal cells and interneurons particularly reliable in the gamma frequency band.

EGFP-positive interneurons may differentially affect target cells according to their firing properties: a simulation model

From the present experiments it is clear that EGFP-positive interneurons in *stratum oriens* constitute a heterogeneous group of cells with different firing properties. Therefore, according to the relative weight of a particular firing pattern, electrically coupled interneurons may differentially affect target cells. As already mentioned, the probability of finding inhibitory connections between *stratum oriens* interneurons and principal cells was extremely low. To figure out the possible functional consequences of the different firing behaviours, we implemented a simple qualitative model using the same morphology of an O-LM interneuron but with different active properties. We found that regularly firing interneurons could be appropriately modelled using only Na^+ and a fast inactivating K^+ current (K_f ; Figure 10A, O_R). The inclusion of a K_s was sufficient to obtain clusters of action potentials (Fig.10A, O_C). Next, we investigated the coupling caused by a dendritic gap junction connecting two cells with different firing properties as observed from the soma (Figure 10B). In agreement with experimental finding, in both cases, a somatic current injected into an O_R (Figure 10B, middle) or an O_C cell (Figure 10B, right) resulted in the same depolarization pattern in both cells, independently from the intrinsic firing properties of the neuron driven by the gap junction conductance. This is a potentially important result, because it implies that the output of the same network of interneurons can be modulated and delivered to the target cells as a regular or clustered train of synaptic activations, according to which kind of cells (O_R or O_C) is receiving the main input. Because of the short-term depression of the synapses formed by interneurons the different output could result in drastically different overall inhibitory effects. We show the prediction of our model in the simulations of Figure 10C, where we modelled, in qualitative agreement with experiments, a short-term depression of the synaptic conductance according to the instantaneous interspike interval. From the simulations, it is

clear that cells firing regularly at approximately the gamma frequency (as in Figure 10C, middle) would result, within a few hundreds of ms from the beginning of the stimulus, in a strong depression of the inhibitory conductance. In striking contrast, for clustered action potentials the conductance would have enough time to recover its full amplitude during the silent intercluster periods (Figure 10C, right). The net result predicted by the model in the latter case is a strong pacemaker inhibitory effect on the target cells.

Discussion

Here we show that in the hippocampus of GIN mice, EGFP-positive interneurons in *stratum oriens* constitute a heterogeneous population of cells exhibiting different firing patterns. These neurons which were electrically coupled *via* gap junctions, established a well-defined inhibitory network able to provide a coordinated inhibition of distal dendrites of principal cells targeted by entorhinal inputs. Moreover, pair recordings from principal cells and EGFP-positive interneurons revealed a frequency and use-dependent facilitation of glutamatergic synaptic connections in response to trains of spikes occurring in the gamma range.

GABAergic interneurons have been divided into different subclasses according to their morphological, physiological or neurochemical properties (Maccaferri & Lacaille, 2003). However, this distinction may be incorrect because, at the molecular level, the same marker can be found in anatomically or electrically distinct cell types (see Markram *et al.* 2004). An alternative method for identifying GABAergic interneurons consists in labelling a neuronal population containing a particular peptide or calcium binding protein with an *in vivo* marker such as the green fluorescent protein (Monyer & Markram, 2004). This allows controlling the network properties of an ensemble of cells with similar molecular characteristics. This powerful tool has been successfully used to characterize the functional properties of parvalbumin positive (Meyer *et al.* 2002) or parvalbumin and calbindin positive GABAergic cells (Blatow *et al.* 2003). In the present study hippocampal slice cultures obtained from GIN mice (Oliva *et al.* 2000) were used to record EGFP-positive, somatostatin-containing interneurons in *stratum oriens* of the CA1 hippocampal region. As recently described for cortical interneurons (Halabisky *et al.* 2006), not all somatostatin-positive cells were EGFP-positive (see also Oliva *et al.* 2000).

Like O-LM cells previously identified in rats, in the present experiments EGFP-positive interneurons also expressed the splicing form of mGluR1, which was sometimes associated with NPY. (Baude *et al.* 1993; Freund & Buzsaki, 1996; Katona *et al.* 1999; Maccaferri *et al.* 2000; Oliva *et al.* 2000; Losonczy *et al.* 2002). All cells tested were immunonegative for parvalbumin (but see Klausberger *et al.* 2003 and Ferraguti *et al.* 2004). Similar to previously identified O-LM interneurons (McBain *et al.* 1994; Ali & Thomson, 1998; Maccaferri *et al.* 2000; Oliva *et al.* 2000; Losonczy *et al.* 2002), most of the recorded cells displayed dendrites running parallel to the strata borders. However, it was not always possible to identify a clear axonal projection towards *stratum lacunosum-moleculare*. In addition, all EGFP-positive cells exhibited a prominent sag in response to hyperpolarizing current injection (Maccaferri & McBain, 1996; see Maccaferri & Lacaille, 2003; Maccaferri, 2005 for reviews) and a pronounced spike after-hyperpolarization (Ali & Thomson, 1998). Moreover, a minority of recorded cells exhibited fast subthreshold membrane oscillations independent of synaptic transmission which could trigger high frequency trains of action potentials. These oscillations are known to confer resonance characteristics to interneurons (Jonas *et al.* 2004). However, while O-LM interneurons were identified as fast spiking cells with modest spike frequency adaptation, (Lacaille & Williams, 1990; Zhang & McBain, 1995; Oliva *et al.* 2000; Maccaferri & Lacaille, 2003; Jonas *et al.* 2004; Lawrence *et al.* 2006) EGFP-positive cells in *stratum oriens* exhibited different firing patterns, suggesting the involvement of different cell types. For instance, in the outermost layer of the hippocampus, EGFP-positive cells may belong to oriens-bistratified (Maccaferri *et al.* 2000) or trilaminar cells (Somogyi & Klausberger, 2005) whose axons do not project to *stratum lacunosum-moleculare*. However, unlike oriens-bistratified cells (Losonczy *et al.* 2002) EGFP-positive neurons were immunopositive for both somatostatin and mGluR1 receptors and in contrast with trilaminar cells localized in the CA3 region (Gloveli *et al.* 2005), they exhibited a prominent sag in response to hyperpolarizing current injection. Independently of the cellular type, the present study provides evidence that interneurons with different firing properties could be electrically coupled through gap junctions to form a functional network. In the neocortex and in the dentate gyrus of the hippocampus, inhibitory networks are thought to be composed of electrically coupled neurons with

similar characteristics (Connors & Long, 2004; Hestrin & Galarreta, 2005). For instance, in the neocortex, cells with similar firing patterns such as fast spiking (Galarreta & Hestrin, 1999; Gibson et al. 1999), low threshold spiking (Beierlein et al. 2000), late spiking (Chu et al. 2003), multipolar bursting (Blatow *et al.* 2003), regular and irregular spiking cells (Szabadics et al. 2001; Galarreta et al. 2004) are coupled with each other. This would allow to efficiently co-ordinate in space and time GABA release into selective target neurons giving rise to specific types of oscillatory behaviours. However, coupling between neurons with different firing properties have been also observed, although less frequently. Thus, electrical coupling may exist between fast spiking and low threshold spiking neurons (Gibson et al. 1999), fast spiking cells and pyramidal neurons (Meyer et al, 2002). Recently, it has been reported that interneurons located in *stratum lacunosum moleculare* constitute a heterogeneous population of cells with different intrinsic excitability coupled *via* gap junctions to form a functional syncytium (Zsirios & Maccaferri, 2005). Also O-LM interneurons are electrically coupled as revealed in the intact *in vitro* hippocampal preparation (Zhang *et al.* 2004). However, unlike EGFP positive cells in *stratum oriens*, all coupled cells were found to fire regularly and manifested minimal spike frequency adaptation in response to long depolarizing current pulses.

In comparison with the results obtained from the intact hippocampus (Zhang *et al.* 2004), in the present case electrical coupling was present in a larger percentage of cases (18% *versus* 48%) and the average value of the coupling coefficient was higher (7% *versus* 21%). This could be related to the younger age of mice used to prepare slice cultures (Meyer *et al.* 2002) or to modifications introduced with the slice culture preparation. Interestingly, the present experiments show that when electrical coupling was particularly robust it could induce firing in the coupled cell and filter the firing frequency from the gamma to the theta band.

The reciprocal interaction between cells with various firing patterns found in the present experiments may differently control GABAergic signalling, permitting, as suggested by our simulation data, a wide range of interneuronal communication. Thus, regular firing interneurons would induce a short-term depression of IPSCs (see Maccaferri *et al.* 2000), while clustered cells would allow IPSCs to recover during silent intercluster periods.

While in the first case the dynamic interaction would result in cell silencing, in the second it would result in a powerful pacemaker inhibitory action on the target cells.

Interestingly, due to their passive and active membrane properties, different types of neurons exhibit a frequency preference for action potential generation, which confers to distinct types of cells the ability to engender rhythms at different frequencies (Pike *et al.* 2000; Whittington & Traub, 2003). These rhythms provide the temporal structure for coherent network oscillations, associated *in vivo* to various behavioural states of the animals (Buzsaki, 2002). For instance, O-LM interneurons have been shown to exhibit firing preference in the theta band (Pike *et al.* 2000). Similarly, EGFP-positive cells in *stratum oriens* exhibited a selective enhancement of voltage response to oscillatory input (resonance) in the theta range, which underlies the frequency preference for action potential generation.

Pair recordings from interconnected pyramidal cells and interneurons showed that EGFP-positive cells could be activated by spikes elicited in CA1 principal cells. Like in O-LM interneurons (Ali & Thomson, 1998; Losonczy *et al.* 2002), EPSCs evoked by pairs of presynaptic spikes were strongly facilitated, an effect that largely depends on presynaptic increase in release probability (Zucker, 1989). In addition, our data revealed highly reliable synaptic responses which were able to follow presynaptic spikes in a wide range of frequencies. Interestingly, synaptic currents exhibited a prominent facilitation when short trains of presynaptic spikes were evoked in the gamma range, as revealed by the enhanced probability of successes and the strong potency facilitation between the last and the first EPSC. It is worth noticing that the interneuronal output arises from the complex interplay between passive and active membrane properties of the cells under examination, the nature of their reciprocal connectivity (including gap junctions) and incoming synaptic inputs (Pike *et al.* 2000; Schreiber *et al.* 2004; Lawrence *et al.* 2006).

In conclusions, the present data indicate that EGFP-positive interneurons in *stratum oriens* of the hippocampus of GIN mice, which contain somatostatin, constitute a heterogeneous group of cells with distinct firing patterns. Due to their intrinsic properties, these cells preferentially fire in theta frequency range. Moreover, they are interconnected *via* electrical synapses to form a functional network, whose dynamic interactions may differentially affect targeted neurons. Principal cells communicate with EGFP-positive

cells through reliable glutamatergic connections which are particularly efficient at the gamma frequency. The overlapping of these two rhythms may be crucial for encoding complex information. In particular, low frequency oscillations would constitute the carrier wave over which barrages of high frequency synaptic currents would be nested as pieces of informational input, in a similar way as described for short-term memories processing (Bragin *et al.* 1995; Lisman & Idiart, 1995).

References

- Ali AB & Thomson AM (1998). Facilitating pyramid to horizontal oriens-alveus interneurone inputs: dual intracellular recordings in slices of rat hippocampus. *J Physiol* **507**, 185-199.
- Baude A, Nusser Z, Roberts JD, Mulvihill E, McIlhinney RA & Somogyi P (1993). The metabotropic glutamate receptor (mGluR1 alpha) is concentrated at perisynaptic membrane of neuronal subpopulations as detected by immunogold reaction. *Neuron* **11**, 771-787.
- Beierlein M, Gibson JR & Connors BW (2000). A network of electrically coupled interneurons drives synchronized inhibition in neocortex. *Nat Neurosci* **3** 904-910.
- Blasco-Ibanez JM & Freund TF (1995). Synaptic input of horizontal interneurons in stratum oriens of the hippocampal CA1 subfield: structural basis of feed-back activation. *Eur J Neurosci* **7**, 2170-2180.
- Blatow M, Rozov A, Katona I, Hormuzdi SG, Meyer AH, Whittington MA, Caputi A & Monyer H (2003). A novel network of multipolar bursting interneurons generates theta frequency oscillations in neocortex. *Neuron* **38**, 805-817.
- Bragin A, Jando G, Nadasdy Z, Hetke J, Wise K & Buzsaki G (1995). Gamma (40-100 Hz) oscillation in the hippocampus of the behaving rat. *J Neurosci* **15**, 47-60.
- Buzsaki G (2002). Theta oscillations in the hippocampus. *Neuron* **33**, 325-340.
- Buzsaki G & Draguhn A. (2004). Neuronal oscillations in cortical networks. *Science* **304**, 1926-1929.
- Chu Z, Galarreta M & Hestrin S (2003). Synaptic interactions of late-spiking neocortical neurons in layer 1. *J Neurosci* **23**, 96-102.
- Connors BW & Long MA (2004). Electrical synapses in the mammalian brain. *Annu Rev Neurosci* **27**, 393-418.
- De Simoni A Griesinger CB & Edwards FA (2003). Development of rat CA1 neurones in acute versus organotypic slices: role of experience in synaptic morphology and activity. *J Physiol* **550**, 135-147.
- Ferraguti F, Cobden P, Pollard M, Cope D, Shigemoto R, Watanabe M & Somogyi P (2004). Immunolocalization of metabotropic glutamate receptor 1alpha

- (mGluR1alpha) in distinct classes of interneuron in the CA1 region of the rat hippocampus. *Hippocampus* **14**, 193-215.
- Freund TF & Buzsaki G (1996). Interneurons of the hippocampus. *Hippocampus* **6**, 347-470.
- Galarreta M & Hestrin S (1999). A network of fast-spiking cells in the neocortex connected by electrical synapses. *Nature* **402**, 72-75.
- Galarreta M, Erdelyi F, Szabo G & Hestrin S (2004). Electrical coupling among irregular-spiking GABAergic interneurons expressing cannabinoid receptors. *J Neurosci* **24**, 9770-9778.
- Gibson JR, Beierlein M & Connors BW (1999). Two networks of electrically coupled inhibitory neurons in neocortex. *Nature* **402**, 75-79.
- Gloveli T, Dugladze T, Saha S, Monyer H, Heinemann U, Traub RD, Whittington MA & Buhl EH (2005). Differential involvement of oriens/pyramidal interneurons in hippocampal network oscillations in vitro. *J Physiol* **562**, 131-147.
- Halabisky B, Shen F, Huguenard JR & Prince DA (2006). Electrophysiological classification of somatostatin-positive interneurons in mouse sensorimotor cortex. *J Neurophysiol* **96**, 834-845.
- Hestrin S & Galarreta M (2005). Electrical synapses define networks of neocortical GABAergic neurons. *Trends Neurosci* **28**, 304-309.
- Hines M & Carnevale T (1997). The NEURON simulation environment. *Neural Comp* **9**, 178-1209.
- Jonas P, Bischofberger J, Fricker D & Miles R (2004). Interneuron Diversity series: Fast in, fast out--temporal and spatial signal processing in hippocampal interneurons. *Trends Neurosci* **27**, 30-40.
- Katona I, Acsady L & Freund TF (1999). Postsynaptic targets of somatostatin-immunoreactive interneurons in the rat hippocampus. *Neuroscience* **88**, 37-55.
- Klausberger T, Magill PJ, Marton LF, Roberts JD, Cobden PM, Buzsaki G & Somogyi P (2003). Brain-state- and cell-type-specific firing of hippocampal interneurons in vivo. *Nature* **421**, 844-848.

- Klausberger T, Marton LF, Baude A, Roberts JD, Magill PJ & Somogyi P (2004). Spike timing of dendrite-targeting bistratified cells during hippocampal network oscillations in vivo. *Nat Neurosci* **7**, 41-47.
- Lacaille JC, Mueller AL, Kunkel DD & Schwartzkroin PA (1987). Local circuit interactions between oriens/alveus interneurons and CA1 pyramidal cells in hippocampal slices: electrophysiology and morphology. *J Neurosci* **7**, 1979-1993.
- Lacaille JC & Williams S (1990). Membrane properties of interneurons in stratum oriens-alveus of the CA1 region of rat hippocampus in vitro. *Neuroscience* **36**, 349-359.
- Lawrence JJ, Grinspan ZM, Statland JM & McBain CJ (2006). Muscarinic receptor activation tunes mouse stratum oriens interneurons to amplify spike reliability. *J Physiol* **571**, 555-562.
- Lisman JE & Idiart MA (1995). Storage of 7 +/- 2 short-term memories in oscillatory subcycles. *Science* **267**, 1512-5.
- Lohmann C, Finski A & Bonhoeffer T (2005). Local calcium transients regulate the spontaneous motility of dendritic filopodia. *Nat Neurosci* **8**, 305-12.
- Losonczy A, Zhang L, Shigemoto R, Somogyi P & Nusser Z (2002). Cell type dependence and variability in the short-term plasticity of EPSCs in identified mouse hippocampal interneurons. *J Physiol* **542**, 193-210.
- Maccaferri G (2005). Stratum oriens horizontal interneurone diversity and hippocampal network dynamics. *J Physiol* **562**, 73-80.
- Maccaferri G & Lacaille JC (2003). Interneuron Diversity series: Hippocampal interneuron classifications--making things as simple as possible, not simpler. *Trends Neurosci* **26**, 564-571.
- Maccaferri G & McBain CJ (1995). Passive propagation of LTD to stratum oriens-alveus inhibitory neurons modulates the temporoammonic input to the hippocampal CA1 region. *Neuron* **15**, 137-145.
- Maccaferri G & McBain CJ (1996). The hyperpolarization-activated current (I_h) and its contribution to pacemaker activity in rat CA1 hippocampal stratum oriens-alveus interneurons. *J Physiol* **497**, 119-130.

- Maccaferri G, Roberts JD, Szucs P, Cottingham CA & Somogyi P (2000). Cell surface domain specific postsynaptic currents evoked by identified GABAergic neurons in rat hippocampus in vitro. *J Physiol* **524**, 91-116.
- Markram H, Toledo-Rodriguez M, Wang Y, Gupta A, Silberberg G & Wu C (2004). Interneurons of the neocortical inhibitory system. *Nat Rev Neurosci* **5**, 793-807.
- McBain CJ, DiChiara TJ & Kauer JA (1994). Activation of metabotropic glutamate receptors differentially affects two classes of hippocampal interneurons and potentiates excitatory synaptic transmission. *J Neurosci* **14**, 4433-4445.
- Meyer AH, Katona I, Blatow M, Rozov A & Monyer H. (2002). In vivo labeling of parvalbumin-positive interneurons and analysis of electrical coupling in identified neurons. *J Neurosci* **22**, 7055-7064.
- Migliore M, Hoffman DA, Magee JC & Johnston D (1999). Role of an A-type K⁺ conductance in the back-propagation of action potentials in the dendrites of hippocampal pyramidal neurons. *J Comput Neurosci* **7**, 5-15.
- Miles R, Toth K, Gulyas AI, Hajos N & Freund TF (1996). Differences between somatic and dendritic inhibition in the hippocampus. *Neuron* **16**, 815-823.
- Monyer H & Markram H (2004). Interneuron Diversity series: Molecular and genetic tools to study GABAergic interneuron diversity and function. *Trends Neurosci* **27**, 90-97.
- Oliva AA Jr, Jiang M, Lam T, Smith KL & Swann JW (2000). Novel hippocampal interneuronal subtypes identified using transgenic mice that express green fluorescent protein in GABAergic interneurons. *J Neurosci* **20**, 3354-3368.
- Parra P, Gulyas AI & Miles R (1998). How many subtypes of inhibitory cells in the hippocampus? *Neuron* **20**, 983-993.
- Pike FG, Goddard RS, Suckling JM, Ganter P, Kasthuri N & Paulsen O (2000). Distinct frequency preferences of different types of rat hippocampal neurons in response to oscillatory input currents. *J Physiol* **529**, 205-213.
- Pouille F & Scanziani M (2004). Routing of spike series by dynamic circuits in the hippocampus. *Nature* **429**, 717-723.
- Ramón y Cajal S (1911). *Histologie de systeme nerveux de l'Homme et des vertebres*. tome II. Maloine, Paris.

- Saraga F, Wu CP, Zhang L & Skinner FK (2003). Active Dendrites and Spike Propagation in Multi-compartment Models of Oriens-Lacunosum/Moleculare Hippocampal Interneurons. *J Physiol* **552**, 502-504.
- Schreiber S, Fellous JM, Tiesinga P & Sejnowski TJ (2004). Influence of ionic conductances on spike timing reliability of cortical neurons for suprathreshold rhythmic inputs. *J Neurophysiol* **91**, 194-205.
- Somogyi P & Klausberger T (2005). Defined types of cortical interneurone structure space and spike timing in the hippocampus. *J Physiol* **562**, 9-26.
- Stoppini L, Buchs PA & Muller DA (1991). A simple method for organotypic cultures of nervous tissue. *J Neurosci Methods* **37**, 173-182.
- Szabadics J, Lorincz A & Tamas G (2001). Beta and gamma frequency synchronization by dendritic gabaergic synapses and gap junctions in a network of cortical interneurons. *J Neurosci* **21**, 5824-5831.
- Wang XJ (2002). Pacemaker neurons for the theta rhythm and their synchronization in the septohippocampal reciprocal loop. *J Neurophysiol* **87**, 889-900.
- Wang XY, McKenzie JS & Kemm RE (1996). Whole-cell K⁺ currents in identified olfactory bulb output neurones of rats, *J Physiol* **490**, 63-77.
- Whittington MA & Traub RD (2003). Interneuron diversity series: inhibitory interneurons and network oscillations in vitro. *Trends Neurosci* **26**, 676-682.
- Zhang L & McBain CJ (1995). Potassium conductances underlying repolarization and after-hyperpolarization in rat CA1 hippocampal interneurons. *J Physiol* **488**, 661-672.
- Zhang XL, Zhang L & Carlen PL (2004). Electrotonic coupling between stratum oriens interneurons in the intact in vitro mouse juvenile hippocampus. *J Physiol* **558**, 825-839.
- Zsiros V & Maccaferri G (2005). Electrical coupling between interneurons with different excitable properties in the stratum lacunosum-moleculare of the juvenile CA1 rat hippocampus. *J Neurosci* **25**, 8686-8695.
- Zucker RS (1989). Short-term synaptic plasticity. *Annu Rev Neurosci* **12**, 13-31.

Acknowledgements

We are grateful to Lara Masten and Beatrice Pastore for preparing organotypic slice cultures; to Majid H. Mohajerani and Paola Zacchi for helping with electroporation and confocal acquisition. This work was supported by grants from Ministero Istruzione Università e Ricerca (MIUR, PRIN 2005) and from the European Union (Project 503221) to EC; MJ was supported by the Program for Training and Research in Italian Laboratories, International Centre for Theoretical Physics, Trieste, Italy.

Table 1
Passive and active membrane properties of *stratum oriens* EGFP-positive interneurons exhibiting different firing patterns

	Regular	Irregular	Clustered	Total
Number of cells (<i>n</i>)	10	10	10	30
R _{in} (MΩ)	304 ± 61	285 ± 31	160 ± 21 *	249 ± 26
C _m (pF)	109 ± 7	108 ± 8	114 ± 11	110 ± 5
V _m (mV)	- 70.0 ± 2.0	- 70.4 ± 1.9	- 71.1 ± 1.4	- 70.5 ± 1.0
Spike amplitude (mV)	78.9 ± 3.0	77.4 ± 2.1	77.4 ± 2.2	77.9 ± 1.4
Spike threshold (mV)	- 52.8 ± 0.7	- 51.6 ± 0.9	- 51.3 ± 0.8	- 51.9 ± 0.5
Spike width (ms)	0.87 ± 0.05	0.86 ± 0.07	0.78 ± 0.06	0.84 ± 0.03

R_{in}: membrane input resistance; C_m: membrane capacitance; V_m: resting membrane potential. The values are expressed as mean ± SEM; * p<0.05.

Figure legends

Figure 1. Distribution pattern and immunocytochemical characterization of EGFP-expressing interneurons in the hippocampus of GIN mice

A: Coronal section of the hippocampus showing the distribution of EGFP-expressing interneurons at P8. *a*: Higher magnification of the inset shown in A. B-D: Organotypic hippocampal slices (3 weeks in culture) showing preserved morphology and distribution of EGFP positive cells. Images were acquired with 20X (B) and 40X (C, D) immersion objectives and confocal microscopy. Note the extensive distribution of EGFP-positive axon terminals in SLM in B. C: A couple of EGFP-positive cells, electroporated with sulforhodamine B. D: Merging picture (in yellow) of two electrically coupled EGFP-positive interneurons (arrows) injected with neurobiotin. EGFP positive cells (green) were co-immunostained with an antibody against neurobiotin (red). Electrical coupling was assessed by electrophysiological experiments. In C and D, EGFP-positive cells are localized in stratum oriens. E-G: EGFP positive cells (left) are stained (middle) with antibodies against somatostatin (E), mGluR1 (F) and NPY (G). The merge pictures are on the right. Note that the vast majority of EGFP-expressing CA1 interneurons were immunopositive for somatostatin. The asterisks in E indicate a somatostatin positive cell that is not expressing EGFP.

SO: *stratum oriens*; SP: *stratum pyramidale*; SR: *stratum radiatum*; SLM: *stratum lacunosum-moleculare*. Scale bars, in A: 100 μm , in *a* and in E-G: 20 μm ; in B: 60 μm ; in C-D: 30 μm .

Figure 2. Membrane properties of the EGFP-positive interneurons

A: Electrotonic potentials induced by hyperpolarizing current pulses in control and during bath application of ZD7288 (100 μM). B: Membrane oscillations on the top of an electrotonic potential induced in another interneuron by a steady depolarising current pulse. Increasing the amplitude of the current pulse induced high-frequency firing (left). Both membrane oscillations and spikes were abolished by TTX (1 μM ; right). C: Membrane oscillations in B (square) are shown on an expanded time scale (left). The power spectrum of the oscillations has a peak around 40 Hz (right).

Figure 3. Stratum oriens interneurons exhibit different firing patterns

Representative traces from three different interneurons exhibiting different firing patterns in response to depolarizing current pulses (left). On the right, the interspike interval probability histogram is plotted for each cell. For the histograms, 100 consecutive sweeps with the same depolarizing current pulse were used.

Figure 4. Increasing membrane depolarization does not change the characteristic firing pattern of individual interneurons

On the left, representative traces of regular (*A*), clustered (*C*) and irregular (*E*) firing patterns in three different cells in response to two depolarizing current pulses of different intensities. The graphs on the right represent the instantaneous frequency corresponding to the first 3 interspike intervals (open symbols) and to the last interspike interval (filled circles) versus current intensities (*B*, *D* and *F*).

Figure 5. Resonance properties of EGFP-positive interneurons in *stratum oriens*

A: Membrane response (upper trace) of an EGFP-positive interneuron to the injection of a sinusoidal current pulse at 2 Hz (lower trace). *B*: Membrane response of the same interneuron to a pulse at 20 Hz. Note that at 20 Hz the membrane response was smaller in amplitude and significantly out of phase with the injected current (dashed lines). *C*: The membrane impedance of the same cell at various frequencies (from 0.5 to 100 Hz) is plotted on the left. On the right, the impedance normalised to the 0.5 Hz value is plotted as a function of frequency (average of 7 cells).

Figure 6. Interneurons are electrically coupled via gap junctions

A: Paired recordings from interconnected interneurons showing spontaneous firing in one cell (cell 1) associated with spikelets in the other one (cell 2). *B*: In another pair, electrical coupling (left) was blocked by carbenoxolone (200 μ M; right). *C*: Same cells as in *B*. In the presence of carbenoxolone a sustained increase in spontaneous glutamatergic activity occurred. On the left, spikes in cell 1 are truncated while the corresponding spikelets in cell 2 are fully represented.

Figure 7. Electrical coupling occurs between neurons exhibiting different firing patterns

A: Paired recordings from two electrically coupled interneurons exhibiting regular (cell 1) and irregular (cell 2) firing patterns. On the left, a depolarizing current pulse evoked irregular firing in cell 2, which is associated in cell 1 (recorded in voltage clamp) with inward spikelet-like currents followed by outward currents corresponding to the after-hyperpolarizations. On the right, a depolarizing current pulse evoked regular firing in cell 1, which is associated with spikelet-like currents in cell 2 (recorded in voltage clamp). *B:* In another pair, electrotonic potentials evoked by hyperpolarizing current pulses in one cell were associated with electrotonic potentials of smaller amplitude in the other cell.

Figure 8. Low-pass filter properties of electrical connections with high coupling coefficient

A: In a pair of cells with high coupling coefficient (0.47), the spontaneous firing of cell 1 caused firing in cell 2 only when the spikelets were sufficiently close in time. Spikelets in cell 2 were coincident with spikes in cell 1 (dotted lines). The arrow marks a spike in cell 2 which, in turn, evoked a spikelet in cell 1. *B:* In the same couple of interneurons, high frequency firing (gamma range) in cell 1 was able to evoke lower frequency firing in cell 2 (theta range) and vice versa.

Figure 9. Synaptic connectivity between EGFP positive interneurons and principal cells

A, B: The graphs on the left represent the experimental arrangement of paired recordings from interconnected interneurons and principal cells. In the case of GABAergic synapses (*A*), a train of action potentials at 20 Hz (upper trace) evoked in the pyramidal cell (lower trace) IPSCs which undergo short-term depression. In the case of glutamatergic synapses (*B*), the same train of spikes in the pyramidal cell (upper trace) elicited in the interneuron (lower trace) EPSCs which undergo short-term facilitation. *C:* Short-term facilitation of EPSCs evoked in another interneuron by trains of spikes in the principal cell at 20, 50 and 100 Hz. In *A-C* each recording is the average of 20 consecutive sweeps. *D:* Plots of

the probability of successes and the potency ratio between the 10th (a_{10}) and the 1st (a_1) response versus different frequencies. Each point represents the average of 10 (probability) and 9 (potency) individual values obtained from different pairs. Vertical bars represent the SEM. Note that, on average, the connections were more reliable during activity at 50 Hz. * $p < 0.05$; ** $p < 0.01$; *** $p < 0.001$ (Tukey test for pairwise multiple comparison).

Figure 10. Simulation modelling reveals differential signalling of interneurons with various firing patterns

A: Simulation of the basic firing properties. Somatic recordings of a regularly firing cell (O_R ; left) under different 800ms somatic current injections; somatic recordings of a cell firing clusters of action potentials (O_C ; right). *B*: Effect of a 1.5 nS gap junction connecting two neurons with different firing properties. Schematic representation of the circuit (left); somatic membrane potential of the two cells during a 0.3 nA current injection in the O_R neuron (middle); somatic membrane potential during a 0.4 nA current injection in the O_C neuron (right). *C*: simulation of the GABAergic output expected from the two kind of cells. Schematic representation of the two kind of neurons (O_R and O_C) and their output (out_R and out_C , respectively; left); somatic membrane potential (bottom) and percent of inhibitory synaptic activation (top) during a somatic current injection into an O_R neuron (middle); somatic potential (bottom) and percent of inhibitory synaptic activation (top) during a current injection into an O_C neuron (right). The same current pulse (0.3 nA, 800 ms) was used in both cases.

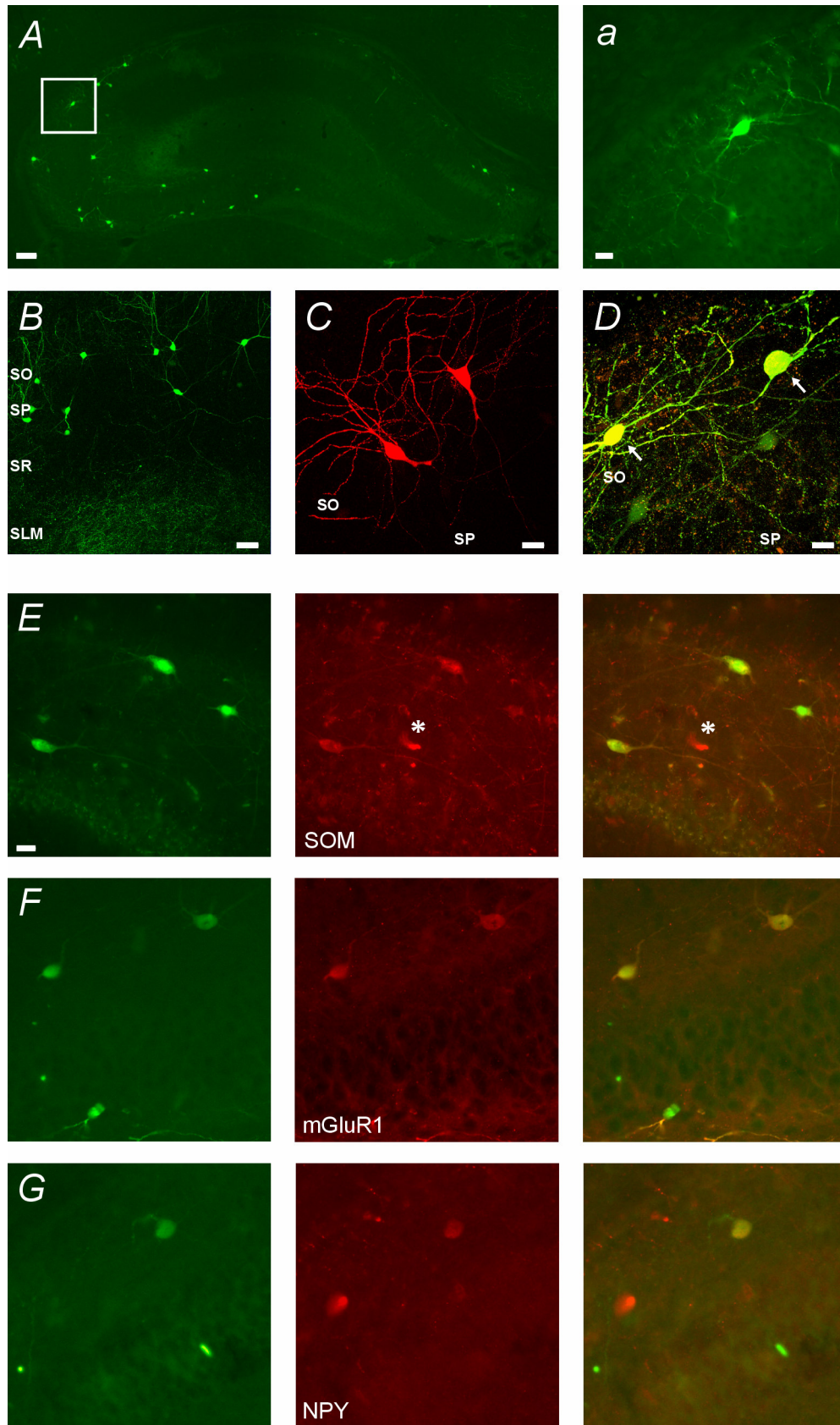


Figure 1

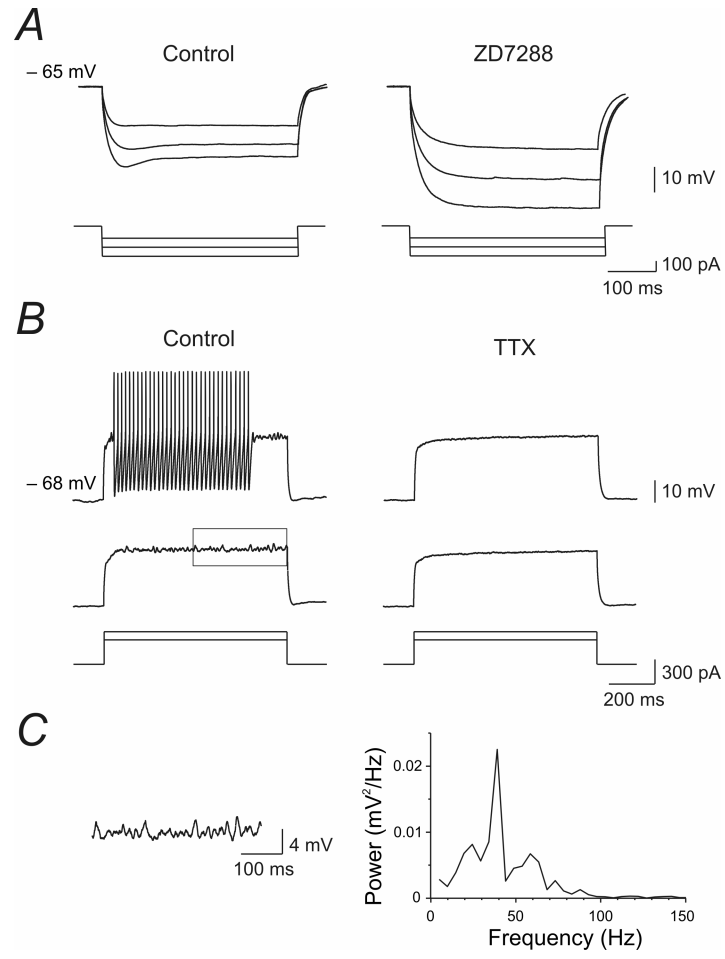


Figure 2

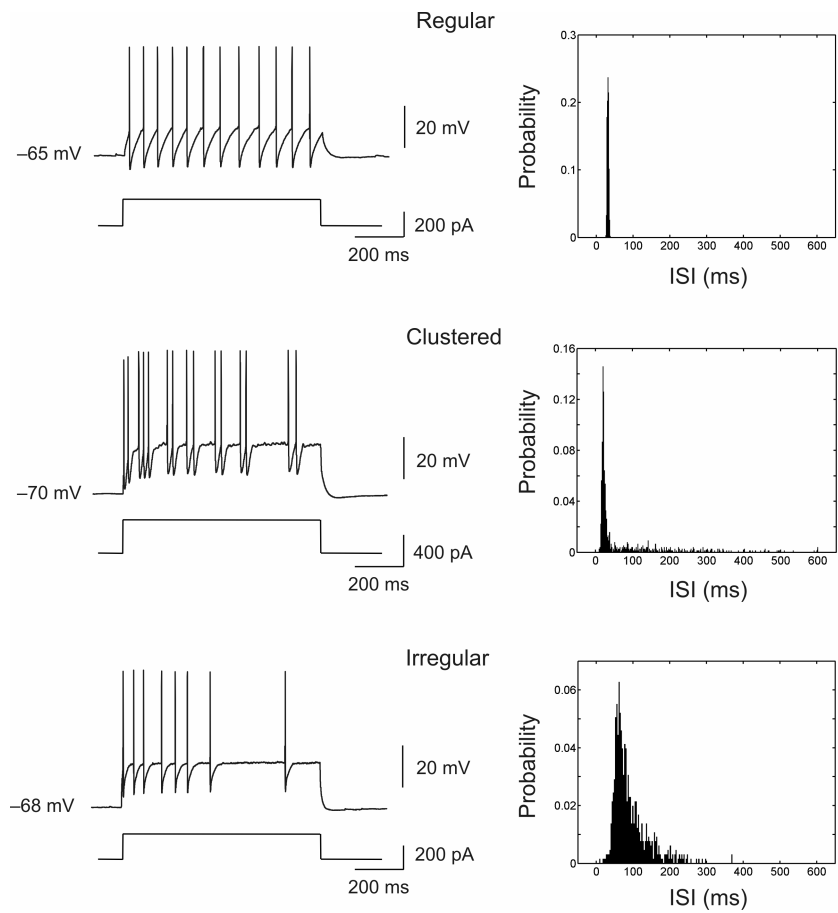


Figure 3

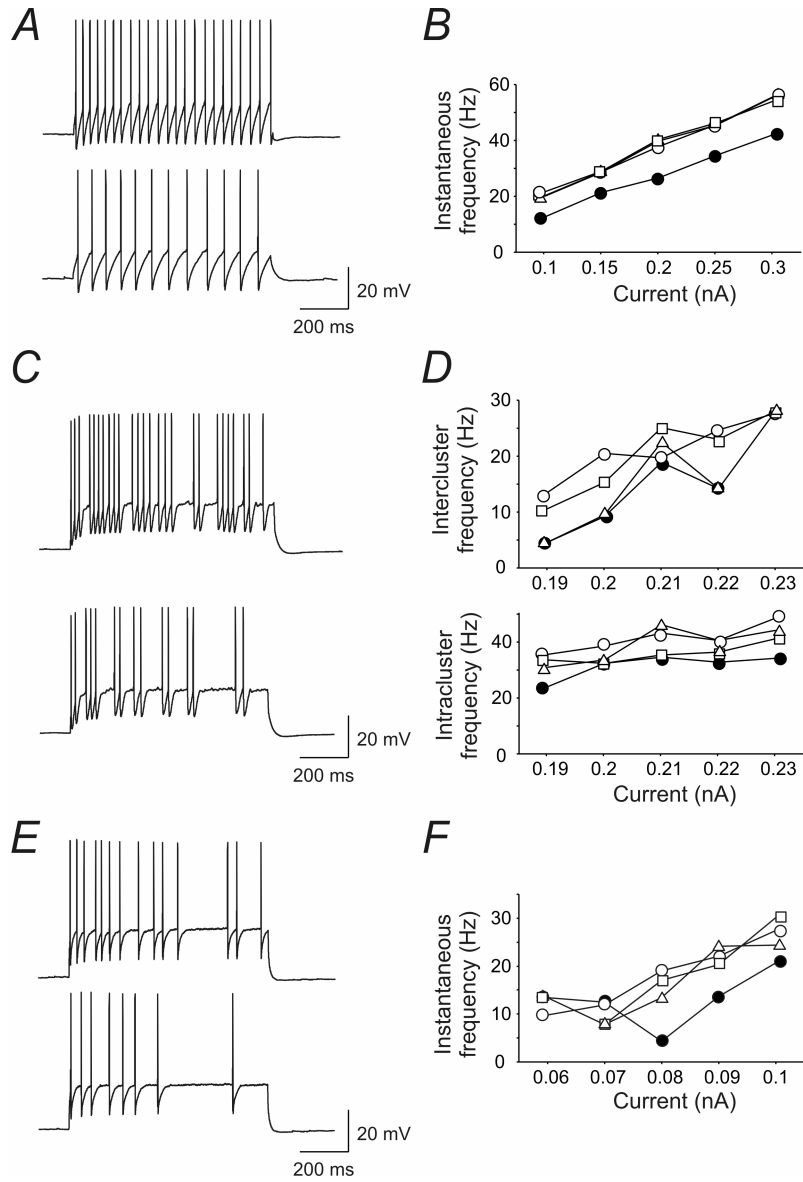


Figure 4

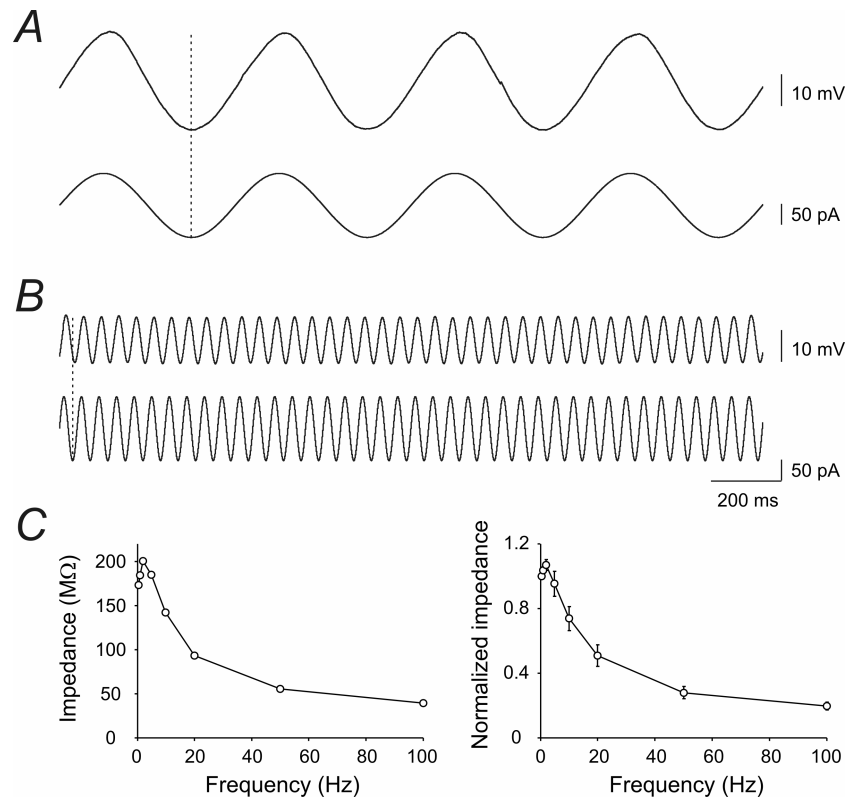


Figure 5

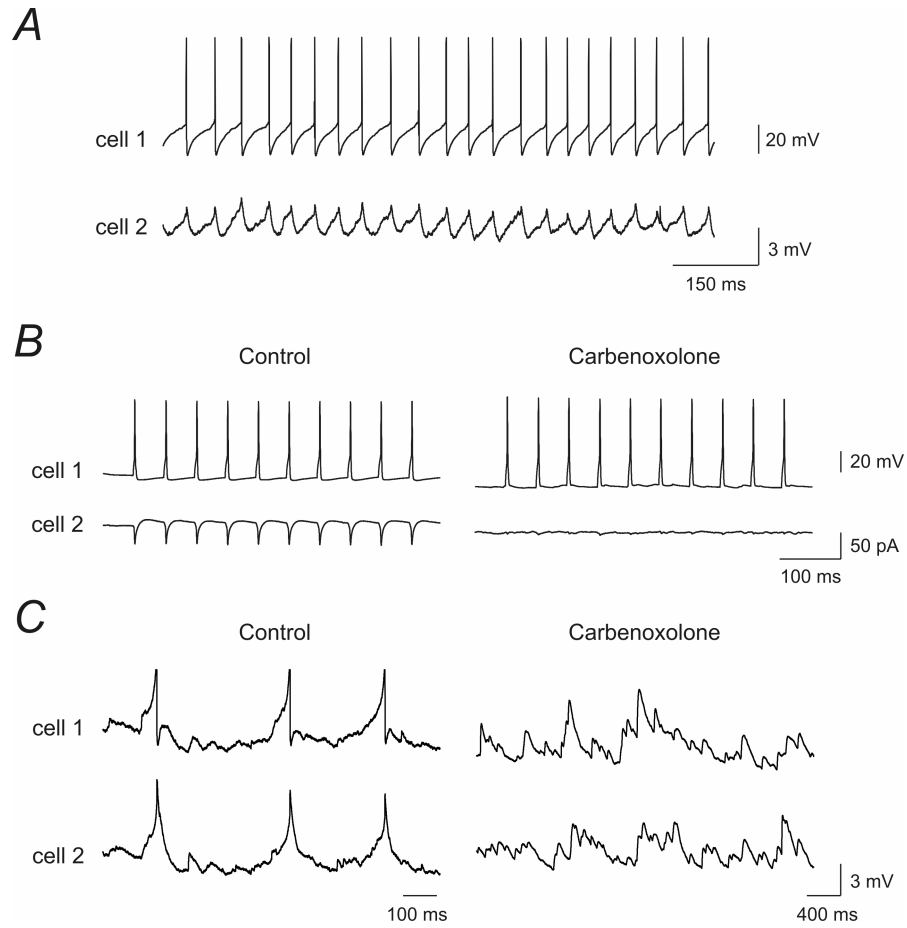


Figure 6

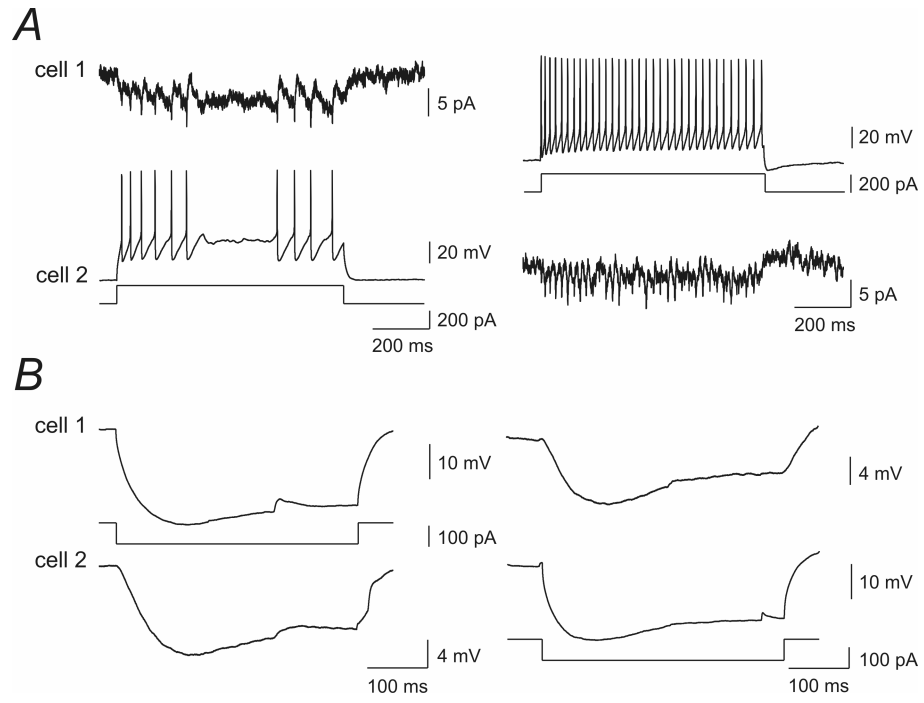


Figure 7

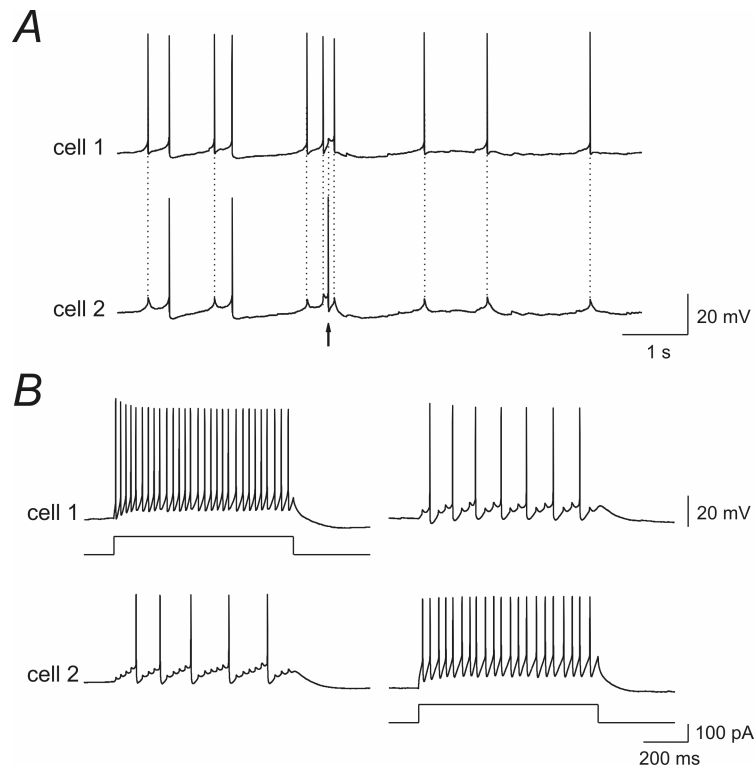


Figure 8

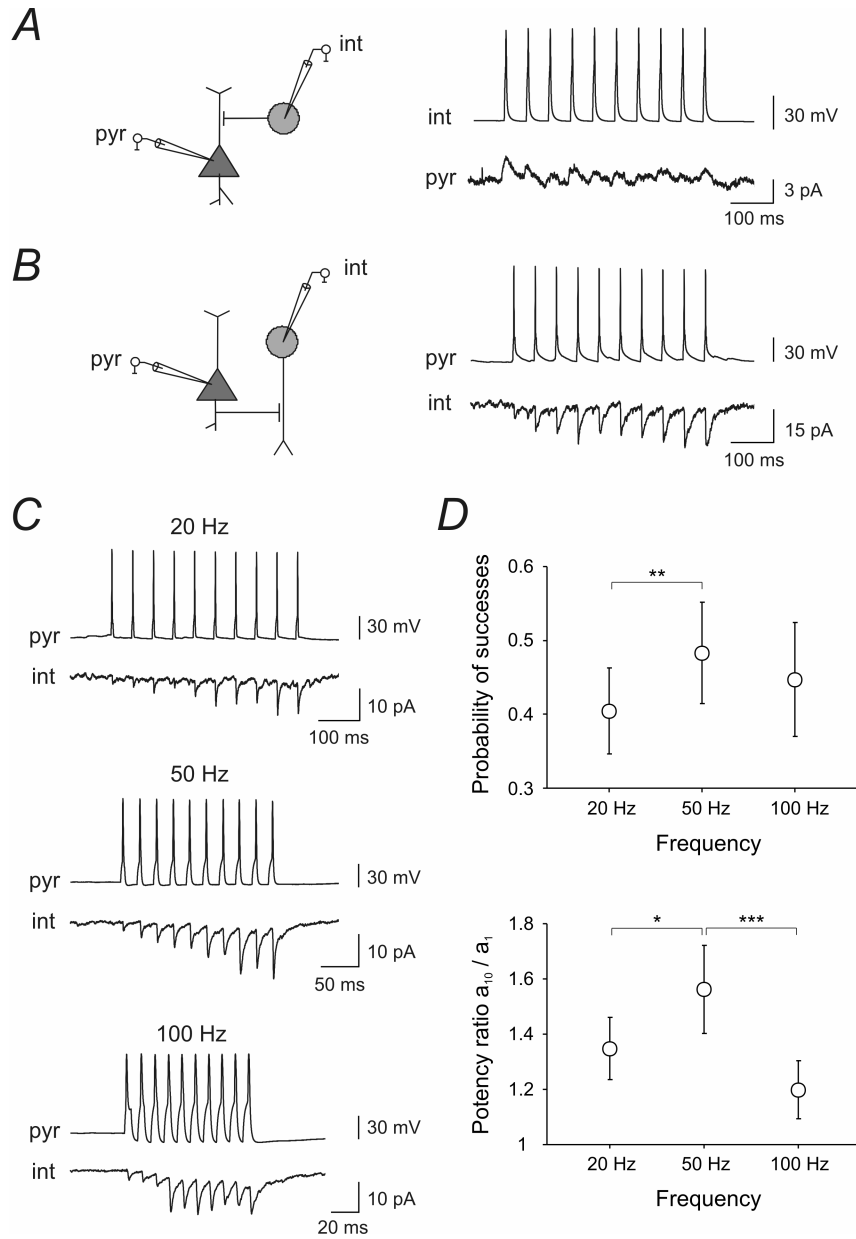


Figure 9

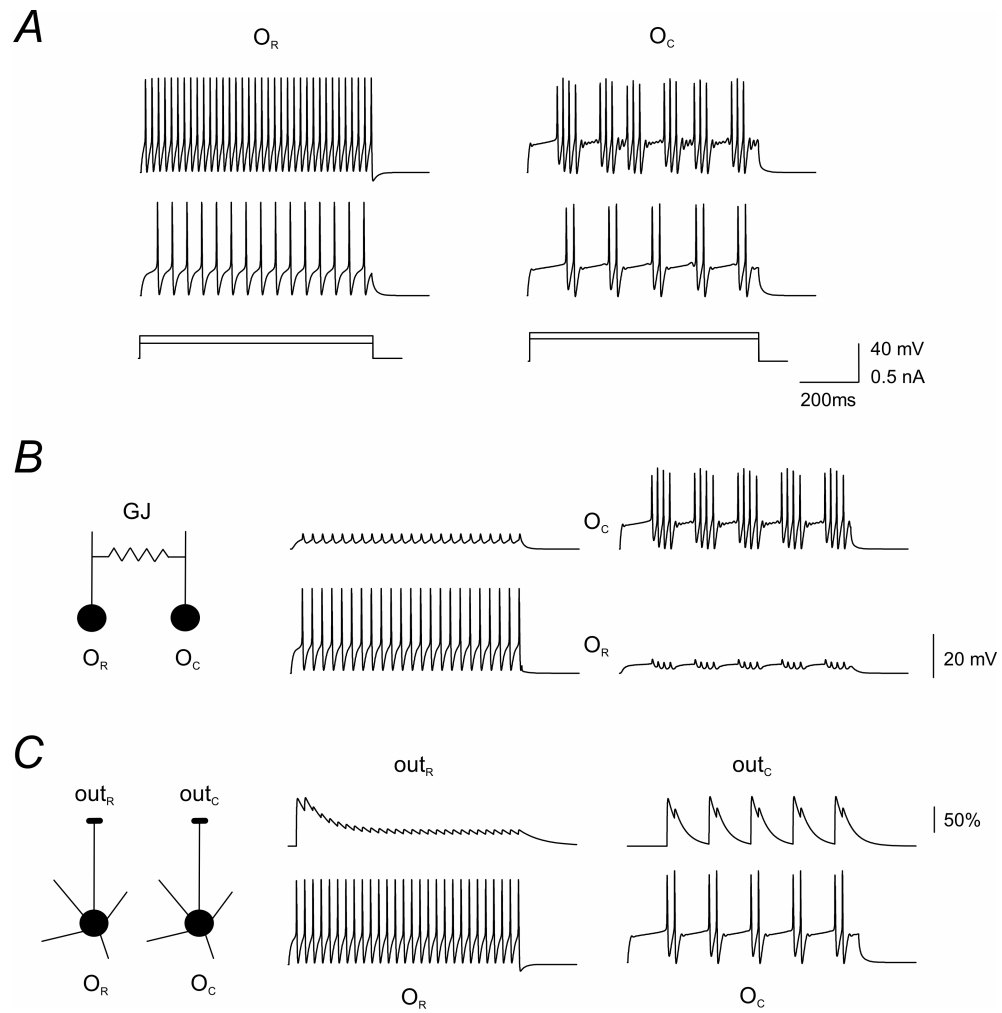


Figure 10

CONCLUSIONS AND FUTURE PERSPECTIVES

In my work, I have used combined theoretical and experimental approaches to examine different aspects of synaptic signalling in the rodent hippocampus. In the first part of my study, I developed a novel analytic model of quantal transmission at chemical synapses. This model describes the release process using some classic quantal parameters, like the probability of a single vesicle being released after stimulation, and other relevant quantities like the distribution of vesicles ready to be released before the arrival of each action potential. In this way, the model can include a wide range of situations in which the size of the readily releasable pool of vesicles may change with time. Moreover, either in the case of univesicular or multivesicular release the calculations were performed with or without the constraint that the release of one vesicle inhibits the release of other vesicles for the same stimulation. The model connects these parameters to quantities that are usually measured experimentally, like the probability of release and the amplitude of the postsynaptic response, with simple mathematical formulas. Using these results with sets of experimental data, previously obtained at single CA3-CA1 synapses in the developing rat hippocampus, allowed estimating quantal parameters. These, were in good agreement with those reported previously in the literature and fitted quite well with a multivesicular model of synaptic transmission.

In the second part of my study, I analyzed some relevant signalling properties of a network of EGFP-positive somatostatin-containing interneurons of the CA1 region of the mouse hippocampus. I performed patch clamp experiments from a single cell or from pair of interconnected neurons in cultured slices obtained from GIN mice. I focussed on the population of EGFP-positive interneurons of the *stratum oriens*. From this work, I can conclude that these interneurons constitute a heterogeneous population of cells with diverse excitable properties. In particular, these neurons exhibit regular, irregular or clustered-type firing patterns in response to similar stimuli. Independently from their single-cell properties, interneurons were interconnected by electrical synapses in a network expressing a high level of connectivity and strong coupling coefficients. The interplay among interneurons with different firing properties may influence information processing in this hippocampal region. I found also that interneurons were connected with principal cells by chemical synapses. Although GABAergic inhibitory synapses to

pyramidal cells were difficult to detect and examine, glutamatergic synapses to interneurons showed a remarkable modulation of their activity with higher reliability and synaptic strength for inputs encoded in the gamma frequency range, which was not observed elsewhere.

Regarding this second part of my work, many aspects are suitable for further investigations.

First of all, since the organotypic culturing procedure may partially affect the network properties of the hippocampal circuitry, it would be interesting to perform similar experiments on acute hippocampal slices obtained from mice of the same strain, in order to validate the present findings. This is true especially in the perspective of analyzing the importance of this interneuronal network in the physiology of hippocampal rhythms. To this aim, experiments on acute slices obtained from P14–P21 animals are presently being performed in our laboratory.

Another interesting issue to investigate is how the interneuronal network is modulated by neurotransmitters and modulators in GIN mice. For instance, it has been demonstrated that cannabinoids exert a powerful control on both glutamatergic and GABAergic circuitry in the hippocampus (for a review see Wilson & Nicoll, 2002). It would be of interest to see how activation of nicotine acetylcholine receptors (nAChRs) by nicotine or endogenous acetylcholine, modulates interneuronal network. nAChRs are widely distributed within the brain where they contribute to regulate high cognitive functions. The hippocampus, a key structure in learning and memory processes, receives a large cholinergic innervation and is endowed with a variety of nAChRs, which are thought to regulate important processes such as transmitter release, cell excitability and neuronal integration, which are crucial to determine network operation and high cognitive functions. Deficits in the cholinergic system produce impairment of cognitive functions, which are particularly relevant during senescence and in age-related neurodegenerative pathologies. Acetylcholine, released from cholinergic fibres, acts on muscarinic and nicotinic receptors. The effects of muscarinic receptors on stratum oriens interneurons have been partially elucidated. In a recent work (Lawrence *et al.*, 2006a,b) important effects of muscarinic receptors activation on the precise tuning of the activity of stratum oriens interneurons have been described. However, similar experiments on nAChRs are

lacking. In a previous work in collaboration with Laura Maggi (Maggi *et al.*, 2004), not included in this thesis, we have shown that, at immature glutamatergic CA3-CA1 synapses in acute hippocampal slices from P1-P6 old rats, activation of nAChRs by nicotine is able to bidirectionally modify synaptic strength, according to the initial probability of the synapses. Thus, it would be useful to investigate the effects of nAChRs on EGFP-positive interneurons to elucidate how this alkaloid regulates cell excitability (as in Lawrence *et al.*, 2006b) and gap junction properties. In preliminary experiments on organotypic cultures, similar to the ones described in this thesis, I have found that EGFP-positive interneurons are sensitive to nicotine which can have a variety of effects. A brief (100 ms) pulse of nicotine delivered by pressure from a pipette (concentration of nicotine into the pipette 1mM), localized close to the soma of the interneurons voltage-clamped near their resting membrane potential (-60 mV), induced in most cases a fast inward current followed by a slow one (see Figure 6B). In some neurons nicotine produced only a fast inward current. These currents are similar to those previously described in non-identified CA1 interneurons by Jones and Yakel (1997). According to McQuiston and Madison (1999) and Alkondon *et al.*, (1999) the fast response would be mediated by $\alpha 7$

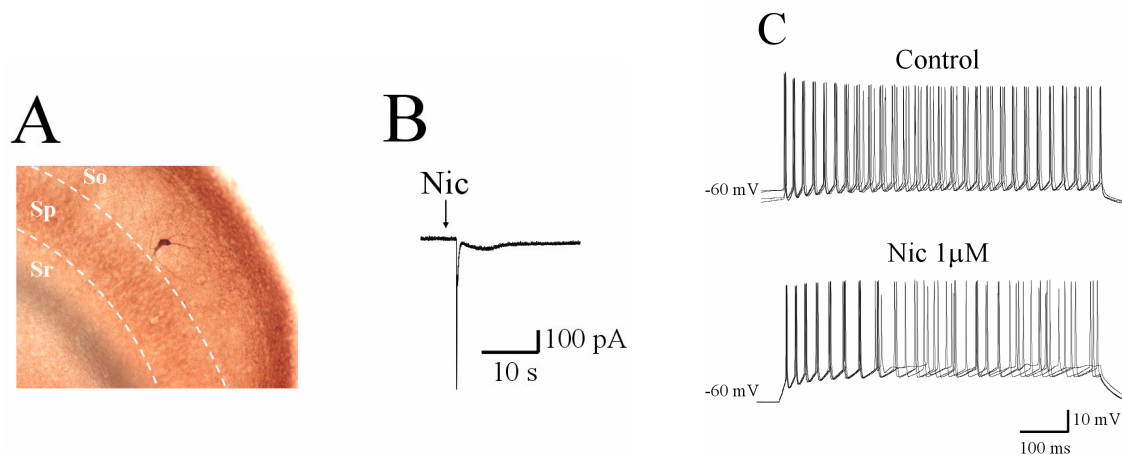


Figure 6. EGFP-positive interneurons bear nAChRs. A. Biocytin labelled EGFP-positive interneuron of the *stratum oriens*. Dashed lines delimit stratum pyramidale (Sp). So: stratum oriens; Sr: stratum radiatum. B. Application of nicotine by pressure (arrow) from a pipette positioned close to the soma of the interneuron evokes a fast inward current followed by a slow one. C. In another regular firing EGFP-positive interneuron bath application of nicotine (1 μ M for 3 min) modifies the firing pattern induced by a steady depolarizing current pulse (four traces are superimposed in control and during nicotine application). (Unpublished observations)

nAChRs while the slow one by non- $\alpha 7$ nAChRs. In addition, other data suggest that nicotine can modify the firing patterns of EGFP-positive interneurons (Figure 6C).

Finally, it would be interesting to use cDNA microarray techniques to characterize differences in gene profile between pyramidal cells and EGFP positive interneurons. It is possible to harvest cytoplasm from identified interneurons for potential single-cell studies. In combination with the described electrophysiological characteristics, this achievement could be used to correlate the diverse excitable properties of interneurons to different gene expression.

REFERENCES

- Abenavoli A, Forti L, Bossi M, Bergamaschi A, Villa A & Malgaroli A (2002). Multimodal quantal release at individual hippocampal synapses: evidence for no lateral inhibition. *J Neurosci.* 22: 6336-6346.
- Aggleton JP & Brown MW (1999). Episodic memory, amnesia, and the hippocampal–anterior thalamic axis. *Behav. Brain Sci.* 22: 425-489.
- Alger B & Nicoll RA (1982). Feed-forward dendritic inhibition in rat hippocampal pyramidal cells studied in vitro. *J Physiol.* 328: 105-123.
- Alkondon M, Pereira EF, Eisenberg HM & Albuquerque EX (1999). Choline and selective antagonists identify two subtypes of nicotinic acetylcholine receptors that modulate GABA release from CA1 interneurons in rat hippocampal slices. *J Neurosci.* 19: 2693-2705.
- Amaral DG & Witter MP (1989). The three dimensional organization of the hippocampal formation: a review of anatomical data. *Neuroscience* 31: 571-591.
- Andersen P, Eccles JC & Loynning Y (1964). Location of synaptic inhibitory synapses on hippocampal pyramids. *J Neurophysiol.* 27: 592-607.
- Andersen P, Bliss TVP & Skrede K (1971). Lamellar organization of hippocampal excitatory pathways. *Exp. Brain Res.* 13: 222-238.
- Aradi I, Santhakumar V, Chen K & Soltesz I (2002). Postsynaptic effects of GABAergic synaptic diversity: regulation of neuronal excitability by changes in IPSC variance. *Neuropharmacology* 43: 511-522.
- Auger C & Marty A (1997). Heterogeneity of functional synaptic parameters among single release sites. *Neuron* 19: 139-150.
- Auger C, Kondo S & Marty A (1998). Multivesicular release at single functional synaptic sites in cerebellar stellate and basket cells. *J Neurosci.* 18: 4532-4547.
- Auger C & Marty A (2000). Quantal currents at single-site central synapses. *J Physiol.* 526: 3-11.
- Barberis A, Petrini EM & Cherubini E (2004). Presynaptic source of quantal size variability at GABAergic synapses in rat hippocampal neurons in culture. *Eur J Neurosci.* 20: 1803-1810.
- Barton SB & Cohen IS (1977). Are transmitter release statistics meaningful? *Nature* 268: 267-268.

Bartos M, Vida I, Frotscher M, Meyer A, Monyer H, Geiger JR & Jonas P (2002). Fast synaptic inhibition promotes synchronized gamma oscillations in hippocampal interneuron networks. *Proc Natl Acad Sci USA* 99: 13222-13227.

Battistin T & Cherubini E (1994). Developmental shift from long-term depression to long-term potentiation at the mossy fibre synapses in the rat hippocampus. *Eur J Neurosci.* 6: 1750-1755.

Bekkers JM, Richerson GB & Stevens CF (1990). Origin of variability in quantal size in cultured hippocampal neurons and hippocampal slices. *Proc Natl Acad Sci USA* 87: 5359-5362.

Bekkers JM (1994). Quantal analysis of synaptic transmission in the central nervous system. *Curr Opin Neurobiol.* 4: 360-365.

Bekkers JM (1995). Synchronous and asynchronous EPSCs evoked in hippocampal slices: a test of the quantal model of neurotransmission. *Soc. Neurosci. Abstr.* 21: 1091.

Bekkers JM & Stevens CF (1995). Quantal analysis of EPSCs recorded from small numbers of synapses in hippocampal cultures. *J Neurophysiol.* 73: 1145-1156.

Bekkers JM & Clements JD (1999). Quantal amplitude and quantal variance of strontium-induced asynchronous EPSCs in rat dentate granule neurons. *J Physiol.* 516: 227-248.

Ben-Ari Y & Cossart R (2000). Kainate: a double agent that generates seizures: two decades of progress. *Trends Neurosci.* 23: 580-587.

Benfenati F, Onofri F & Giovedi S (1999). Protein-protein interactions and protein modules in the control of neurotransmitter release. *Philos Trans R Soc Lond B Biol Sci.* 354: 243-257.

Bennett MVL, Barrio LC, Bargiello TA, Spray DC, Hertzberg E & Saez JC (1991). Gap junctions: new tools, new answers, new questions. *Neuron* 6: 305-320.

Bennett MR & Kearns JL (2000). Statistics of transmitter release at nerve terminals. *Prog Neurobiol.* 60: 545-606.

Blatow M, Rozov A, Katona I, Hormuzdi SG, Meyer AH, Whittington MA, Caputi A & Monyer H (2003). A novel network of multipolar bursting interneurons generates theta frequency oscillations in neocortex. *Neuron* 38: 805-817.

Bliss TVP & Lomo T (1973). Long-lasting potentiation of synaptic transmission in the dentate area of the anaesthetized rabbit following stimulation of the perforant path. *J Physiol.* 232: 331-356.

Bliss TVP & Collingridge GL (1993). A synaptic model of memory: long-term potentiation in the hippocampus. *Nature* 361: 31-39.

Borst JG, Helmchen F & Sakmann B (1995). Pre- and postsynaptic whole-cell recordings in the medial nucleus of the trapezoid body of the rat. *J Physiol.* 489: 825-840.

Bragin A, Jando G, Nadasdy Z, Hetke J, Wise K & Buzsáki G (1995). Gamma (40-100 Hz) oscillation in the hippocampus of the behaving rat. *J Neurosci.* 15: 47-60.

Brown TH, Perkel DH & Feldman MW (1976). Evoked neurotransmitter release: statistical effects of nonuniformity and nonstationarity. *Proc Natl Acad Sci USA.* 73: 2913-2917.

Bruzzone R, White TW & Paul DL (1996). Connections with connexins: the molecular basis of direct intercellular signaling, *Eur. J. Biochem.* 238: 1-27.

Buhl DL, Harris KD, Hormuzdi SG, Monyer H & Buzsáki G (2003). Selective impairment of hippocampal gamma oscillations in connexin-36 knock-out mouse in vivo. *J Neurosci.* 23: 1013-1018.

Buhl EH, Halasy K & Somogyi P (1994). Diverse sources of hippocampal unitary inhibitory postsynaptic potentials and the number of synaptic release sites. *Nature* 368: 823-828.

Buhl EH, Cobb SR, Halasy K & Somogyi P (1995). Properties of unitary IPSPs evoked by anatomically identified basket cells in the rat hippocampus. *Eur J Neurosci.* 7: 1989-2004.

Buhl DL, Harris KD, Hormuzdi SG, Monyer H & Buzsáki G (2003). Selective impairment of hippocampal gamma oscillations in connexin-36 knock-out mouse in vivo. *J Neurosci.* 23: 1013-1018.

Buzsáki G, Leung LW & Vanderwolf CH (1983). Cellular bases of hippocampal EEG in the behaving rat. *Brain Res.* 287: 139-171.

Buzsáki G (1984). Feed-forward inhibition in the hippocampal formation. *Prog Neurobiol.* 22: 131-153.

Buzsáki G & Draguhn A (2004). Neuronal oscillations in cortical networks. *Science* 304: 1926-1929.

Buzsáki G, Geisler C, Henze DA & Wang XJ (2004). Interneuron Diversity series: Circuit complexity and axon wiring economy of cortical interneurons. *Trends Neurosci.* 27: 186-193.

Callaway JC & Ross WN (1995). Frequency-dependent propagation of sodium action potentials in dendrites of hippocampal CA1 pyramidal neurons *J. Neurophysiol* 74: 1395-1403.

Ceccarelli B, Hurlbut WP & Mauro A (1973). Turnover of transmitter and synaptic vesicles at the frog neuromuscular junction. *J Cell Biol.* 57: 499-524.

Chapman CA & Lacaille JC (1999). Intrinsic theta-frequency membrane potential oscillations in hippocampal CA1 interneurons of stratum lacunosum-moleculare. *J Neurophysiol.* 81: 1296-1307.

Chapman CA & Lacaille JC (1999). Cholinergic induction of theta-frequency oscillations in hippocampal inhibitory interneurons and pacing of pyramidal cell firing. *J Neurosci.* 19: 8637-8645.

Christie JM & Jahr CE (2006). Multivesicular release at Schaffer collateral-CA1 hippocampal synapses. *J Neurosci.* 26: 210-216.

Clements JD (1991). Quantal synaptic transmission? *Nature* 353: 396.

Clements JD, Lester RA, Tong G, Jahr CE & Westbrook GL (1992). The time course of glutamate in the synaptic cleft. *Science* 258: 1498-1501.

Clements JD (1996). Transmitter timecourse in the synaptic cleft: its role in central synaptic function. *Trends Neurosci.* 19: 163-171.

Clements JD & Silver RA (2000). Unveiling synaptic plasticity: a new graphical and analytical approach. *Trends Neurosci.* 23: 105-113.

Clements JD (2003). Variance-mean analysis: a simple and reliable approach for investigating synaptic transmission and modulation. *J Neurosci Methods.* 130: 115-125.

Cobb SR, Buhl EH, Halasy K, Paulsen O & Somogyi P (1995). Synchronization of neuronal activity in hippocampus by individual GABAergic interneurons. *Nature* 378: 75-78.

Conti R & Lisman J (2003). The high variance of AMPA receptor- and NMDA receptor-mediated responses at single hippocampal synapses: evidence for multiquantal release. *Proc Natl Acad Sci USA.* 100: 4885-4890.

Deans MR, Gibson JR, Sellitto C, Connors BW & Paul DL (2001). Synchronous activity of inhibitory networks in neocortex requires electrical synapses containing connexin36. *Neuron* 31: 477-485.

Debanne D, Guérineau NC, Gähwiler B & Thompson SM (1996). Paired-pulse facilitation and depression at unitary synapses in the rat hippocampus: quantal fluctuation affects subsequent release. *J Physiol.* 491: 163-176.

del Castillo J & Katz B (1954). Quantal component of the end plate potential. *J Physiol.* 124: 560-573.

Dermietzel R, Traub O, Hwang TK, Beyer E, Bennett MVL, Spray DC & Willecke K (1989). Differential expression of three gap junction proteins in developing and mature brain tissues. *Proc. Natl. Acad. Sci. USA* 86: 10148-10152.

Dobrunz LE & Stevens CF (1997). Heterogeneity of release probability, facilitation and depletion at central synapses. *Neuron* 18: 995-1008.

Dodge FA Jr & Rahamimoff R (1967). Co-operative action of calcium ions in transmitter release at the neuromuscular junction. *J Physiol.* 193: 419-432.

Draguhn A, Traub RD, Schmitz D & Jefferys JG (1998). Electrical coupling underlies high-frequency oscillations in the hippocampus in vitro. *Nature* 394: 189-192.

Dudek SM & Bear MF (1993). Bidirectional long-term modification of synaptic effectiveness in the adult and immature hippocampus. *J Neurosci.* 13: 2910-2918.

Eccles JC (1964). *The Physiology of Synapses*. Springer-Verlag.

Edwards FA, Konnerth A & Sakmann B (1990). Quantal analysis of inhibitory synaptic transmission in the dentate gyrus of rat hippocampal slices: a patch-clamp study. *J Physiol.* 430: 213-249.

Edwards FA (1995). Anatomy and electrophysiology of fast central synapses lead to a structural model for long-term potentiation. *Physiol Rev.* 75: 759-787.

Eichenbaum H & Cohen NJ (2001). *From Conditioning to Conscious Recollection*. Oxford University Press, New York.

Faber DS & Korn H (1991). Applicability of the coefficient of variation method for analyzing synaptic plasticity. *Biophys. J* 60: 1288-1294.

Faber DS, Korn H, Redman SJ, Thompson SM & Altman JS (1998). "Central Synapses: Quantal Mechanisms and Plasticity". HFSP, Strasbourg.

Fisahn A, Pike FG, Buhl EH & Paulsen O (1998). Cholinergic induction of network oscillations at 40 Hz in the hippocampus in vitro. *Nature* 394: 186-189.

Foldy C, Aradi I, Howard A & Soltesz I (2004). Diversity beyond variance: modulation of firing rates and network coherence by GABAergic subpopulations. *Eur J Neurosci.* 19: 119-130.

Forti L, Bossi M, Bergamaschi A, Villa A & Malgaroli A (1997). Loose-patch recordings of single quanta at individual hippocampal synapses. *Nature* 388: 874-878.

Foster KA, Kreitzer AC & Regehr WG (2002). Interaction of postsynaptic receptor saturation with presynaptic mechanisms produces a reliable synapse. *Neuron* 36: 1115-1126.

Foster KA & Regehr WG (2004). Variance-mean analysis in the presence of a rapid antagonist indicates vesicle depletion underlies depression at the climbing fiber synapse. *Neuron* 43: 119-131.

Franks KM, Stevens CF & Sejnowski TJ (2003). Independent sources of quantal variability at single glutamatergic synapses. *J Neurosci.* 23: 3186-3195.

Frerking M & Wilson M (1996). Effects of variance in mini amplitude on stimulus-evoked release: a comparison of two models. *Biophys. J* 70: 2078-2091.

Freund TF (2003). Interneuron Diversity series: Rhythm and mood in perisomatic inhibition. *Trends Neurosci.* 26: 489-495.

Freund TF & Buzsáki G (1996). Interneurons of the hippocampus. *Hippocampus* 6: 347-470.

Fries P, Reynolds JH, Rorie AE & Desimone R (2001). Modulation of oscillatory neuronal synchronization by selective visual attention. *Science* 291: 1560-1563.

Fukuda T & Kosaka T (2000). Gap junctions linking the dendritic network of GABAergic interneurons in the hippocampus. *J Neurosci.* 20: 1519-1528.

Gaffan D (2001). What is a memory system? Horel's critique revisited. *Behav. Brain Res.* 127: 5-11.

Gaiarsa JL, Tseeb V & Ben-Ari Y (1995). Postnatal development of pre- and postsynaptic GABAB-mediated inhibitions in the CA3 hippocampal region of the rat. *J Neurophysiol.* 73: 246-255.

Geppert M, Goda Y, Stevens CF & Sudhof TC (1997). The small GTP-binding protein Rab3A regulates a late step in synaptic vesicle fusion. *Nature* 387: 810-814.

Gillies MJ, Traub RD, LeBeau FEN, Davies CH, Gloveli T, Buhl EH & Whittington MA (2002). A model of atropine-resistant theta oscillations in rat hippocampal area CA1. *J Physiol.* 543: 779-793.

Gloveli T, Dugladze T, Saha S, Monyer H, Heinemann U, Traub RD, Whittington MA & Buhl EH (2005). Differential involvement of oriens/pyramidal interneurons in hippocampal network oscillations in vitro. *J Physiol.* 562: 131-147.

Good M & Honey RC (1991). Conditioning and contextual retrieval in hippocampal rats. *Behav. Neurosci.* 105: 499-509.

Goodenough DA, Goliger JA & Paul DL (1996). Connexins, connexons, and intercellular communication. *Annu. Rev. Biochem.* 65: 475-502.

Gray CM, König P, Engel AK & Singer W (1989). Oscillatory responses in cat visual cortex exhibit inter-columnar synchronization which reflects global stimulus properties. *Nature* 338: 334-337.

Gray CM & Singer W (1989). Stimulus-specific neuronal oscillations in orientation columns of cat visual cortex. *Proc Natl Acad Sci USA* 86: 1698-1702.

Groc L, Gustafsson B & Hanse E (2002). Spontaneous unitary synaptic activity in CA1 pyramidal neurons during early postnatal development: constant contribution of AMPA and NMDA receptors. *J Neurosci.* 22: 5552-5562.

Gulyas AI, Miles R, Hajos N & Freund TF (1993). Precision and variability in postsynaptic target selection of inhibitory cells in the hippocampal CA3 region. *Eur J Neurosci.* 5: 1729-1751.

Gulyas AI, Megias M, Emri Z & Freund TF (1999). Total number and ratio of excitatory and inhibitory synapses converging onto single interneurons of different types in the CA1 area of the rat hippocampus. *J Neurosci.* 19: 10082-10097.

Halasy K, Buhl EH, Lorinczi Z, Tamas G & Somogyi P (1996). Synaptic target selectivity and input of GABAergic basket and bistratified interneurons in the CA1 area of the rat hippocampus. *Hippocampus* 6: 306-29.

Hanse E & Gustafsson B (2001a). Quantal variability at glutamatergic synapses in area CA1 of the rat neonatal hippocampus. *J Physiol.* 531: 467-480.

Hanse E & Gustafsson B (2001b). Factors explaining heterogeneity in short-term synaptic dynamics of hippocampal glutamatergic synapses in the neonatal rat. *J Physiol.* 537: 141-149.

Hefft S & Jonas P (2005). Asynchronous GABA release generates long-lasting inhibition at a hippocampal interneuron-principal neuron synapse. *Nat Neurosci.* 8: 1319-1328.

Hirsh R (1974). The hippocampus and contextual retrieval of information from memory: a theory. *Behav. Biol.* 12: 421-444.

Hjelmstad GO, Nicoll RA & Malenka RC (1997). Synaptic refractory period provides a measure of probability of release in the hippocampus. *Neuron* 19: 1309-1318.

Hjelmstad GO, Isaac JT, Nicoll RA & Malenka RC (1999). Lack of AMPA receptor desensitization during basal synaptic transmission in the hippocampal slice. *J Neurophysiol.* 81: 3096-3099.

Hoffman DA, Magee JC, Colbert CM & Johnston, D (1997). K⁺ channel regulation of signal propagation in dendrites of hippocampal pyramidal neurons. *Nature* 387: 869-875.

Holt GR & Koch C (1997). Shunting inhibition does not have a divisive effect on firing rates. *Neural Comput.* 9: 1001-1013.

Hormuzdi SG, Pais I, LeBeau FE, Towers SK, Rozov A, Buhl EH, Whittington MA & Monyer H (2001). Impaired electrical signaling disrupts gamma frequency oscillations in connexin 36-deficient mice. *Neuron* 31: 487-95.

Hormuzdi SG, Filippov MA, Mitropoulou G, Monyer H & Bruzzone R (2004). Electrical synapses: a dynamic signaling system that shapes the activity of neuronal networks. *Biochim Biophys Acta.* 1662: 113-137.

Hsia AY, Malenka RC & Nicoll RA (1998). Development of excitatory circuitry in the hippocampus. *J Neurophysiol.* 79: 2013-2024.

Isaacson JS & Walmsley B (1995). Counting quanta: direct measurements of transmitter release at a central synapse. *Neuron* 15: 875-884.

Johnston D & Amaral DG (1998). Hippocampus. In “The synaptic organization of the brain” (ed. by G.M Shepherd). Oxford University Press.

Jonas P, Major G & Sakmann B (1993). Quantal components of unitary EPSCs at the mossy fibre synapse on CA3 pyramidal cells of rat hippocampus. *J Physiol.* 472: 615-663.

Jonas P (2000). The time course of signaling at central glutamatergic synapses. *News Physiol Sci.* 15: 83-89.

Jones MV & Westbrook GL (1996). The impact of receptor desensitization on fast synaptic transmission. *Trends Neurosci.* 19: 96-101.

Jones MS & Barth DS (1997). Sensory-evoked high-frequency (gamma-band) oscillating potentials in somatosensory cortex of the unanesthetized rat. *Brain Res.* 768: 167-176.

Jones S & Yakel JL (1997). Functional nicotinic ACh receptors on interneurons in the rat hippocampus. *J Physiol.* 504: 603-610.

Kamiya H, Shinozaki H & Yamamoto C (1996). Activation of metabotropic glutamate receptor type 2/3 suppresses transmission at rat hippocampal mossy fibre synapses. *J Physiol.* 493: 447-455.

Kandel ER (2001). The molecular biology of memory storage: a dialogue between genes and synapses. *Science* 294: 1030-1038.

Katona I (1999). Postsynaptic targets of somatostatin-immunoreactive interneurons in the rat hippocampus. *Neuroscience* 88: 37-55.

Katsumaru H, Kosaka T, Heizmann CW & Hama K (1988). Gap junctions on GABAergic neurons containing the calcium-binding protein parvalbumin in the rat hippocampus (CA1 region). *Exp. Brain Res.* 72: 363-370.

Katz B & Miledi R (1965). The measurement of synaptic delay, and the time course of acetylcholine release from motor nerve terminals. *Proceedings of the Royal Society B* 161: 483-495.

Katz B (1969). The release of neural transmitter substance. Springfield, IL: Thomas.

Kawaguchi Y & Hama K (1988). Physiological heterogeneity of non-pyramidal cells in the rat hippocampal CA1 region. *Exp. Brain Res.* 72: 494-502.

Kemp N & Bashir ZI (2001). Long-term depression: a cascade of induction and expression mechanisms. *Prog Neurobiol.* 65: 339-365.

Klausberger T, Roberts JD & Somogyi P (2002). Cell type- and input-specific differences in the number and subtypes of synaptic GABA(A) receptors in the hippocampus. *J Neurosci.* 22: 2513-2521.

Klausberger T, Magill PJ, Marton LF, Roberts JD, Cobden PM, Buzsaki G & Somogyi P (2003). Brain-state- and cell-type-specific firing of hippocampal interneurons in vivo. *Nature* 421: 844-848.

Klausberger T, Marton LF, Baude A, Roberts JD, Magill PJ & Somogyi P (2004). Spike timing of dendrite-targeting bistratified cells during hippocampal network oscillations in vivo. *Nat Neurosci.* 7: 41-47.

Klausberger T, Marton LF, O'Neill J, Huck JH, Dalezios Y, Fuentealba P, Suen WY, Papp E, Kaneko T, Watanabe M, Csicsvari J & Somogyi P (2005). Complementary roles of cholecystokinin- and parvalbumin-expressing GABAergic neurons in hippocampal network oscillations. *J Neurosci.* 25: 9782-9793.

Korn H, Mallet A, Triller A & Faber DS (1982). Transmission at a central inhibitory synapse. II. Quantal description of release, with a physical correlate for binomial n. *J Neurophysiol.* 48: 679-707.

Korn H & Faber DS (1991). Quantal analysis and synaptic efficacy in the CNS. *Trends Neurosci.* 14: 439-445.

Kosaka T (1983). Neuronal gap junctions in the polymorph layer of the rat dentate gyrus. *Brain Res.* 277: 347-351.

Kosaka T & Hama K (1985). Gap junctions between non-pyramidal cell dendrites in the rat hippocampus (CA1 and CA3 regions): a combined Golgi-electron microscopy study. *J Comput. Neurol.* 231: 150-161.

Kosaka T, Katsumaru H, Hama K, Wu JY & Heizmann CW (1987). GABAergic neurons containing the Ca²⁺-binding protein parvalbumin in the rat hippocampus and dentate gyrus. *Brain Res.* 419: 119-130.

Kwok SC & Buckley MJ (2006). Fornix transection impairs exploration but not locomotion in ambulatory macaque monkeys. *Hippocampus* 16: 655-663.

Lacaille J-C, Meuller AL, Kunkel DD & Schwartzkroin PA (1987). Local circuit interactions between oriens/alveus interneurons and CA1 pyramidal cells in hippocampal slices: electrophysiology and morphology. *J. Neurosci* 7: 1979-1993.

Lacaille J-C & Schwartzkroin PA (1988). Stratum lacunosum-moleculare interneurons of hippocampal CA1 region. 11. intrasomatic and intradendritic recordings of local circuit synaptic interactions. *J Neurosci.* 8:1411-1424.

Lacaille JC (1991). Postsynaptic potentials mediated by excitatory and inhibitory aminoacids in interneurons of stratum pyramidale of the CA1 region of rat hippocampal slices in vitro. *J Neurophysiol.* 66: 1441-1454.

Laezza F, Doherty JJ & Dingledine R (1999). Long-term depression in hippocampal interneurons: joint requirement for pre- and postsynaptic events. *Science* 285: 1411-1414.

Lambert NA & Wilson WA (1993). Heterogeneity in presynaptic regulation of GABA release from hippocampal inhibitory neurons. *Neuron* 11: 1057-1067.

Larkman AU & Jack JJ (1995). Synaptic plasticity: hippocampal LTP. *Curr Opin Neurobiol.* 5: 324-334.

Lawrence JJ, Statland JM, Grinspan ZM & McBain CJ (2006a). Cell type-specific dependence of muscarinic signalling in mouse hippocampal stratum oriens interneurons. *J Physiol.* 570: 595-610.

Lawrence JJ, Grinspan ZM, Statland JM & McBain CJ (2006b). Muscarinic receptor activation tunes mouse stratum oriens interneurons to amplify spike reliability. *J Physiol.* 571: 555-562.

Lein ES, Callaway EM, Albright TD & Gage FH (2005). Redefining the boundaries of the hippocampal CA2 subfield in the mouse using gene expression and 3-dimensional reconstruction. *J Comp Neurol.* 485: 1-10.

Liu G, Choi S & Tsien RW (1999). Variability of neurotransmitter concentration and nonsaturation of postsynaptic AMPA receptors at synapses in hippocampal cultures and slices. *Neuron.* 22: 395-409.

Liu G (2003). Presynaptic control of quantal size: kinetic mechanisms and implications for synaptic transmission and plasticity. *Curr Opin Neurobiol.* 13: 324-31.

Lorente de Nó R (1934). Studies on the structure of the cerebral cortex – II. Continuation of the study of the ammonic system. *J. Psychol* 46: 113-177.

Losonczy A, Zhang L, Shigemoto R, Somogyi P & Nusser Z (2002). Cell type dependence and variability in the short-term plasticity of EPSCs in identified mouse hippocampal interneurons. *J Physiol.* 542: 193-210.

Lynch GS, Dunwiddie T & Gribkoff V (1977). Heterosynaptic depression: a postsynaptic correlate of long-term potentiation. *Nature* 266: 737-739.

Maccaferri G & McBain CJ (1996). Long-term potentiation in distinct subtypes of hippocampal nonpyramidal neurons. *J Neurosci.* 16: 5334-5343.

Maccaferri G, Toth K & McBain CJ (1998). Target-specific expression of presynaptic mossy fiber plasticity. *Science* 279: 1368-1370.

Maccaferri G, Roberts JD, Szucs P, Cottingham CA & Somogyi P (2000). Cell surface domain specific postsynaptic currents evoked by identified GABAergic neurons in rat hippocampus in vitro. *J Physiol.* 524: 91-116.

Maccaferri G & Lacaille JC (2003). Interneuron Diversity series: Hippocampal interneuron classifications--making things as simple as possible, not simpler. *Trends Neurosci.* 26: 564-571.

Maggi L, Sola E, Minneci F, Le Magueresse C, Changeux JP & Cherubini E (2004). Persistent decrease in synaptic efficacy induced by nicotine at Schaffer collateral-CA1 synapses in the immature rat hippocampus. *J Physiol.* 559: 863-74. E-pub 22 Jul 2004.

Mainen ZF, Malinow R & Svoboda K (1999). Synaptic calcium transients in single spines indicate that NMDA receptors are not saturated. *Nature* 399: 151-155.

Malenka RC & Nicoll RA (1999). Long-term potentiation--a decade of progress? *Science* 285: 1870-1874.

Markram H & Tsodyks H (1996). Redistribution of synaptic efficacy between neocortical pyramidal neurons. *Nature* 382: 807-810.

Markram H, Toledo-Rodriguez M, Wang Y, Gupta A, Silberberg G & Wu C (2004). Interneurons of the neocortical inhibitory system. *Nat Rev Neurosci* 5: 793-807.

Marr D (1971). Simple memory: a theory for archicortex. *Phil. Trans. R. Soc. Lond. B* 262: 23-81.

Martin AR (1977). Junctional transmission. II. Presynaptic mechanisms. In: Handbook of physiology, section 1, volume I, part 1 (ed. Kandel ER), Bethesda: American Physiological Society.

Martin SJ, Grimwood PD & Morris RG (2000). Synaptic plasticity and memory: an evaluation of the hypothesis. *Annu Rev Neurosci.*23: 649-711.

Martina M, Schultz JH, Ehmke H, Monyer H & Jonas P (1998). Functional and molecular differences between voltage gated K⁺ channels of fast-spiking interneurons and pyramidal neurons of rat hippocampus. *J Neurosci.* 18: 8111-8125.

Matthies H, Frey U, Reymann K, Krug M, Jork R & Schroeder H (1990). Different mechanisms and multiple stages of LTP. *Adv. Exp. Med. Biol.* 268: 359-368.

McAllister AK & Stevens CF (2000). Nonsaturation of AMPA and NMDA receptors at hippocampal synapses. *Proc Natl Acad Sci USA.* 97: 6173-6178.

McBain CJ, DiChiara TJ & Kauer JA (1994). Activation of metabotropic glutamate receptors differentially affects two classes of hippocampal interneurons and potentiates excitatory synaptic transmission. *J Neurosci.* 14: 4433-4445.

McBain CJ, Freund TF & Mody I (1999). Glutamatergic synapses onto hippocampal interneurons: precision timing without lasting plasticity. *Trends Neurosci.* 22: 228-235.

McBain CJ (2000). Multiple forms of feedback inhibition by str. oriens inhibitory interneurons? *J Physiol.* 524: 2.

McBain CJ & Fisahn A (2001). Interneurons unbound. *Nat Rev Neurosci.* 2: 11-23.

McClelland JL, McNaughton BL & O'Reilly RC (1995). Why there are complementary learning systems in the hippocampus and neocortex: insights from the successes and failures of connectionist models of learning and memory. *Psychol. Rev.* 102: 419-457.

- McGehee DS & Role LW (1995). Physiological diversity of nicotine acetylcholine receptors expressed by vertebrate neurons. *Annu Rev Physiol.* 57: 521-546.
- McLean HA, Caillard O, Khazipov R, Ben-Ari Y & Gaiarsa JL (1996). Spontaneous release of GABA activates GABAB receptors and controls network activity in the neonatal rat hippocampus. *J Neurophysiol.* 76: 1036-1046.
- McMahon L & Kauer JA (1997). Hippocampal interneurons express a novel form of synaptic plasticity. *Neuron* 18: 295-305.
- McNaughton BL & Morris RGM (1987). Hippocampal synaptic enhancement and information storage within a distributed memory system. *Trends Neurosci.* 10: 408-415.
- McQuiston AR & Madison DV (1999). Nicotinic receptor activation excites distinct subtypes of interneurons in the rat hippocampus. *J Neurosci.* 19: 2887-2896.
- Meyer AH, Katona I, Blatow M, Rozov A & Monyer H (2002). In vivo labeling of parvalbumin-positive interneurons and analysis of electrical coupling in identified neurons. *J Neurosci.* 22: 7055-7064.
- Michelson HB & Wong RK (1994). Synchronization of inhibitory neurones in the guinea-pig hippocampus in vitro. *J Physiol.* 477: 35-45.
- Miles R & Wong RKS (1986). Excitatory synaptic interactions between CA3 neurones in the guinea-pig hippocampus. *J Physiol.* 373: 397-418.
- Miles R, Toth K, Gulyas AI, Hajos N & Freund TF (1996). Differences between somatic and dendritic inhibition in the hippocampus. *Neuron* 16: 815-823.
- Mishkin M, Suzuki WA, Gadian DG & Vargha_Khadem F (1997). Hierarchical organization of cognitive memory. *Phil. Trans. R. Soc. Lond. B Biol. Sci.* 352: 1461-1467.
- Mitchell SJ & Silver RA (2003). Shunting inhibition modulates neuronal gain during synaptic excitation. *Neuron* 38: 433-445.
- Mody I, De Koninck Y, Otis TS & Soltesz I (1994). Bridging the cleft at GABA synapses in the brain. *Trends Neurosci.* 17: 517-525.
- Monyer H & Markram H (2004). Interneuron Diversity series: Molecular and genetic tools to study GABAergic interneuron diversity and function. *Trends Neurosci.* 27: 90-97.
- Morris RGM, Garrud P, Rawlins JN & O'Keefe J (1982). Place navigation impaired in rats with hippocampal lesions. *Nature* 297: 681-683.

Morris RGM & Frey U (1997). Hippocampal synaptic plasticity: role in spatial learning or the automatic recording of attended experience? *Phil. Trans. R. Soc. Lond. B Biol. Sci.* 352: 1489-1503.

Morris RGM (2006). Elements of a neurobiological theory of hippocampal function: the role of synaptic plasticity, synaptic tagging and schemas. *Eur J Neurosci.* 23: 2829-2846.

Mott DD, Turner DA, Okazaki MM & Lewis DV (1997). Interneurons of the dentate-hilus border of the rat dentate gyrus: morphological and electrophysiological heterogeneity. *J Neurosci.* 17: 3990-4005.

Muller R (1996). A quarter of a century of place cells. *Neuron* 17: 813-822.

Nakazawa K, Quirk MC, Chitwood RA, Watanabe M, Yeckel MF, Sun LD, Kato A, Carr CA, Johnston D, Wilson MA & Tonegawa S (2002). Requirement for hippocampal CA3 NMDA receptors in associative memory recall. *Science* 297: 211-218.

Nelson SB & Turrigiano GG (1998). Synaptic depression: a key player in the cortical balancing act. *Nat Neurosci.* 1: 539-541.

Nicoll RA & Malenka RC (1995). Contrasting properties of two forms of long-term potentiation in the hippocampus. *Nature* 377: 115-118.

Nimchinsky EA, Yasuda R, Oertner TG & Svoboda K (2004). The number of glutamate receptors opened by synaptic stimulation in single hippocampal spines. *J Neurosci.* 24: 2054-2064.

Oertner TG, Sabatini BL, Nimchinsky EA & Svoboda K (2002). Facilitation at single synapses probed with optical quantal analysis. *Nat Neurosci.* 5: 657-664.

O'Keefe J & Nadel L (1978). *The Hippocampus as a Cognitive Map*. Clarendon Press, Oxford.

Oliva AA Jr, Jiang M, Lam T, Smith KL & Swann JW (2000). Novel hippocampal interneuronal subtypes identified using transgenic mice that express green fluorescent protein in GABAergic interneurons. *J Neurosci.* 20: 3354-3368.

O'Reilly RC & Rudy JW (2001). Conjunctive representations in learning and memory: principles of cortical and hippocampal function. *Psychol. Rev.* 108: 311-345.

Owens DF & Kriegstein AR (2002). Is there more to GABA than synaptic inhibition? *Nat Rev Neurosci.* 3: 715-727.

Palade GE (1954). Electron microscope observation of interneuronal and neuromuscular synapses. *Anatomical Record* 118: 335-336.

Palay SL (1954). Electron microscope study of the cytoplasm of neurons. *Anatomical Record* 118: 336.

Parra P, Gulyas AI & Miles R (1998). How many subtypes of inhibitory cells in the hippocampus? *Neuron* 20: 983-993.

Penttonen M, Kamondi A, Acsady L & Buzsaki G (1998). Gamma frequency oscillation in the hippocampus of the rat: intracellular analysis in vivo. *Eur J Neurosci* 10: 718-728.

Pike FG, Goddard RS, Suckling JM, Ganter P, Kasthuri N & Paulsen O (2000). Distinct frequency preferences of different types of rat hippocampal neurones in response to oscillatory input currents. *J Physiol.* 529: 205-213.

Raghavachari S & Lisman JE (2004). Properties of quantal transmission at CA1 synapses. *J Neurophysiol.* 92: 2456-2467.

Ramón y Cajal, S (1893). Estructura del asta de Ammon y fascia dentate. *Ann. Soc. Esp. Hist. Nat.* 22.

Ramón y Cajal S (1911). Histologie de systeme nerveux de l'Homme et des vertebres tomme 11. Paris: Maloine.

Redman S (1990). Quantal analysis of synaptic potentials in neurons of the central nervous system. *Physiol. Rev.* 70: 165-198.

Reid CA & Clements JD (1999). Postsynaptic expression of long-term potentiation in the rat dentate gyrus demonstrated by variance-mean analysis. *J Physiol.* 518: 121-130.

Revel JP & Karnovsky MJ (1967). Hexagonal array of in intercellular junctions of the mouse heart and liver. *J Cell Biol.* 33: C7-C12.

Ribak CE (1978). Aspinous and sparsely-spinous stellate neurons in the visual cortex of rats contain glutamic acid decarboxylase. *J Neurocytol.* 7: 461-478.

Ritz R & Sejnowski TJ (1997). Synchronous oscillatory activity in sensory systems: new vistas on mechanisms. *Curr Opin Neurobiol.* 7: 536-546.

Rizzoli SO & Betz WJ (2005). Synaptic vesicle pools. *Nat Rev Neurosci.* 6: 57-69.

Rolls ET & Treves A (1998). Neural Networks and Brain Function. Oxford University Press, Oxford.

Rosenmund C, Clements JD & Westbrook GL (1993). Nonuniform probability of glutamate release at a hippocampal synapse. *Science* 262: 754-757.

Rosemund C & Stevens CF (1996). Definition of the readily releasable pool of vesicles at hippocampal synapses. *Neuron* 16: 1197-1207.

Sabatini BL & Regehr WG (1997). Control of neurotransmitter release by presynaptic waveform at the granule cell to Purkinje synapse. *J Neurosci* 17: 3425-3435.

Sara Y, Virmani T, Deak F, Liu X & Kavalali ET (2005). An isolated pool of vesicles recycles at rest and drives spontaneous neurotransmission. *Neuron* 45: 563-573.

Scanziani M, Gahwiler BH & Charpak S (1998). Target cell-specific modulation of transmitter release at terminals from a single axon. *Proc. Natl Acad. Sci. USA* 95: 12004-12009.

Scheuss V & Neher E (2001). Estimating synaptic parameters from mean, variance, and covariance in trains of synaptic responses. *Biophys. J* 81: 1970-1989.

Scheuss V, Schneggenburger R & Neher E (2002). Separation of presynaptic and postsynaptic contributions to depression by covariance analysis of successive EPSCs at the calyx of held synapse. *J Neurosci*. 22: 728-739.

Schneider SW (2001). Kiss and run mechanism in exocytosis. *J Membr Biol*. 181: 67-76.

Schreiber S, Fellous JM, Tiesinga P & Sejnowski TJ (2004). Influence of ionic conductances on spike timing reliability of cortical neurons for suprathreshold rhythmic inputs. *J Neurophysiol*. 91: 194-205.

Segal M (1990). A subset of local interneurons generate slow inhibitory postsynaptic potentials in hippocampal neurons. *Brain Res*. 511: 163-164.

Sik A, Penttonen M, Ylinen A & Buzsaki G (1995). Hippocampal CA1 interneurons: an in vivo intracellular labeling study. *J Neurosci*. 15: 6651-6665.

Silver RA (1998). Neurotransmission at synapses with single and multiple release sites. In: "Central Synapses: Quantal Mechanisms and Plasticity". Eds D.S. Faber, H. Korn, S.J. Redman, S.M. Thompson and J.S. Altman. HFSP, Strasbourg.

Silver RA, Momiyama A & Cull-Candy SG (1998). Locus of frequency-dependent depression identified with multiple-probability fluctuation analysis at rat climbing fibre-Purkinje cell synapses. *J Physiol*. 510: 881-902.

Silver RA (2003). Estimation of nonuniform quantal parameters with multiple-probability fluctuation analysis: theory, application and limitations. *J Neurosci Methods*. 130: 127-141.

Singer W & Gray CM (1995). Visual feature integration and the temporal correlation hypothesis. *Annu Rev Neurosci* 18: 555-586.

Sohal VS & Huguenard JR (2005). Inhibitory coupling specifically generates emergent gamma oscillations in diverse cell types. *Proc Natl Acad Sci USA* 102: 18638-18643.

Soltesz I & Deschenes M (1993). Low- and high-frequency membrane potential oscillations during theta activity in CA1 and CA3 pyramidal neurones of the rat hippocampus under ketamine-xylazine anesthesia. *J Neurophysiol.* 70: 97-116.

Soltesz I & Mody I (1994). Patch-clamp recordings reveal powerful GABAergic inhibition in dentate hilar neurons. *J Neurosci.* 14: 2365-2376.

Somogyi P, Hodgson AJ, Smith AD, Nunzi MG, Gorio A & Wu JY (1984). Different populations of GABAergic neurons in the visual cortex and hippocampus of cat contain somatostatin- or cholecystinin-immunoreactive material. *J Neurosci.* 4: 2590-603.

Somogyi P & Klausberger T (2005). Defined types of cortical interneurone structure space and spike timing in the hippocampus. *J Physiol.* 562: 9-26.

Squire LR (1986). Mechanisms of memory. *Science* 232:1612-1619.

Stevens CF & Wang Y (1995). Facilitation and depression at single central synapses. *Neuron* 14: 795-802.

Stevens CF (1998). A million dollar question: does LTP = memory? *Neuron* 20: 1-2.

Storm-Mathisen J, Leknes AK, Bore AT, Vaaland JL, Edminson P, Haug FM & Ottersen OP (1983). First visualization of glutamate and GABA in neurones by immunocytochemistry. *Nature* 301: 517-20.

Strata F, Atzori M, Molnar M, Ugolini G, Tempia F & Cherubini E (1997). A pacemaker current in dye-coupled hilar interneurons contributes to the generation of giant GABAergic potentials in developing hippocampus. *J Neurosci.* 17: 1435-1446.

Südhof TC (1995). The synaptic vesicle cycle: a cascade of protein-protein interactions. *Nature* 30: 171-182.

Sutherland RJ & Rudy JW (1989). Configural association theory: The role of the hippocampal formation in learning, memory, and amnesia. *Psychobiology* 17: 129-144.

Szentagothai J (1975). The 'module-concept' in cerebral cortex architecture. *Brain Res* 95: 475-496.

Tang CM, Margulis M, Shi QY & Fielding A (1994). Saturation of postsynaptic glutamate receptors after quantal release of transmitter. *Neuron* 13: 1385-1393.

Tang VW & Goodenough DA (2003). Paracellular ion channel at the tight junction. *Biophys. J* 84: 1660-1673.

Thomson AM & Deuchars J (1994). Temporal and spatial properties of local circuits in neocortex. *Trends Neurosci.* 17: 119-126.

Thomson AM, West DC & Deuchars J (1995). Properties of single axon excitatory postsynaptic potentials elicited in spiny interneurons by action potentials in pyramidal neurons in slices of rat neocortex. *Neurosci.* 69: 727-738.

Thomson AM (2000). Molecular frequency filters at central synapses. *Prog. Neurobiol.* 62: 159-196.

Toledo-Rodriguez M, Blumenfeld B, Wu C, Luo J, Attali B, Goodman P & Markram H (2004). Correlation maps allow neuronal electrical properties to be predicted from single-cell gene expression profiles in rat neocortex. *Cereb Cortex.* 14: 1310-1327.

Toledo-Rodriguez M, Goodman P, Illic M, Wu C & Markram H (2005). Neuropeptide and calcium-binding protein gene expression profiles predict neuronal anatomical type in the juvenile rat. *J Physiol.* 567: 401-413.

Tong G & Jahr CE (1994a). Multivesicular release from excitatory synapses of cultured hippocampal neurons. *Neuron* 12: 51-59.

Tong G & Jahr CE (1994b). Block of glutamate transporters potentiates postsynaptic excitation. *Neuron* 13: 1195-1203.

Toth K, Soares G, Lawrence JJ, Philips-Tansey E & McBain CJ (2000). Differential mechanisms of transmission at three types of mossy fiber synapse. *J Neurosci.* 20: 8279-8289.

Traub RD, Miles R & Wong RKS (1987). Models of synchronized hippocampal bursts in the presence of inhibition. I. Single population events. *J Neurophysiol.* 58: 739-751.

Traub RD & Miles R (1991). Neuronal networks of the hippocampus. Cambridge University Press.

Traub RD, Whittington MA, Colling SB, Buzsáki G & Jefferys JGR (1996). Analysis of gamma rhythms in the rat hippocampus in vitro and in vivo. *J Physiol.* 493: 471-484.

Traub RD, Draguhn A, Whittington MA, Baldeweg T, Bibbig A, Buhl EH & Schmitz D (2002). Axonal gap junctions between principal neurons: a novel source of network oscillations, and perhaps epileptogenesis. *Rev. Neurosci.* 13: 1-30.

Traub RD, Bibbig A, LeBeau FE, Buhl EH & Whittington MA (2004). Cellular mechanisms of neuronal population oscillations in the hippocampus in vitro. *Annu Rev Neurosci.* 27: 247-278.

Triller A & Korn H (1982). Transmission at a central inhibitory synapse. III. Ultrastructure of physiologically identified and stained terminals. *J Neurophysiol.* 48: 708-736.

Tsodyks M & Markram H (1997). The neural code between neocortical pyramidal neurons depends on neurotransmitter release probability. *Proc Natl Acad Sci USA* 94: 719-723.

Tulving E (1983). *Elements of Episodic Memory*. Oxford University Press, New York.

Vargha-Khadem F, Gadian DG, Watkins KE, Connely A, Van Paesschen W & Mishkin M (1997). Differential effects of early hippocampal pathology on episodic and semantic memory. *Science* 277: 376-380.

Venance L, Rozov A, Blatow M, Burnashev N, Feldmeyer D & Monyer H (2000). Connexin expression in electrically coupled postnatal rat brain neurons. *Proc. Natl. Acad. Sci. USA* 97: 10260-10265.

Vida I, Bartos M & Jonas P (2006). Shunting inhibition improves robustness of gamma oscillations in hippocampal interneuron networks by homogenizing firing rates. *Neuron* 49: 107-117.

von Gersdorff H, Schneggenburger R, Weis S & Neher E (1997). Presynaptic depression at a Calyx synapse: the small contribution of metabotropic glutamate receptors. *J Neurosci.* 17: 8137-8148.

Wadiche JI & Jahr CE (2001). Multivesicular release at climbing fiber-Purkinje cell synapses. *Neuron* 32: 301-313.

Walmsley B (1995). Interpretation of 'quantal' peaks in distributions of evoked synaptic transmission at central synapses. *Proc. R. Soc., Lond. B Biol. Sci.* 261: 245-250.

Wasling P, Hanse E & Gustafsson B (2004). Developmental changes in release properties of the CA3-CA1 glutamate synapse in rat hippocampus. *J Neurophysiol.* 92: 2714-24.

Whittington MA, Traub RD & Jefferys JG (1995). Synchronized oscillation in interneuron networks driven by metabotropic glutamate receptor activation. *Nature* 373: 612-615.

Whittington MA & Traub RD (2003). Interneuron diversity series: inhibitory interneurons and network oscillations in vitro. *Trends Neurosci.* 26: 676-682.

Whittington MA, Traub RD & Jefferys JG (1995). Synchronized oscillations in interneuron networks driven by metabotropic glutamate receptor activation. *Nature* 373: 612-615.

Willecke K, Eiberger J, Degen J, Eckardt D, Romualdi A, Guldenagel M, Deutsch U & Sohl G (2002). Structural and functional diversity of connexin genes in the mouse and human genome. *Biol. Chem.* 383: 725-737.

Wilson RI & Nicoll RA (2002). Endocannabinoid signaling in the brain. *Science* 296: 678-682.

Witter MP, Naber PA, van Haeften T, Machielsen WC, Rombouts SA, Barkhof F, Scheltens P & Lopes da Silva FH (2000). Cortico-hippocampal communication by way of parallel parahippocampal-subicular pathways. *Hippocampus* 10: 398-410.

Yeckel MF, Kapur A & Johnston D (1999). Multiple forms of LTP in hippocampal CA3 neurons use a common postsynaptic mechanism. *Nat Neurosci.* 2: 625-633.

Zola-Morgan S & Squire LR (1993). Neuroanatomy of memory. *Annu Rev Neurosci.* 16: 547-563.

Zucker RS & Regehr WG (2002). Short-term synaptic plasticity. *Annu. Rev. Physiol.* 64: 355-405.

ACKNOWLEDGEMENTS

I would like to thank all the people around me who have made my stay more enjoyable and more interesting throughout this long adventure in Trieste.

In particular, I want to warmly thank my supervisor, Enrico Cherubini, for teaching me how to deal with neurobiology and experimental science, for triggering me with a lot of interesting ideas, and for supporting me in the bad moments. I also want to say thank you to my family, for assisting me continuously, though from a great distance.

I am extremely grateful to many people with whom I have spent my time, both inside and outside the lab, for helping me to learn my new job, for dealing with me in my best and worst periods, for giving me the opportunity to know them, and for sharing with me a lot of nice moments that I will never forget.